Determining the effects of market mechanisms on the power flow for a prosumer building

An analysis of feed-in tariff, capacity mechanism and frequency regulation on power flow of a building with its own generation and storage

A. Subrahmanya Rao

Technische Universiteit Delft

TU Delft

Determining the effects of market mechanisms on the power flow for a prosumer building

An analysis of feed-in tariff, capacity mechanism and frequency regulation on power flow of a building with its own generation and storage

by

A. Subrahmanya Rao

to obtain the degree of Master of Science
at the Delft University of Technology,
to be defended publicly on Friday, November 27, 2020 at 12:00.

Student number:	4780094	
Project duration:	December 1, 2019 – November 27, 2020	
Thesis committee:	Prof. dr. ir. P. Bauer,	TU Delft
	Dr. G. R. Mouli,	TU Delft
	Dr. A. Stefanov,	TU Delft
	Ir. W. Vermeer,	TU Delft

An electronic version of this thesis is available at `http://repository.tudelft.nl/`.

TU Delft

Preface

Energy has always fascinated me, ever since as a 10 year old who was dumbfounded when he first realised that it was possible to convert sunlight to electricity. I have always been a very curious person and it has led me to many places. I like to think that it is because of my curiosity that I decided to pursue my Master at TU Delft.

This project has been quite a challenge but it has helped me acquire new skills. Looking back to the last twelve months of the project makes me realise how important people around me are. Firstly, I would like to thank my supervisor Dr. Gautham Ram for motivating me and believing in me. He was an immense support during this tenuous period and always gently pushed me to do better. Gautham's calm demeanor and eye for fine detail is something that I would like to incorporate in myself.

Next, I would like to thank my daily supervisor, Wiljan for showing me how to think critically and helping me see things from a different perspective. I also thank him for helping me get out of the many blocks that I suffered during the last twelve months. His attitude of diving deep enough into any topic is what I would like inculcate in myself as well.

I would like to thank my roommate, Hajo for ensuring that I stay sane, healthy, and on track during my entire stay in Delft starting in 2018. His practical approach to any problem and a can do attitude is something I admire. I also thank him for getting the coffee grinder which has worked wonders for my productivity during the past 5 months.

I would like to thank Bram, Calvin, Lode and Saumitra for becoming my unspoken thesis support group during the initial period of my thesis. I miss the lunches we used to have together at the EWI cafetaria. I also thank Bertram for the interesting talks over coffee and showing me how cool a place the city library is to work. I also want to take my opportunity to thank Stella for making me try bubble tea for the first time and Khushboo for all the interesting conversations and walks around the city. I also show my appreciation to Anamitra, Ezra, Yang, Reinier and everyone from IAESTE who helped me stay in good spirits. I thank for Roberto for telling me, "Hey, you got this. Don't worry." whenever we met.

Lastly, I want to thank my family for believing in me and motivating me to do better during my entire period at TU Delft. None of this would have been possible without their immense and unwavering support.

As I am writing this down, I am just realising what a whirlwind this past year has been. The pandemic definitely added a lot of strain on my thesis and my life. But it has also taught me to be grateful for everything that I have. I am grateful to be healthy and safe during this tumultuous period. I learnt a lot of things at TU Delft but I think the two most important lessons that I learnt here were that it is okay to ask for help and perseverance is the key to get things done. If you are reading this, I want to tell you to be easy on yourself and that you are doing the best you can.

A. Subrahmanya Rao
Delft, November 2020

Abstract

With distributed energy sources becoming prominent, it is expected that new market mechanisms would become necessary to overcome the issues caused by the intermittency of those sources. This research determines the effect of certain market mechanisms, which have been proposed to either incentivize the distributed generation or to reduce their undesirable effects, on power flow of a prosumer household. The prosumer household was assumed to consist of PV generation system, an Electric Vehicle which was capable of V2G and a household battery. The market mechanisms used were Feed-in tariffs, Capacity Mechanism and Frequency Containment Reserve. An Energy Management System which determines both, the optimal system size and the optimal power flow by minimizing the operational costs was used to achieve this. It was observed that different level of feed in tariff affected the optimal system size and the power flow. At high feed-in tariff, the system size was the largest and high grid peak power was observed. Furthermore, the introduction of the capacity mechanism in the form of capacity tariffs per kW led to reduction in grid power consumption and feeding in. Finally, it was observed that the energy management system was able to reserve power for the frequency regulation market. Compared to an uncontrolled case, a reduction of 70.26% in total costs was achieved when the EMS control was introduced. A cost reduction of 52.02% compared to the uncontrolled case was achieved when an additional capacity tariff was also introduced to the control. Finally, introduction of the frequency regulation mechanism in the EMS control led to even further reduction in costs with a drop of 1205.07% compared to the uncontrolled case.

Contents

Acronyms

BES Battery Energy Storage.

BSP Balancing Service Providers.

CHP Combined Heat Pump.

CM Capacity Mechanism.

CT Capacity Tariffs.

DG Distributed Generation.

DR Demand Response.

DSM Demand Side Management.

DSO Distribution System Operator.

EBT Energy Based Tariff.

EMS Energy Management System.

EV Electric Vehicles.

FCR Frequency Containment Reserve.

FIT Feed-in tariff.

LCOE Levelised Cost of Electricity.

MPPT Maximum Power Point Tracking.

NLP Non Linear Programming.

OCV Open Circuit Voltage.

PBT Power Based Tariff.

PV Photovoltaic.

RES Renewable Energy Sources.

RP Retail Price.

RTP Real Time Price.

SoC State of Charge.

ToU Time of Use.

TSO Transmission System Operator.

V2G Vehicle to Grid.

WTP Willingness to Pay.

1 Introduction

1.1. Background and Motivation

Energy transition is a necessity for preventing further climate change. This requires more non-carbon based energy sources. Examples are solar and wind energy. This has also led to interest in electric vehicles as an alternative to conventional fossil fuel powered automobiles.

The introduction of intermittent renewable energy sources (RES) causes uncertainty of energy supply. This happens because of the strong dependence of these sources on the local climate. Due to this reason, the energy scheduling of the conventional power plants becomes difficult. Traditionally, the total supply was easily predictable, but now the supply is strongly dependent on external factors such as weather conditions. On a day with abundant sunlight or wind, RES might be able to generate required energy to satisfy the demand, but on other days, the scarcity is noticed. In the current distribution grid with increasing penetration of RES, a decreasing number of controllable power plants and low storage penetration can lead to price spikes with abnormally high and low prices. In the un-bundled energy markets of Europe, this leads to challenges which pertain to the the stability of the electricity grid and new investment in renewable energy sources.

Because of the new dependencies, there occur gaps in the energy markets that did not exist before, such as requirement of new actors who specialise in demand side response. Since the energy availability can also become intermittent, it becomes interesting to schedule the usage based on the energy availability (though this is also leading to investment in storage technologies). This has an advantage that the energy generated by RES is consumed and since they are relatively cheaper compared to conventional plants, energy cost is also lower. The gaps in the energy markets are being filled by Aggregrators who offer demand side response by incentivizing consumption/changing consumption patterns. The current energy markets face the challenge of accommodating aggregators due to lack of regulation.

Decentralised generation is also becoming popular in the form of having solar panels on rooftops and having storage devices such as batteries and electric vehicles (EV). Such instruments can lead to a bi-directional flow of current, which is either grid to household or household to grid. These operations can cause problems in the grid at the distribution level such as congestion, lower voltage levels, issues related to active and reactive power, overloading leading to heat dissipation etc. It is because the grid was not designed to allow bi-directional power flow.

As mentioned, these issues are not prevalent yet in the grids, which is because the penetration of RES is still comparatively lower. But the issues are predicted to play a bigger role in electricity grids in the coming years. Various proposals have been put forward for solving these problems via mechanisms like demand side management and smart charging of EV. Demand side management involves scheduling the consumption of energy during off-peak hours or moving the consumption of energy from peak hours to off-peak hours to reduce the consumption costs and to maintain the network stability. Smart charging of EV is also becoming interesting because of the increasing number of EV. Smart charging involves charging the vehicle during the times with low tariff but at the same time avoiding grid congestion and making sure that there are no new

peaks formed due to the shifting of charging sessions.

These mechanisms suggest increasing roles for aggregators and a more pro-active roles for the Distribution System Operators (DSO) and prosumers. This also means more close involvement of DSOs with the Transmission System Operators (TSO). However, these market mechanisms are more focused on providing an economic perspective and do not present the technical results. Research has to be done to further understand their effects on the energy grid.

With the knowledge of such parameters, the DSO and TSO can determine which market policies are best suited for the electricity grids and make the necessary modifications. This ensures the grid safety and energy adequacy along with the grid stability. Also, it is intended to create benchmarks on different market mechanisms by evaluating different grid parameters. Such information can help governments and other entities involved make an informed decision as to what market mechanism(s) can be used.

This research is necessary as it can be a good starting option to choose a specific market mechanism for distribution grids. The aim of this research is to identify the different market mechanisms that have been proposed for the energy markets of the future and try to quantify their effects on the distribution grids.

1.2. Research questions

To this end the objective of this thesis was:

Analyse the effects of certain market instruments that are proposed/in place for energy transition on power flows of a prosumer household with Electric Vehicle (EV), Battery Energy Storage (BES) and Photvoltaic power generation (PV).

This was done by answering the following questions:

- **How are feed-in tariffs (FIT) affecting the energy consumption, energy feeding behaviour, system sizing and costs to a prosumer household?** What are the effects of different level of FIT on system sizing and what are the optimal sizes for each level?

  What are the different kind of FIT being considered in the current electricity regime? What are the differences among them and what are their advantages and disadvantages?

  How does different level of FIT affect the power flow within a household? How does the feeding in and consumption behaviour change when there is a change in the FIT?

  What is the optimal system size for each level of FIT? How does the system sizing vary when FIT changes and how do the total energy costs change?

  What are prospective challenges and opportunities that can be seen with the above effects of FIT on power flow and system size?

- **What Capacity Mechanisms (CM) are being discussed to ensure grid stability and reduce grid peak power level on a distribution level and what effects would such a mechanism would have on power flow of a prosumer household?**

  What are the different CM proposed? How are they different from each other?

  What are the assumptions these mechanisms make for prosumer households? What are the drawbacks of these assumptions?

  What are different capacity tariffs (CT) being proposed for such a mechanism?

  How does such a mechanism affect the power flow and consumption of a prosumer household? Does such a mechanism increase the self-consumption and if so to what extent?

  What are the different challenges to implement such a mechanism in the Netherlands?

- **How can prosumers participate in the primary frequency regulation market (FCR) in the Netherlands and how would reserving the power for regulation affect the power flow of a prosumer household?**

What is frequency regulation and why is it necessary? What are the challenges for frequency regulation when the share of renewables increase in the distribution grid?

How does the Frequency Containment Reserve (FCR) market in the Netherlands work? What are the provisions provided by the TSO and what are the requirements?

How does reserving the power for FCR affect the power flow and the total costs for a household?

1.3. Methodology

The goal of the thesis was achieved by first performing a literature review of the electricity regime of the Netherlands. Different market mechanisms which were relevant were identified and they were simulated to determine their effects on power flow for a single household. Real prices were considered wherever available and assumptions were made when the prices were not available.

An EMS designed as a part of the FlexGrids project at TU Delft was used to simulate the market mechanism effects on the power flow of the household. The household was considered to have a V2G-capable EV, PV and BES system available. Investment costs were considered for BES and PV system while EV was assumed to be obtained independently of the study.

This EMS was simulated in GAMS and relevant market mechanism equations along with their prices were added in the smart control model. The results of the optimization to minimize the system cost under the influence of the market mechanisms were studied. The plots were plotted on MATLAB and the results were analysed. Discussions pertaining to the observed power flows and the current energy ecosystem were then made.

The market mechanisms being considered are Feed-in tariff (FIT), Capacity Mechanism (CM), and Frequency regulation. FIT have been proposed to increase the penetration of distributed energy sources such as PV and Battery Energy Storage (BES). However, the increasing presence of renewable energy sources have resulted in frequent power peaks in the distribution grid. As a result, Capacity Mechanism (CM) was proposed to reduce these power peaks and increase the reliance on storage devices. Furthermore, the increasing penetration of renewables also cause issues in grid frequency due to their intermittent behaviour. To this end, the frequency regulation using energy sources present at a prosumer household have been investigated in this work.

2

Literature Review

To prevent further damage from climate change, countries across the world have started to adapt to renewable energy sources to meet their energy demand. Moving from conventional power plants powered by fossil fuels is difficult due to the fact that the solar and wind energy, which are predominant form of renewables, are often available intermittently. In other words, they have a very strong dependence on the weather conditions in a locality.

This change in the generation patterns inevitably affect the energy markets which are in place to ensure the supply to customers from producers.

2.1. Retail electricity costs in the Netherlands.

In the Netherlands, energy utilities have been un-bundled since 2008[1]. The un-bundling has led to separation of various energy network related activities as transmission and distribution networks are considered as monopoly activities. Thus, the production, transmission and distribution of energy was separated to incentivize competition and to reduce prices.

The authors in [2] concluded that the authority for regulation of costs in the Netherlands, ACM regulates the retail energy prices rather strictly and as a result, the energy suppliers are required to get their tariffs approved before making changes in the retail tariffs. To this end, on analysing the current retail prices, the following components were observed [3].

- Variable costs
- Fixed costs
- Network management costs
- Resident tax deduction
- Government taxes
- Contract end date and price differences

Variable costs

Variable costs included the costs of energy consumption. These costs depend on the energy consumption and thus, larger the consumption, larger the costs. For energy acquired from wind parks, these prices include the normal and the low rate and vary between 0.22 €/kWh and 0.20 €/kWh. These costs are inclusive of the energy tax which the supplier had to pay to the government, which amount to 0.12 €/kWh.

Fixed costs

Fixed costs are the tariffs to be paid by the consumer regardless of the consumption. They can be attributed to a cost similar to the network charges which are charged by the DSO to their consumers.

Network management costs

These are the costs which were charged by the DSO to consumers for using the distribution network. These costs depend on the connection size and vary based on the maximum power which can be drawn from the grid at any instant. For a household with a connection of 3x25 A, the network costs were determined to be €230.36.

Resident tax deduction

If the energy supply is used by the consumers for residential purposes, the consumers received tax benefits by the government in the form of resident tax deduction. These were the costs which relate to the discount amount set by the government and they amounted to €527.17.

Government taxes

Government taxes are the costs paid by the supplier to the government for the energy production and supply operations. These costs included the government levies and VAT for an annual consumption of set amount of energy and gas. Additionally, government taxes also included the energy tax and the energy storage tax.

Contract end date and price differences

The contract end date also affected the retail price for energy as the fixed prices were calculated based on the contract period. Furthermore, the costs were also rounded off to reflect even tariffs and that part of the costs were reflected by the price differences component of the total cost.

From the above described costs, it was observed that the only the variable energy costs were dependent on the energy usage. Additionally, it also reflected that regardless of time, only two different retail prices were available. This showed that the price changes in the wholesale market were not reflected in the retail costs. Additionally, the network component of the fixed costs also formed a significant portion of the costs. For example, the total energy costs for a 3x25A connection was found to be €831.87 per year. Of this, €230.36 was the capacity tariff. This amounted to 27.8% of the total costs. As noted, these costs are fixed as well and irrespective of time did not change. Thus, the network costs also did not reflect the conditions of the distribution network at any instant. Finally, the reduction in energy costs for residential purposes were equal to €527.17 which reduced the total energy costs by 63%.

From the cost split up, it was observed that the suppliers charge only for the energy supplied. The variable costs and the fixed cost for consumers are the revenue generating components for the suppliers. The network management costs are the revenue obtained by the DSO, but due to regulation, the DSO is not allowed to design their own tariffs. As already mentioned in the literature, the retail prices needed to be approved by the government which leads to significant involvement of the government in designing the tariffs. Thus, it was observed that the governmental regulation affects the retail tariffs significantly. Changes in the regulation are necessary for there to be changes in the retail price structure.

2.2. Issues caused by the presence of renewable energy source and additional loads in the current grid

Distributed energy generation has increased drastically in the last decade in the Netherlands [4] and as of 2018, the total installation of Photovoltaic (PV) systems on rooftops of houses amount to 2.3 GW [5]. As the penetration of renewables in the grid increase, problems caused by them become more noticeable. Issues which are relevant for this thesis are discussed in detail. It should be noted that issues presented here are not exhaustive and there might also arise further market issues in the future.

In the current day-ahead energy markets, energy bids are placed by different suppliers for particular time blocks of the day. These time blocks are usually fifteen minutes long and are called as Programme Time Units (PTU). Currently, the energy markets only account for the energy at the start and at the end of the PTU. The energy balance during the fifteen minute interval is not being addressed. This causes system imbalances due to the fact that the demand can be stochastic [6]. Increasing number of the renewables leads to changes in the supply as well. This additional stochasticity in the generation further causes more imbalance issues in

the grid. To solve this problem of imbalance, ancillary service markets are operated. The imbalances caused by the renewables in the system lead to more trading in the imbalance markets which can lead to larger electricity prices.

Currently, one of the main challenges faced by the electricity industry is how to integrate the large number of renewables in the system. This is challenging in a decentralized European electricity industry as the processes of generation, transmission and distribution are un-bundled and different actors are involved in each of the process involved. Authors of [7] conclude that one of the main regulatory challenges that the electricity industry is facing is the lack of co-ordination between different actors and they recommend all the actors involved to play a more pro-active role.

At the national (transmission level), challenges related to congestion and cross border co-ordination for investment in transmission networks were found to be the major issues. At the distribution level, challenges related to grid congestion, rooftop PV and flexible charging of Electric Vehicles (EV) were determined to be the big challenges. It is also uncertain how the governments are going to fix these issues, i.e. allow new aggregators or assign the responsibilities to the DSO. Another key challenge was the integration with the wholesale markets as the retail prices do not really reflect the additional volatility that is being introduced by the increasing number of the renewable sources. In [7], authors also commented that a new challenge was the market design to allocate local flexibility so that the grids are no longer designed to allow peak loads, but rather lower loads for increased hours. They recommended that energy needs to be traded more close to real time which can help in reducing the volatility of forecast errors for renewable energy sources. However, they did not comment upon the requirement of new additional ancillary services that might be necessary when there are much higher penetration levels of renewable sources.

The climate goals of the European Union (EU) for the year 2030 requires member nations to reduce their emissions by 40% from the 1990 levels and 32% of the total energy to be supplied from renewables [8]. Additionally, the 2050 goals of going climate neutral [9] has led to investment in distributed energy generation by large suppliers and small residential consumers alike. In the Netherlands, this was observed by the increasing number of PV installations as [5] shows.

However, it was observed that distributed generation (DG) also causes issues, both in distribution as well as transmission grids. These issues can affect the power losses in the grid, the voltage levels and grid congestion. In [10], the authors simulate a IEEE 34 node test feeder using DIGSilent PowerFactory to determine the effects of distributed generation sources on power losses, voltage profiles, system imbalances, and faults. They determine this by varying the penetration of DG as well as the position of the sources in the feeder. It should be noted that in [10], the authors only consider PV as DG sources. All the analysis have been done for various penetrations of PV sources. Penetration level has been defined as the total DG generation capacity with respect to the rated capacity of the network. The impact of DGs at penetrations of 10% and 20% were analysed. It was observed that DGs led to increase in voltage levels at the nodes that they were placed. This occurred due to change in the power flow from lower voltage to higher voltage. This reversal in power can lead to potential damages to the grid equipments such as transformers and relays which are relatively expensive to replace. This phenomenon of reversal of power flow was also observed by the authors in [11].

Furthermore, in [12], authors determine the effects of the distributed generation (only hydro, wind and thermal plants are considered) on transmission level. A 60 kV feeder network is considered in this work and the distributed generation is considered on 30 kV and 15 kV networks. In the results of [12], it was again found that the voltage levels in the distribution network were reduced when the DG units were disconnected. Voltage changes (on disconnection of the DG units) were highest in the substations that were close to the DG unit and with lower loads. However, this increase in voltage levels can lead to overloading of the line which was observed in [10] and [11]. This increase in line voltage could result in expensive voltage correction steps [13]. In brief, the increasing penetration of DG caused increased fault current infiltration, larger risk to protection systems such as failures in relays and circuit breakers, and lower sensitivity for detection of fault. As already discussed, the intermittent behaviour also led to imbalance and as a result the DGs might not be able to provide the required power for regulation without the presence of storage devices. Authors in [13] provide an exhaustive review of various issues caused by the PV systems in distributed generation.

One of the key contributors to CO_2 emissions is the transport sector. In Q3 of 2019, the transportation sector accounted for 17.3 % of the total emissions [14]. As one of the policies implemented to meet the 2050 EU goals, the Dutch government announces a plant to ban sales of new fossil fuel powered vehicles [15]. Infact, the city of Amsterdam has also planned to outright ban polluting fossil fuel powered vehicles [16]. This has led to an increase in the number of EVs (Electric Vehicles) in the Netherlands. As of February 2019, there are 202,624 EVs (all the types) registered in the Netherlands and this number has been increasing rapidly ,from 151,752 in 2016 [17], [18]. This increase in the number of EVs has led increase the electricity consumption from the grid.

When the number of large loads like EVs increase in the grid, problems such as congestion occur [19]. This happens due to the fact that the users would try to charge their EVs, which is a large load, during the hours with lower tariffs. With significantly large number of EVs and increased penetration of DERs (Distributed Energy Sources), congestion problems are just going to increase. DSOs in the Netherlands have been facing congestion issues in their distribution networks which occur due to a result of increasing number of EVs and home energy generation [20], [21]. In [22], the authors add increasing number of EVs to the existining grid networks in the UK to determine their effects on the grid. Under their uncontrolled charging scenario, the authors in [22] assumed that there are no incentives for DSM. This was also observed to be the current scenario in the Netherlands as technologies such as V2G are relatively expensive. In [22], under uncontrolled charging, it was observed that in the local grid, the peak load increased by 18% when the EVs got back from the work trip (at 18:00). This increase would lead to the overloading of the grid and lead to increase in costs due to damage to components. When the charging of EVs was pushed to off peak hours, the peak demand just moved from 18:00 to the off peak hour (which was set at 01:00). When the effect of EV loading on voltage profile was tested, similar observations were observed as well. When the EV penetration rose by 30%, the grid voltage limits for low voltage distribution grids were exceeded.

Going carbon neutral would also require moving away from conventional natural gas powered heating systems to electric heat pumps. The number of open air heat pumps has increased in the Netherlands in the recent years and statistics also show how much energy from fossil fuel can be avoided by switching to heat pumps. It is estimated that in 2017, almost nine hundred tera joules of energy from fossil fuel was avoided. The amount of energy consumed by the open air heat pumps is two percent of the total renewable energy [23]. In [24], the authors try to determine the effects of distributed heat pumps and micro Combined Heat Pumps (CHP) on the grid. The authors try to create models which can replicate the effects of the heat pumps. This was done by measuring the the data pertaining to heat pumps and understanding what parameters affect the load profile of the heat pumps. They determined that the heat demand is directly related to the total heat demand of the household, the outside temperature, the type of the household, and the individual preferences. Larger the number of heat pumps in the grid, higher the demand. Similar effects observed under the increasing presence of EV were observed when the number of heat pumps increased. The authors determined that heating demand would be larger for the case of space heating compared to heating demand for hot water. For space heating, heat pump had to supply higher power for a longer duration while for water heating, the duration was fairly low [24].

However, these mentioned issues in the grid could be solved by efficient use of the energy sources along with energy storage and incentivizing certain required behaviour through market mechanisms.

2.3. Proposals to prevent grid issues by using market mechanisms

In [6], the authors proposed trading power instead of energy in the markets to prevent momentary imbalances within a particular PTU. However this market is based on the transmission level and for large producers and prosumers are not considered in this work. As discussed, the imbalances caused by the increasing penetration of the renewable generation leads to increasing costs in the ancillary services market. Analysis of the retail market in the Netherlands by the authors of [2] showed that the price increases in the wholesale market are usually passed on to the consumers faster than price decreases. Thus, if the costs to the suppliers go up due to the increasing number of the renewables in the grid, the costs for the consumers might also inevitably rise. Another conclusion from [2] is that the competition in the Dutch retail energy market is quite high which is determined from the number of "green products" which are available for the consumers to choose from. Green products are different energy products offered by energy suppliers to the consumers which have ori-

gins from renewable energy sources such as wind or solar farms. Additionally, energy suppliers also offer the consumers a product which allows them to use energy produced by distributed energy sources such as solar panels which have been installed on a large roof in a neighbourhood [25].

Since the current energy markets were not designed for a high penetration of renewables, they need modifications which can be in the form of additional storage mechanisms or flexibility mechanisms such as demand response. It should also be noted that these mechanisms are able to alleviate energy scarcity for only a short duration of time. In other words, for a system with high renewable penetration, the energy output depends significantly on the weather conditions. For example, for a system with high solar and wind energy penetration, when the solar output is low and the wind availability is almost zero, in the absence of controllable power plants or battery storage, the prices of energy can increase drastically [26]. Moreover, this does not give a good idea of investment in the storage systems on a transmission level because such energy shortages might be rare and it would not be feasible for different stakeholders to invest in assets that might be used for a very few hours a year. [26] Additionally, in all these cases, ancillary markets are needed to ensure the safe operation of the power grid. In the Netherlands, the ancillary services are also provided via the ancillary markets. The ancillary market is set up by the TSO, TenneT TSO B.V. and involves all the balance service parties (BSP).

To prevent the high prices during scarcities, different capacity mechanisms would be necessary. Broadly speaking these mechanisms can be either price based or volume based [27]. This means either changing the prices to influence the energy demand or supplying the required energy demand without changing the prices. Volume based mechanisms include running old power plants as reserve. These are also called as mothball plants and are mainly used in countries such as Sweden, Poland and Belgium. These power plants are activated in times of scarcity [27]. But this is not in line with the EU 2050 goals mentioned above since these plants are conventional power plants and thus conflict with the goals of complete de-carbonization in the fields of energy generation. Price based capacity mechanisms include capacity payments which are pre-determined fees that are paid by the regulator (TSO) to capacity providers [27]. This can, however, be complicated as it requires accurately predicting the necessary capacity and fees are pre-determined which may lead to disproportionate payments.

2.3.1. Incentives for distributed generation

As observed from the EU climate goals of 2030 and 2050, there needs to be reduction in carbon emissions and a requirement to go carbon neutral. To achieve these goals, it is pertinent for the share of renewable energy sources to increase in the energy production.

Countries in the EU have various support mechanisms for the promotion of renewables, both for large suppliers and prosumers. The support schemes in the Netherlands include feed-in tariffs, net metering, loans at lower interest (for projects except biomass) and tax benefits [28] [29]. Net metering was also an option available for small consumers who have the connection size of up to 3x80A (3 phase, 80 A total). Net metering meant that the remuneration that was obtained by the residents for feeding-in the energy to grid was equal to the retail price that they paid. However, net-metering was not considered suitable for many reasons. Some of which are:

- This approach in reality is a subsidy to those who were capable of investing in small-scale generation. Consumer that cannot invest (e.g. because they have no available area for PV or lack financial resources.) miss out on this subsidy and does not lead to reduction of costs for them.
- Households avoid taxes and levies and in many cases also network charges when their electricity injections to the grid are netted with their electricity withdrawals. This is an implicit subsidy that may be unreasonably high and may lead to grid defection.
- Net-metering ignores the time value of electricity in case of static prices. This means that the households receive the same remuneration when they sell during a surplus of renewables in the grid and when there is scarcity. So when the number of fossil fuel powered plants reduce and the prices vary depending on renewables, this will still lead to unfair remuneration to the households which have PV systems installed. [26]

As mentioned, large suppliers are incentivized to invest in renewable sources of energy by the use of subsidies. The subsidy programme that is made available in the Netherlands was the SDE+ subsidy programme which was changed to SDE++. Under this scheme, the large energy producers can apply for generation compensation when they produce energy from renewable sources. The government allots a fixed base amount for a project. Generators whose generation costs are larger than or equal to the base amount are eligible for the subsidy. However it is unclear how the subsidy is going to change after 2020. [30] SDE+ subsidy at its core is a feed-in tariff (FIT) which has been used by countries across the EU to stimulate the renewable energy generation. FIT are the amount that are received when the energy generated by renewables is fed in to the grid. This subsidy is designed to remunerate the large producers for the costs incurred while generating electricity as well as a guarantee that the energy generated will be paid for. [30]

Based on the remuneration policy, the feed-in tariffs can be classified as market-dependent and market-independent [31]. Market independent FIT do not get affected by the market prices. Irrespective of the wholesale prices, the producers get the same levels of remuneration. These FIT can also be termed as static FIT. The static FIT is independent of changes in inflation, retail price changes and changes in Levelised Cost of Electricity (LCOE) of generation. This independence of FIT from the market prices can lead to high costs to the government if the retail costs or generation costs decrease. But it may also lead to high costs to the energy producers if the retail prices rise and the FIT has been set at low levels.

The Netherlands uses the spot market gap model. In this model, the FIT is set by the government and the revenues of the generators is the difference between the spot price and the feed-in tariff. However, if the retail prices rise above the FIT, the costs are not passed on to the customers, but the producers are rather paid by the government subsidy. [31]

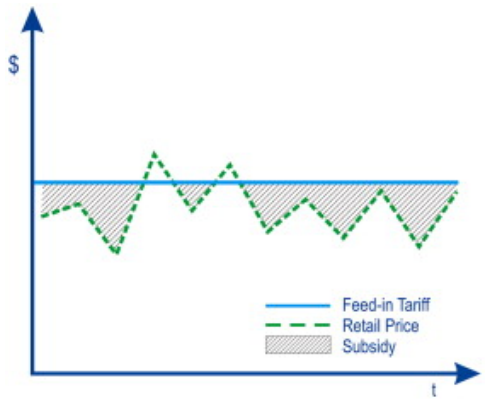

Figure 2.1: Market-independent FIT: Spot Market Gap Model [31]

Market dependent FIT policies get affected by the market prices. The changes in the market prices and the renewable energy generation are reflected in the changes in the FIT that might be obtained. At the same time the dependency on the market prices make it so that the producers are more exposed to the price risks and do not make disproportionate profits.

A market dependant FIT model that was used in Germany, Denmark and Spain is the percentage of the retail price model. Under this policy, the FIT is fixed at a certain percentage of the retail price and the suppliers get remunerated the amount proportional to the retail price depending upon the set percentage. This may vary from 80% to 575% depending upon the technology's costs[31]. These FIT are relevant to large producers but a similar structure can be applied for the producers at distribution level as well.

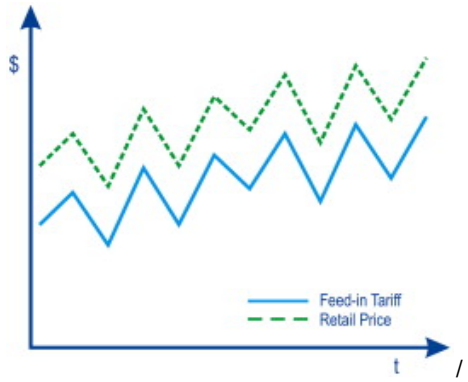

Figure 2.2: Market-dependent FIT: Percent of retail price

However, these policies have been used for remuneration for large suppliers. The policies mentioned can also be scaled to be used at the distribution level rather than only at the transmission level where the suppliers operate. To incentivize consumers to install solar panels at their houses, for example, FIT can be very effective. Furthermore, the disadvantages of net-metering were discussed which make FIT comparatively more appealing.

There can be significant impact of FIT in the distribution grid as well. Since the number of distributed energy installations would rise under the influence of FIT, the issues discussed in section 2.2 still remain relevant. Depending on the level of FIT, the power level of different households might also vary. Furthermore, the revenue which could be generated under the presence of FIT could also lead to variations in system size. The effects of FIT on power flow and system size were discussed in this research. The FIT used in this research were considered to be market dependent and varying in time.

Research has been done on how prosumers can be better aligned with the wholesale market to increase their PV self-consumption. This alignment is necessary because the wholesale prices are a good indicator of the energy availability. Lower wholesale prices can signify excess generation or low demand and higher prices signify shortage in generation or excess in demand. Authors of [32] conclude that the self-consumption of generated PV increases when prosumers are exposed to the wholesale price. In their modelling, they have added a cost component to the wholesale price to reflect retail prices. The retail price, related to the wholesale price is determined as shown in equation 2.1.

$$P_{electricity}(t) = P_{wholesale}(t) + c \tag{2.1}$$

Where $P_{wholesale}(t)$ is the wholesale price of electricity at that instant and c is a constant associated with the additional fee (administrative and service) that is associated with acquiring electricity. The constant ,c is calculated by 2.2 which is:

$$c = \frac{P_{electricityAcq} \cdot \sum_{t=1}^{T} - P_{wholesale}(t).\lambda(t)}{\sum_{t=1}^{T} \lambda(t)} \tag{2.2}$$

Where $P_{electricityAcq}$ was the component of the electricity bill allocated for electricity acquirement and λ was the hourly load. It should be noted that when using this equation, the consumer with a PV system installed will pay the same price as a consumer without, based on the hourly load.

The dynamic retail prices are interesting because the retail suppliers in the Netherlands do not offer purely dynamic prices or purely static prices. The prices, depending on the supplier, have two levels: Peak prices and off-peak prices[33]. These can also be called as Time of Use prices (ToU). ToU prices used in this work are represented in table 2.1. Real time pricing (RTP) vary in time and the prices can be different for each time instance. RTP is comparatively better than static retail prices and can be helpful for aggregators to avoid grid congestion[34].

Table 2.1: Time of Use tariffs in the Netherlands [33]

Tariff Type	Time	Value (euros/kWh)
Peak	9-20	0.2202
Off-Peak	0-9, 20-24	0.2062
Feed-in	0-24	0.092

Moreover, RTP also gives the opportunities for aggregators for peak shaving which can be desirable with increasing distributed generation and increase in loads such as electric vehicles. Despite the economic incentives, it is also necessary to avoid large power peaks in the distribution grid for stability. In [35], the authors discuss why dynamic and capacity tariffs are necessary. They argue that with the increasing penetration of renewable energy in the distribution grid and the increasing electricity usage for services such as transportation, there are load peaks which can cause blackouts if not regulated. In such cases, either grid expansion or incentivizing demand side response becomes necessary. But grid expansion is very costly and can result in sub-optimal solutions which can further exacerbate the problems.

In [32], the authors provide the mathematical expressions for calculation of FIT and the RP. However, the authors do not consider the presence of EV at prosumer households. The load in their work was determined to be the sum of the demands of the household. They also assumed that this demand was known and would not vary. However, in the future, the prosumer households would also contain loads which arise as result of electrification of transport and heating. These demands due to the EV and heat pump are larger than the household demands and as a result, the equations for retail price and FIT presented in [32] were not used.

2.3.2. Market mechanisms for grid stability and congestion management

Authors of [35] say that the grid expansion depends upon the peaks that are experienced. But if the peaks can be reduced by shifting loads, unnecessary costs can be avoided. They give the example of Australian power networks where in between 2009 and 2013, $17.6 billion was invested, but $ 7.8 billion could have been avoided by implementing dynamic tariffs. However, the paper does not provide any mathematical equations to determine the dynamic tariffs that are used. Instead, it comments on the acceptance of such tariffs by using the fairness as an argument. It concludes that transport and capacity charges, i.e, charges either based on energy consumed (euros/kWh) or charges based on capacity consumed (euros/kW), are more likely to be accepted by the public.

As discussed, using dynamic tariffs can lead to significant savings and avoids unnecessary costs which means that grid expansion costs are significantly reduced. Another potential solution that can be used for preventing grid congestion and prospective issues is provided in [36]. Authors of this research come up with a linear model of the Low Voltage (LV) network and then plug it to a community battery which is placed at the local feeder level. A linear model is chosen because the X/R ratio in the distribution grids (LV grids) are comparatively much smaller than Medium Voltage (MV) grids. X represents the imaginary part of the impedance and R the real part. This means that the LV grids are more resistive and MV grids are more inductive. The battery control in [36] is determined by linear optimization and the power supplied by the battery is to be minimized. However, this solution is not further explored as this solution was implemented on the distribution feeder level. Furthermore, this work does not comment on how the ownership of such a community battery would work. From [1], it was observed that the DSO's actions were limited due to the unbundling of energy systems in the Netherlands. This unbundling meant that the DSO cannot participate in market activites which could lead to generation of profits for the DSO. Additionally, the DSOs are not allowed to charge the consumers for acquiring new assets by changing their network costs. Distribution grids are often under the control of the DSO and as a result there are incentives to manipulate the grid to generate revenue. The regulatory challenges are not discussed in detail in this work but are relevant nonetheless.

But the increasing presence of renewable generation and EV in the distribution grid has called for reform in grid tariffs. Abdelmottelebab et. al. [37] discuss the importance of new distribution or capacity tariffs. They claimed that the current network tariffs do not ensure cost recovery for the DSO and are not incentivizing the consumers to use their network more efficiently. They also mentioned that the scenario where the consumers are not just a passive agent (just consuming from grid) but transitioning towards being active agents (gener-

ating energy and supplying it back) requires reshaping of the distribution tariffs. The prosumers do not just use the network to consume energy from the grid but also feed energy back to the grid and as a result, the usage of network increased. With these reasoning, they mention that new capacity tariff (with the unit of €/kW) would become necessary for maximizing the efficiency of network consumption and minimizing the costs to the consumers. To do so, they proposed a network charge consisting of two different network components. These components were the peak coincidence network charge and the fixed charge. The peak coincidence network charge was a forward charge which took into account the costs required to reinforce the grid during peak hours of the network utilization. This utilization depended on the consumer's consumption behaviour. A minimum base tariff was set so that the consumers could not avoid the grid costs if they installed their own generation systems. Fixed charges depended on the size of the capacity required by the household and they varied based on the maximum limit. Fixed charges also consisted of the residual costs which were not included in the peak coincidence network tariff (such as taxes). However, they do not conclude with actual recommended tariffs but rather provide information about the economic advantage.

In [38], the authors discussed certain challenges that the DSOs across Western Europe are facing with regard to effects of energy transition on the distribution grid. They discuss the importance of the power tariffs and provide insights on how to optimally design the tariffs from the DSO perspective to minimize the losses. But no specific methods to design tariffs were proposed but rather an argument for the necessity of regulatory changes were provided. In [39], the authors also reached to the conclusion that the majority of the issues caused by the renewable energy sources and electric loads would affect the distribution grid. They determine the effectiveness of tariff based demand response (DR) by using different tariffs. The authors in [39] concluded that peak shaving reduced the financial losses and reduced the investment costs. But they also state that further investments in the grid would be driven by the peak demand. However, they do not perform grid simulations but rather discuss the differences between various tariffs. They conclude by stating that reforms in grid tariffs are necessary and that the design of efficient tariffs needs more research.

Steen et. al. in [40] determine the effects of different kinds of grid tariffs on the distribution grid with the help of DR consumers. They consider dynamic energy prices, or energy based tariffs (EBT, €/kWh) and power based tariffs (PBT, €/kW). The dynamic energy prices were based on the Swedish day ahead market where consumers have the option to switch to dynamic retail prices. The authors designed a mixed integer linear program (MILP) which minimized the energy costs of 100 residential consumers. The results showed that PBT were able to reduce the total costs of consumers by €127 per year. Dynamic EBT were also able to reduce the total costs, but a reduction of only €119 was observed. They also concluded that if all the consumers were price responsive, there was a reduction in peak demand by 4%. However, when the EVs were added to the grid, there was a significant increase in grid power losses observed under EBT. Steen et. al. showed the advantages of using PBT over EBT on a grid level. But they do not discuss how this price should be designed and use the available local DSO price. Furthermore, the authors also do not consider the impact of the PV systems on the power generation profile. It was observed in literature that the increasing penetration of PV also lead to increasing voltage fluctuations.

As mentioned in [26], capacity subscriptions can be very effective in preventing energy scarcities and preventing loss of energy during the time of one. This mechanism was proposed to be implemented by the use of a simple load limiting device (LLD) which can be under the control of the DSO. The LLD limits the power to a subscribed level during the time of scarcity. However, it can be tricky to choose the correct level of power subscription. The selection of the subscribed capacity is interesting, as mentioned before, because it makes the energy reliability a priced service. Based upon the willingness-to-pay of the consumers (WTP), the reliability can be identified. WTP shows how much a consumer is willing to pay in order to avoid a complete loss of power during a scarcity. Thus, during an outage or a scarcity, a larger WTP would lead to a higher subscription which makes the reliability a priced service.

The concept of capacity subscription was first proposed in [41] where Doorman used capacity tariff to reduce the peak demands in the distribution grid. They concluded that capacity subscription was a self-rationing scheme which could lead to reduction in grid power peak as the consumers would be able to anticipate their peak demand. With the knowledge of their peak consumption, the consumers have the choice to shift their loads or to reduce their consumption.

Using power subscription was a good way to ensure that all the power levels within a network are always in desirable ranges. From a customer perspective, it is desirable to always have the amount of power that is actually required. Different power levels can be priced differently and a surcharge is applied when one exceeds the power-level that a household is subscribed to. In [42], the authors discuss the capacity subscription that is now in place in Norway. The authors consider three different scenarios. They are enumerated as follows:

- **Static Capacity tariff:** Under this scheme, the households pay a static capacity price per kilo-watt. As long as the consumption is below the subscribed power levels, the cost of energy is low. But once the consumption goes above the subscribed level, the cost of energy rises quickly. Authors of [42] suggest this price increases can be roughly 10 to 20 times higher than the normal price. No LLDs are being used in this scenario, but HEM systems can be, technically, used for load control and preventing increased usage.
- **Dynamic Capacity tariff:** Dynamic capacity tariffs are introduced in [41]. They are further explored in [42] as an alternative to static capacity tariff but only during the cases when there is an actual shortage of energy. As mentioned, the optimal capacity to be subscribed is difficult to estimate because factors such as lost load and willingness-to-pay should also be considered. The main difference between static and dynamic capacity tariff is that the excess costs are zero during the scarcity. This is because the LLDs are activated during the shortage.
- **Dynamic Capacity tariff with flex:** The main difference between the dynamic capacity tariff and dynamic capacity tariff with flex is the presence of battery storage device which is able to provide flexibility. In the absence of flexibility device, the household will lose the access to power and the DSOs/utility companies would be required to pay a penalty equal to the value of the lost load (VoLL). However, this can be avoided by the presence of battery which the consumer uses during the time of shortage.

The pricing equation used in [42] is shown in equation 2.3

$$C_{tot} = C_{fixed} + C_p \cdot P_{sub} + C_{en} \cdot (W - W_{ex}) + C_{ex} \cdot W_{ex} \tag{2.3}$$

In the equation, C_p denotes the cost of the power subscription, which is $€/kW$ and C_{en} is the energy price which is in $€/kWh$. W, W_{ex} denote the annual demand and the annual excess demand respectively. C_{ex} is the extra cost per kW that the consumers need to pay when the subscribed power capacity levels are exceeded. Since this cost is significantly higher than C_p, the consumers have the incentive to keep the consumption within the subscribed limit.

The main advantage of this capacity subscription from the literature is understood to be that having a power capacity subscription leads to optimal usage of the network. By this, capacity subscription also lead to prevention of scarcity and congestion in the grid. From an economical point, DSOs and the utility agencies have incentive to provide a reliable supply to the consumers based upon their subscription. However, the selection of optimal capacity is not commented upon. It was assumed in [42] and [26] that consumers are aware of their consumption and would select an optimal capacity by themselves. Furthermore, from equation 2.3, it was observed that the modified retail costs included the energy costs for extra consumption when deviating from the annual demand. This amount of energy can be particularly difficult to determine as the household loads can be quite stochastic.

A similar, modified, mechanism was used in this work to determine the effects of such a capacity tariff on the power flow for a prosumer household. The objective was to determine if capacity tariffs (euro/kW) are able to reduce the peak grid power consumed from and fed back to the grid.

2.3.3. Ancillary services: Frequency Regulation

Under the problems in the current market, imbalance markets were also discussed. Imbalance markets are relevant for the grid to maintain the supply and demand equilibrium. Maintaining the supply and demand equilibrium in the grid is necessary for its optimal operation. If this equilibrium is not maintained, there are chances that the consumers might lose access to their energy supply. Since maintaining the equilibrium is an essential service for its operation, it is termed as ancillary service. The markets where such services are

traded are termed as ancillary service market. Traditionally, there was only requirement to operate the frequency regulation market to maintain the grid frequency at the nominal value. However, with the increasing presence of distributed energy generation and presence of large loads such as EV, flexibility services have also become prominent [43][44]. However, the frequency regulation market is still expected to be prominent in the future.

Frequency regulation is the process by which the grid frequency is maintained at 50 Hz. The method employed to ensure the grid frequency remains at 50 Hz is called frequency control. In the event of an disturbance, the frequency deviates from the nominal value. This deviation of frequency from the nominal value of 50 Hz is termed as frequency imbalance. It can be defined by:

$$\Delta f = f - f_{nom} \tag{2.4}$$

Frequency control is necessary to ensure that the grid frequency remains stable. Frequency is directly related to energy produced by the synchronous generators via the equation

$$K = \frac{1}{2} J\omega^2 = 2 \cdot \pi^2 \cdot J^2 \cdot f^2 \tag{2.5}$$

Here K is the kinetic energy produced by the generator[J], J is the combined moment of inertia of the generator and turbine [$Kg.m^2$], ω the angular speed[rad/s] and f is the frequency [Hz].

From eq 2.5, it can be seen that the K kinetic energy produced is affected by the changing speed and frequency. Thus, a constant frequency is necessary to supply power at a high quality (constant voltage and frequency). Since the load in the system varies continuously, it essential to maintain the frequency at the nominal value to ensure the security of supply. The security of supply is also one of the goals of the TSO (Transmission System Operator) in the Netherlands [45]. Another key objective of the TSO is to ensure the balance of supply and demand of electricity. Since storing electricity in large quantities is expensive, balancing supply and demand must be done in real-time. This power balance is critical because if the balance is not maintained and a sudden change in load occurs, blackouts may occur as a consequence [46] [47] [48].

As mentioned, the power balance in the grid is maintained by frequency control. If the frequency of the grid goes below 50 Hz, the frequency has to be increased, and if it exceeds 50 Hz, the frequency has to be reduced. When the frequency increases, the power in the grid also increases, and conversely, when the frequency decreases, the power reduces as well. Additional load is necessary to solve the problem of increased frequency, and to solve the issue of under frequency, energy needs to be fed back to the grid. In the Netherlands, the TSO, along with grid balancing parties, is responsible for the frequency regulation and maintains the grid balance.

There are three kinds of frequency control. They are classified based on the time it takes to respond to an imbalance in the grid. They are:

- Primary frequency control
- Secondary frequency control
- Tertiary frequency control

Primary frequency control occurs within seconds of an imbalance and traditionally involved response from the speed governor of a machine. An example of primary frequency control is prime mover control of the generator, which acts as feedback and helps control the speed and frequency. When a disturbance occurs, primary control initiates to restore the balance between the supply and the demand. However, if the change in the frequency caused by the imbalance is too large and exceeds the permissible limits ($> \pm 200 mHz$), contingency measures such as load shedding are required to maintain the system stability [49]. Primary control depends on the reserves (both load and supply) provided to the TSO. When the imbalance is noticed, the primary controllers (of the generators obliged to provide primary control) will alter the output power until a balance is reached. However, the frequency after this equilibrium is attained will not be equal to the nominal grid frequency. This occurs due to the droop effect of the generators and is called the quasi-steady operation.

This operation is termed as quasi-steady-state. This Quasi-steady operation is shown in figure 2.3. The generators delivering primary supply together for an area are called primary control reserve or frequency control reserve, which has a maximum 3000 MW size. For deviations that lead to a change of 3000 MW of power, the entire reserve is obligated to supply primary frequency control. [49]

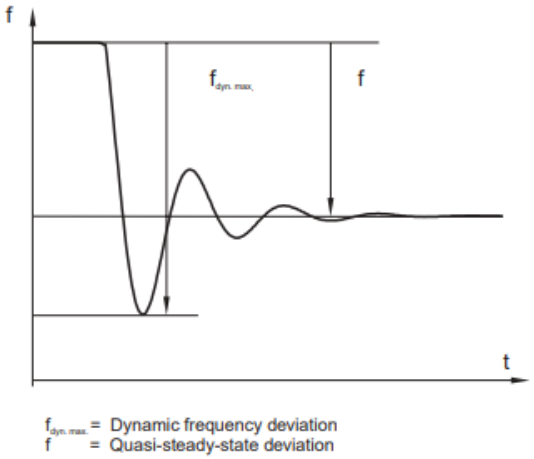

Figure 2.3: Quasi Steady Operation under primary control ([49])

Secondary frequency control is spread over the area where the imbalance occurs. Secondary frequency control occurs 15-30 minutes after the primary frequency control. It takes over the remaining frequency regulation and brings it back to the nominal level. Thus, the function of secondary frequency control is to restore the frequency to 50 Hz. Secondary control also allows the restoration of primary control reserves and the secondary reserves are separate from primary reserves. According to ENTSO-E, secondary regulation may not impair the functioning of primary control. It allows the area to absorb the changes in the load and restores the interconnections between two regions. Tertiary frequency control occurs after primary and secondary frequency control reserves are activated. Tertiary control is equated to the desired optimal performance of each generating unit or the normal functioning of generators. Figure 2.4 shows the order along with the time duration between primary, secondary, and tertiary frequency control. [49]

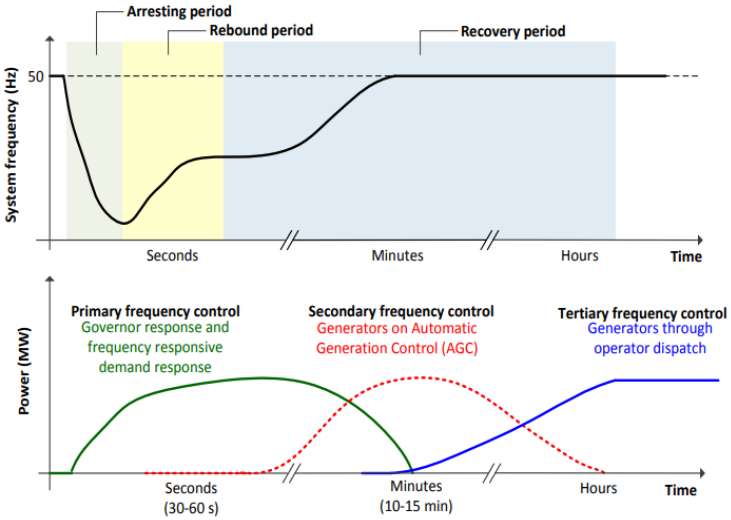

Figure 2.4: Types of frequency regulation and their time-scales [50]

Droop Control

Droop of a generator is a ratio without a dimension and is obtained by the following expression

$$S_G = \frac{-\frac{\Delta f}{f_{nom}}}{\frac{\Delta P}{P_{nom}}} \cdot 100\% \tag{2.6}$$

Here Δf is the frequency deviation from the nominal value f_{nom} whose value is 50 Hz. ΔP is the difference in power caused by the change in frequency and P_{nom} is the rated power of the generator. The contribution of the generator for frequency regulation depends on its droop.

This research mainly focuses on Frequency Containment Reserve (FCR) market. FCR market relates to the operations performed in primary frequency control. Based on the country of operation, the TSO can set up rules which are desirable for the FCR operation in that country. In Western Europe's decentralized markets, the local TSO operates a market where ancillary services such as frequency regulation are traded. In the Netherlands, the participants in this market are termed as Balancing Service Providers (BSP). The BSP enters into a contract with TenneT and agrees to provide the required regulation power in the FCR market. Once the contract is awarded, the BSP has to be continually available for the entire auction period. If a placed bid is accepted and called for FCR, the BSP should provide the regulating power. However, if the bid is accepted and is not called for, the BSP still has to ensure that the reserved power is available until the end of the auction period, which is four hours. The BSP gets paid for reserving the regulation power regardless of whether they supply the regulation power or not.

To participate in the FCR market, the BSP has to meet specific criteria explained in this section. For the contract to be awarded, the BSP needs to pass the pre-qualification tests that prove that the BSP can supply the regulation power whenever necessary. The pre-qualification tests indicate that the BSP can deliver or consume the required power during imbalance situations. Pre-qualification tests are essential because the BSP assets should have the ability to respond to changes in operating setpoints quickly. The full description of the tests can be found at [51]. The key takeaways from this test are:

- At least 50% power change proportional to the change in frequency should be supplied within 15 seconds from the beginning of the frequency step when FCR is called.
- The complete power change proportional to the frequency change should be provided within 30 seconds of the beginning of the frequency step when FCR is called
- The power change between 15 and 30 seconds should be linear after each frequency step.

These tests are performed on the assets under TenneT's supervision. For the BSP to use an asset for FCR, the asset must meet all the above requirements. It should be noted that there are additional requirements for the assets which can be found at [51].

It should also be pointed out that TenneT allows the pooling of multiple individual Reserve Providing Generators (RPGs) to make a Reserve Providing Unit (RPU). This pooling allows for various combinations of assets to be used for required regulation on either side. Here, the side means up or down. Up-regulation occurs when the grid frequency drops below the nominal value, and as a result, energy needs to be fed back to the grid. Down-regulation is the opposite of up-regulation and requires the consumption of excess power in the grid.

Devices such as BES, Combined Heat Pumps, EV batteries, etc. can be pooled together to get the regulation in the desired direction. However, TenneT deems these units as energy-limited units as they cannot continually supply energy because of their characteristic [51].

For energy-limited sources, the following rules apply:

- They must be able to supply power at the standard frequency of 50 Hz
- If a large imbalance occurs, the RPU/RPG must supply the full/contracted FCR for at least 15 minutes.
- If an imbalance of <200 mHz occurs, it should supply partial delivery for a period proportionately longer than 15 minutes.

- After supplying energy for fifteen minutes or a proportionally longer time, the installation must provide the contracted FCR within two hours.
- Unlimited energy sources such as coal or gas-powered plants should deliver for an indefinitely.

TenneT also specifies that the battery system's load management should also be documented along with characteristics related to battery ageing, self-discharge, charging limits, SoC limits, etc. Charging and discharging the battery for load management should only occur when the device does not provide FCR. This rule also means the batteries cannot be used for load management during the periods when the bids have been placed. In brief, the other operations of the battery should not hinder the energy delivery for frequency regulation [51].

At high penetrations of renewable energy sources in the grid, one of the issues that start to become prominent is related to frequency variations. Due to the intermittent nature of renewable energy sources, achieving frequency stability becomes increasingly difficult [52]. Conventional power plants such as coal and gas power plants continuously provided frequency regulation due to their nature of operation. The synchronous generators and the turbines used to generate energy can offer frequency regulation by the rotational inertia. However, in recent years, conventional power plants are being decommissioned due to their comparatively large carbon emissions. Thus, methods for frequency regulation by using renewables are being researched [53], [54]. Stand-alone PV systems without storage are connected to the grid via an inverter that often have an MPPT algorithm designed to ensure optimal operation and maximum power generation by the panels. These PV systems can be de-loaded for frequency regulation. De-loading is essentially reducing operating the system below the optimal point. This operation reduces the power generated by the PV panels and can thus help in down-regulation. De-loading is a form of curtailment of energy generated by renewable power plants. Wind turbines can also be de-loaded, and two kinds of wind turbine de-loading exist; Pitch-angle control and over-speed control [53].

PV and Wind farms, when coupled with an energy storage system, along with the de-loading method, provide an additional way for frequency regulation. With the presence of storage, the power available for frequency regulation increases. It also helps reduce the effect of the intermittent energy generation behavior of renewable energy sources [53]. The increasing presence of EVs in the grid is also an essential factor affecting the total load [22]. The higher presence of EVs inevitably leads to an increase in energy consumption. This increase in load leads to issues in the grid, such as congestion, voltage issues, frequency issues, etc. However, with the development of V2G, several opportunities for using the EV battery to improve the grid performance have become available. V2G can be used to improve grid performance in the areas of grid efficiency, grid reliability, and grid security. Vehicles capable of V2G can offer active power regulation, peak shaving services, grid harmonic filtering, etc. [55].

Aggregators can operate a fleet of vehicles capable of V2G to provide ancillary services and generate revenue [56]. However, the authors also mentioned that these technologies' success in maintaining grid balance and providing ancillary services also depend on the development and standardization of smart grid concepts. Communication between various grid elements needs to be standardized, infrastructure development should happen to allow for future developments and provisions for services. There should be coordination between parties that offer grid services with the DSO/TSO [56]. Various research has been performed where EV, along with PV, has been optimized to increase self-consumption by the prosumers and provide grid balancing services whenever possible [57], [58], [59]. In [57], authors propose an energy management system that integrates EVs with the grid by considering the EV battery as an energy storage system that can supply the energy when the PV is unavailable. The EV charges itself by PV power whenever available and uses the grid when PV is unavailable. The EMS also reduces unexpected peak demand and helps in implementing V2G applications to improve stability. The EV battery can also be used to supply energy when there is a loss of grid power, potentially used to provide power for regulation.

The authors in [57] also proposed that EV and PV's detrimental effects can be reduced if these can be used for frequency regulation and grid balancing. They showed that with a co-ordinated EV charging, extra flexibility could be achieved in the distribution grid. The load flow simulations showed that significant improvement in grid voltage and frequency was observed when the PV inverters and EV were used for load balancing in a co-ordinated manner. In [60], authors present a multi-period optimization problem that minimizes the EV

charging costs to consumers. This optimization is done by implementing centralized control, which focuses on controlling the rate and times over which EVs charge. They conclude that with the rolling optimization method implemented, the charging costs reduced, and the costly network expansions can be deferred. Furthermore, they also conclude that with co-ordinated charging, the costs to both the system operator and the consumers also reduce as grid issues can be prevented. However, they also mention that considerable improvements in error forecasting are necessary to fully deliver the power required by the consumers.

Increasing communication developments between various devices such as IoT and the development of record-keeping technologies such as Blockchain have also benefitted ancillary service provision [61]. With IoT, assets can be controlled remotely, changing the power levels using power electronic devices and communication protocols. The information involved, which include the power delivered, can be kept track of by Blockchain. TenneT conducted a pilot study in 2017 to determine how aggregators could also supply FCR with assets such as heat pumps, EV batteries, etc. [62]. Moreover, TenneT, along with other TSOs in Italy and Switzerland, has built a platform which enables small scale asset owners to participate in energy balancing in the grid [63].

2.3.4. Home Energy Management

With the advances in technology and policy and changes in regulation, it can be assumed that the share of distributed energy generation at households, number of EVs and heat pumps are going to increase. But with this change it is necessary to determine how these new electric loads and generation capacity affect the power flows within a household. Moreover, it also becomes necessary to manage the increase in loads and the generation in an optimal manner. It has been found that a large amount of the greenhouse emissions occur by consumption of energy by buildings. They account for almost 40% of the total energy consumed in the EU [64]. This makes it necessary to reduce the carbon emissions of the building by optimal and efficient ways of energy consumption. For this purpose, Energy Management Systems (EMS) systems could be used to optimise either the cost or the energy consumption by households. They generally minimise the total cost or the total energy consumption within the limits which are set by the user. As the penetration of renewables increase in the grid, it can be more challenging for the HEMS to determine the optimal operation to meet the required outcomes [65].

In [66], the authors discuss a rule-based EMS which integrates a PV, wind farm, and a stationary battery system at a household. Their aim was to provide the energy via the battery system when the energy from the intermittent sources was not available. This would help in dispatching the renewable energy power plants as if they were conventional power plants and this was done using the pv and wind forecast. However, they do not develop a mathematical model and are focused on large energy generation which is not feasible for a prosumer household. Furthermore, the degradation of the batteries are not considered and they also do not look at the costs for the operation of the battery or the PV systems and the wind farm. Moreover, rule-based EMS models cannot accurately reduce the costs as they are not considering the future energy demand. In [67] the authors present an EMS model which used the time series data, consisting of the demand and PV generation for a locality. The EMS develops an optimal schedule for using the household appliances and storage devices (battery and thermal energy storage in this work) with an aim to minimize the costs to the consumers and minimizing the total emissions. Thus, this EMS developed a multi-optimization problem to reduce the costs and emissions by changing the consumption pattern. However, it is not always convenient to re-schedule the loads of a household as the operation of EMS should not lead to discomfort to the occupants.

Authors in [68] present an mixed integer programming problem to minimze the charging costs of the EV. Based on the user preferences, they described three different charging schemes. They consider a charging station equipped with a PV system to charge the EV. Simulation was done for different months and they determined that when the EV users are responsive to the price signals, the charging costs reduced. A reduction of up to 85% in charging costs was observed in summer and a reduction of 83% was observed during winter when all the consumers were considered to be responsive to price signals. However, they do not consider the battery degradation into account. They also do not consider the PV variations in demand.

2.4. Contribution from this research

In this research, the effects of the market instruments are analysed by looking at the power flows within a household and looking at the costs incurred. This was done using a smart control algorithm. The EMS model used in this project is reproduced from [69]. This model solves the NLP (Non Linear Programming) which is formulated by the different constraints that are modelled for optimal operation of PV, battery storage, EV, household loads, and heat pump. Additionally, this model also determines the degradation for the EV battery and the stationary household battery. With the determination of the degradation, associated costs were calculated for an accurate overview of the operational costs. Furthermore, this model also considered the opportunities in revenue generation by reserving power in the FCR market. This consideration was done using the generation and the storage devices available at the household which were the PV system and the batteries. For this study, it was also assumed that the EV was capable of V2G operations. Furthermore, the EMS also allowed for determining the optimal size of the system.

However this model does not consider all the market mechanisms that are going to be analysed in this paper. The price signals from such market mechanisms are going to be additionally added and then their effects are then going to be seen in the form of variations in power flows and costs. The simulation period of half a year is taken to account for the different load profiles caused by the seasonal variations. The results will then help in identifying how the costs of the household are going to vary in the future and help in determining how much investment in storage and PV is going to be necessary, as the model also determines the optimal size for PV and the battery, based upon the power flows and the load.

3

EMS Model

3.1. Introduction

In this chapter, the EMS system used for this research is discussed. This EMS has been adopted from [69]. It should be noted that the EMS smart control method used in this work was provided as a part of the FlexGrid Project (TU Delft-DCES). This EMS differs from the EMS mentioned in the literature review in the aspects that this EMS considers the BES and EV battery degradation as a part of the total system cost and minimizes it. Furthermore, PV output predictions were also made using the PV forecasting data, which have been obtained from the Dutch Meteorological Institute (KNMI). Additionally, this EMS method considers the household and the heating load as unflexible and thus, meets the demand at all times. Thus, acting as a demand-side management (DSM) tool requiring least manual intervention.

3.2. System Description

The EMS controls a multi-port controller to which PV, EV and the BES were connected. Figure 3.1 shows a representation of the system being used for this research. Heat pump was connected to the AC side of the inverter while the other components were connected on the DC side.

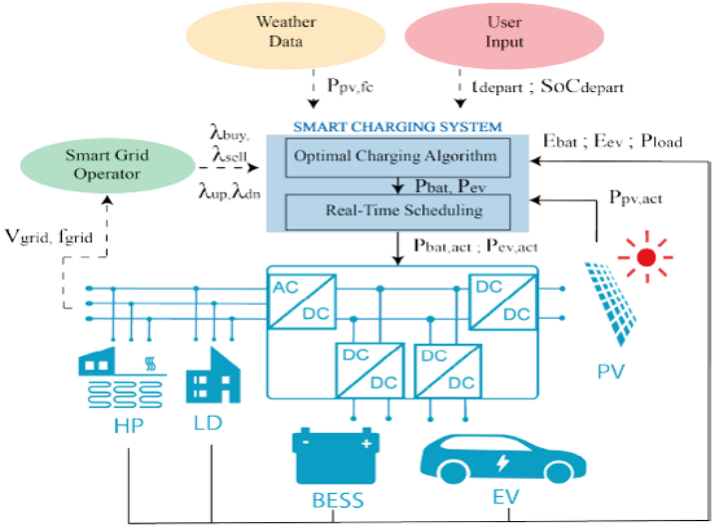

Figure 3.1: Scehmatic representation of the system [69]

Thus, the PV, EV and the BES share the same DC link which added the benefit of avoiding multiple rectifiers and thus reducing the costs. Efficiencies from individual efficiency of the component and the inverter efficiency were present on the DC link.

3.3. EMS Optimization Model

In this section, the EMS algorithm for minmizing the costs was presented. The EMS used is a Non Linear Problem (NLP) which minimizes the costs for the household. Individual components have their own constraints and so does the total system. These were described individually in this section. It should be noted that additions to the model were done over the course of this research. These additions were defined in their relevant chapters. However, the entire given EMS model was defined in this chapter and the equations and inequalities presented here remain valid throughout the work (except for the uncontrolled scenario in chapter 4). The additions should be referred in concurrence with the EMS model. This model also determines the optimal sizing of the component based on the prices. The optimal sizing has been discussed after the model was described. Additionally, the EMS is also able to determine the optimal power flow based on the inputs. This has also been discussed after the model description.

3.3.1. Objective function

The overall objective of the EMS was to minimize the total costs to the system. This was done by individually computing the costs. Equation 3.1 describes the objective function

$$min(C_{total}) = min(C_{bat} + C_{EV} + C_{PV} + C_{grid} + C_{int} + C_{inv}) \tag{3.1}$$

Here, C_{bat}, C_{EV}, C_{PV}, C_{inv} denoted the operational costs of the Battery Energy Storage (BES), Electric Vehicles (EV) and Photovoltaic (PV) system respectively. C_{grid} represents the grid cost while C_{int} were the interest costs of the components.

3.3.2. Costs involved

BES Costs

Lithium Ion batteries were considered in this study. BES operational costs signfied the value of the battery which remained after degradation caused by its use and by the passing of time. The costs were determined by determining the degradation in the BES and then subtracting it from initial capacity which are both in kWh.

Additionally, the value of the BES(V_{bat}) in €/kWh is calculated. This is relevant as the total energy that can be stored in the BES reduces, the value offered by it per kWh also reduces. This was calculated using [70]. Once the battery loses 20% of its maximum capacity, it is considered to enter its second-life. In this study, the value of the battery when it enters the second life was considered to be 50% of the original value (€/kWh). Furthermore, the BES was considered to be in its first life during the beginning of the study. The costs for BES were calculated using the equations 3.2a and 3.2b.

$$V_{bat} = \frac{V_{bat}^{2nd} - V_{bat}^{new}}{0.2} \Delta E_{bat}^{tot} + V_{bat}^{new} \tag{3.2a}$$

$$C_{bat} = V_{bat}^{new} E_{bat}^{max} - V_{bat} \left(E_{bat}^{max} - \Delta E_{bat}^{tot} \right) \tag{3.2b}$$

In 3.2b, the value used for V_{bat}^{2nd} is 0.5 times the value for V_{bat}^{new} which was assumed to be €500/kWh [71]. ΔE_{bat}^{tot} represents the total BES degradation that occurred after the simulation period. E_{bat}^{max} is the total capacity of a new battery. C_{bat} represents the operational costs of the battery which were calculated by subtracting the total remaining value from the total investment costs of a new battery.

EV operation costs

Costs for EV operation are also calculated in a similar way. However, it should be noted that costs due to driving were not considered in this study as they are not under the control of the EMS. But the costs due to V2G operation were controlled by the EMS, so those costs were considered.

$$V_{bat} = \frac{V_{EV}^{2nd} - V_{EV}^{new}}{0.2} \Delta E_{EV}^{tot} + V_{EV}^{new} \tag{3.3a}$$

$$C_{EV} = V_{EV}^{new} E_{EV}^{max} - V_{bat} \left(E_{EV}^{max} - \Delta E_{EV}^{tot} \right) \tag{3.3b}$$

The values considered for V_{EV}^{new} and V_{EV}^{2nd} were the same as that for the battery (500€/kWh and 0.5 times 500). ΔE_{EV}^{tot} represented the EV degradation after the simulation period. E_{EV}^{max} represents the total capacity of the battery in a new EV battery, and for this study, this value was assumed to be $80kWh$.

PV Costs

The investment and installation costs for PV were considered in this study. This investment cost, V_{pv} used was equal to €1350/kW_p. This value was considered to be the installation price of PV per kW_p in the Netherlands in the year 2019 [72]. The equation used to determine PV cost was:

$$C_{PV} = \frac{P_{PV}^{max} \times V_{PV}}{T_{sim} \times T_{life}} \tag{3.4}$$

T_{sim} was the number of times the simulation period fits in a year which was equal to two. T_{life} was the lifetime considered, which was fifteen years. These values for T_{life} and T_{sim} were considered to be the same for all the devices in this work. P_{PV}^{max} was the maximum PV system size which was decided by the EMS.

Grid costs

Grid costs represented the net cost for the consumption of energy from the grid and revenue generated from feeding energy back. Dynamic tariffs based on the day-ahead price of APX (from the year 2018) were used in this study. The prices were modified in a way that the average price over a period of half year was found to be €0.20. APX is the Amsterdam Power Exchange, and energy trading for the day-ahead market in the Netherlands occurs at APX.

$$C_{grid}^{buy} = \sum_{t=1}^{T} P_{grid}^{neg}(t) \times \lambda_{grid}^{buy}(t) \tag{3.5a}$$

$$C_{grid}^{sell} = \sum_{t=1}^{T} P_{grid}^{pos}(t) \times \lambda_{grid}^{sell}(t) \tag{3.5b}$$

$$C_{grid} = C_{grid}^{buy} - C_{grid}^{sell} \tag{3.5c}$$

$\lambda_{grid}^{buy}(t)$ and $\lambda_{grid}^{sell}(t)$ were the grid price for buying and feeding at that particular time step respectively. $P_{grid}^{neg}(t)$ and $P_{grid}^{pos}(t)$ are the consumption and feeding-in power at various time instances.

Inverter Costs

The inverter/converter costs were not considered to be zero in this study. The inverter costs depended on the maximum inverter power and the cost of the converter per kW. Inverter costs were determined by

$$C_{inv} = \frac{V_{inv} \times P_{inv}^{max}}{T_{sim} \times T_{life}} \tag{3.6}$$

P_{inv}^{max} was the maximum rated power of the inverter, determined by the EMS as a part of sizing. V_{inv} was the cost of the inverter per kW and was €200/kW. This was taken from [73]

Interest

Interest denotes the revenue that would have been generated had the investment in the devices were not made. These costs were also considered for the optimization. However, it was assumed that the EV was brought independently and thus, the EV interest rate was not considered. It was calculated using the following

$$C_{int} = C_{investment} \frac{ROI\%}{T_{sim}} \tag{3.7}$$

Investment costs here include the costs to purchase the BES. The investment costs for the BES were calculated in the equation 3.2b's first term ($V_{bat}^{new}.E_{bat}^{new}$), ROI is the rate of interest and was assumed to be 1%.

3.3.3. Constraints

Degradation of Li-ion battery

The degradation of the BES system was calculated by considering the degradation model provided in [74]. In order to calculate the degradation ($\Delta E_{bat}^{tot}(t)$) parameters considered for this calculation were the current of the cell ($I_{bat}^{cell}(t)$), the Ah processed at that instant ($I_{bat}^{cell}(t)\delta t$) and the cell temperature. The cell temperature was assumed to be constant at 35°C. This was done considering the variation in the temperature setpoints provided to the heat pump which varied from 18-20°C. This assumption was also assumed for the EV battery. It should also be noted that there occur differences between the degradation due to the age of the battery and due to its operation. This was differentiated by the symbols ΔE_{bat}^{cal} and ΔE_{bat}^{cycle}. The battery degradation due to age depends on its temperature, SoC, and lifetime. Since the temperature was considered to be considered to be constant, the degradation due to age was also considered to be constant for time steps. As the degradation model proposed in [74] showed the degradation of single cell, the entire battery must be scaled appropriately to determine the total degradation. This was done by determining the open circuit voltage (OCV) ($V_{oc,bat}(t)$) which was calculated as follows:

$$V_{OC\,bat}(t) = N_{bat}^{series}\left(a_1.e^{b_1 SoC_{bat}(t)} + a_2.e^{b_2 SoC_{bat}(t)} + a_3.SoC_{bat}(t)^2\right) \quad ,\forall t \tag{3.8a}$$

$$i_{bat}^{cell}(t) = \frac{P_{BES}(t)}{N_{bat}^{Parallel}.V_{OC\,bat}(t)} \quad ,\forall t \tag{3.8b}$$

a_1, a_2 and a_3 were the curve fitting parameters. These were considered to linearize the curve presented in the figure.

The curve also showed that based on the SoC, the maximum charge and discharge power also varied.

The linearizied equation for the BES OCV was obtained in the form of $y = mx + c$, determined as shown in fig 3.2 [75]. Equation was

$$V_{OC\,bat}(t) = 100(3.42 + 0.7SoC_{bat}(t)) \tag{3.9}$$

Multiplication with 100 was necessary to convert the voltage from percent to a value. The values used in the equation 3.9 were also determined by the figure 3.2 where slope (m) of the line was 0.7 and the y-intercept (c) was 3.42V.

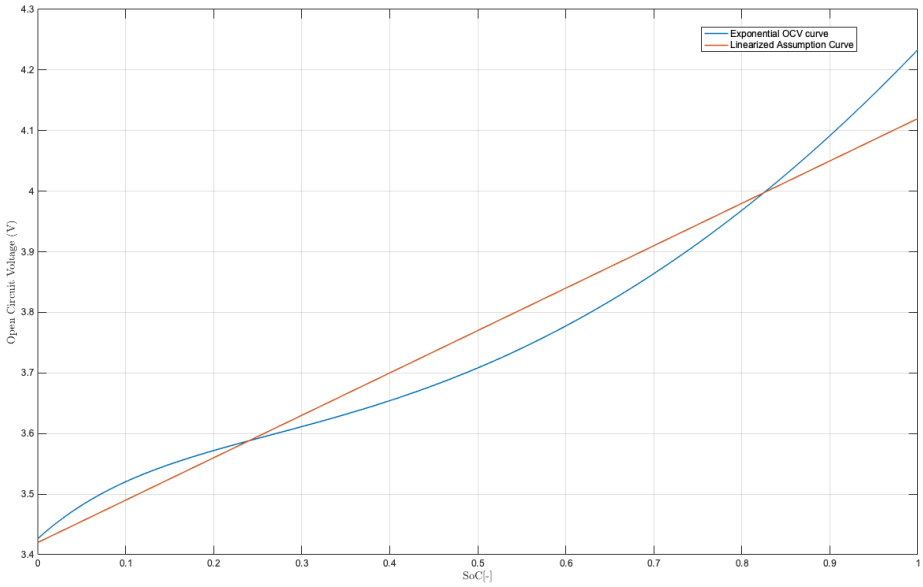

Figure 3.2: Linearized SoC vs OCV for Li-ion batteries [75]

These equations were valid for all time steps. In order to calculate the total degradation at time step t, equation 3.10c was used.

$$\Delta E_{bat}^{cycle}(t) = \left(c_1 e^{c_2 |i_{bat}^{cell}(t)|} |i_{bat}^{cell}(t)| \delta t\right) \frac{E_{bat}^{max}}{100} \quad ,\forall t \tag{3.10a}$$

$$\Delta E_{bat}^{cal}(t) = \left(c_3 \sqrt{t} e^{-24kJ/RT}\right) = (c_4 \Delta t) \frac{E_{bat}^{max}}{100} \quad ,\forall t \tag{3.10b}$$

$$\Delta E_{bat}^{tot} = \sum_{t=1}^{T} \left(\Delta E_{bat}^{cycle}(t) + \Delta E_{bat}^{cal}(t)\right) \tag{3.10c}$$

The multiplication with $\frac{E_{bat}^{max}}{100}$ was done in equations 3.10a and 3.10b in order to determine the actual degradation because the battery degradation model calculates the percentage degradation of the initial capacity.

Table 3.1: Various parameters used to determine Batt. degradation

Symbol	Quantity	Value
N_{bat}^{series}	Number of battery cells in series	100
$N_{bat}^{parallel}$	Number of battery cells in parallel	TBD
a_1	OCV curve fit parameter	3.679
a_2	OCV curve fit parameter	-0.2528
a_3	OCV curve fit parameter	0.9386
b_1	OCV curve fit parameter	-0.1101
b_2	OCV curve fit parameter	-6.829
c_1	Battery ageing curve parameter	5.4 e-3
c_2	Battery ageing curve parameter	0.35
c_3	Calendar ageing parameter	14876
c_4	Ageing averaged over time	1.86 e-4

In table 3.1, the $N_{bat}^{parallel}$ was determined by the EMS for different FIT for different size. These parameters were also used to determine the EV degradation.

BES Constraints

The power balance constraints used for the BES were then defined. The equations 3.11a to 3.11g represented the power balance within the BES. It should be noted that the power of the BES is dependent on its State of Charge (SoC) and varies linearly below a SoC of 10% and above a SoC of 80%. These regions represent the constant current/voltage operation of the BES. Additionally, the round trip of the BES was considered to be constant at 95% This led to obtaining the single-cycle efficiency of 0.975 ($0.975 = \sqrt{0.95} = \eta_{ch}, \eta dis$). This efficiency meant that the positive and negative BES power could not be zero simultaneously, or charging and discharging could not occur at the same time.

$$P_{bat}^{pos}(t) \leq P_{bat}^{max}(t) \quad ,\forall t \tag{3.11a}$$

$$P_{bat}^{max}(t) \leq P_{bat}^{rated} \quad ,\forall t \tag{3.11b}$$

$$P_{bat}^{max}(t) \leq \frac{P_{bat}^{rated}}{1 - D_{ch}} \left(\frac{E_{bat}(t)}{E_{bat}^{max}} - 1\right) \quad ,\forall t \tag{3.11c}$$

$$P_{bat}^{neg}(t) \leq P_{bat}^{min}(t) \quad ,\forall t \tag{3.11d}$$

$$P_{bat}^{min}(t) \leq P_{bat}^{rated} \quad ,\forall t \tag{3.11e}$$

$$P_{bat}^{min}(t) \leq \frac{P_{bat}^{rated}}{D_{dis}} \frac{E_{bat}(t)}{E_{bat}^{max}} \quad ,\forall t \tag{3.11f}$$

$$P_{bat}(t) = \eta_{ch} P_{bat}^{pos}(t) - \frac{1}{\eta_{dis}} P_{bat}^{neg}(t) \qquad ,\forall t \tag{3.11g}$$

In the above constraints, the superscript "max", "min", "pos", "neg" and "rated" denote the maximum allowable, minimum allowable, actual positive, actual negative and rated powers. P_{bat}^{pos} and P_{bat}^{neg} represent the charging and discharging power respectively.

The following set of equations can calculate the energy stored in the BES ($E_{bat}(t)$). The initial and final energy availability in the battery is assumed to be equal so that the costs are not skewed due to the battery's energy availability. The SoC of the BES ($SoC_{bat}(t)$)is a function of the energy available in the battery and can be calculated by the following equations.

$$E_{bat}(t) = \begin{cases} E_{bat}^{init}, & t = 1 \\ E_{bat}(t-1) + P_{bat}(t)\Delta t, & 1 \le t \le t_{final} \\ E_{bat}^{final} & t = t_{final} \end{cases} \tag{3.12}$$

Thus, E_{Ebat}^{Init} equals E_{bat}^{final} and represent the initial and the final values for the battery energy respectively.

$$SoC_{bat}(t) = \frac{E_{bat}(t)}{E_{bat}^{limit}(t)} \qquad ,\forall t \tag{3.13}$$

$$E_{bat}^{limit}(t) = \begin{cases} E_{bat}^{max}, & t = 1 \\ E_{bat}^{limit}(t-1) - \Delta E_{bat}(t) & t > 1 \end{cases} \tag{3.14a}$$

$$E_{bat}(t) \le E_{bat}^{limit}(t) \qquad ,\forall t \tag{3.14b}$$

EV Constraints

The EV battery degradation uses the same equations which are described for BES. They are represented by equations 3.8a - 3.10c

The constraints for the power balance of the EV battery were similar to the constraints and the power balance for the BES. However, an additional parameter was added, which denoted the availability of the EV at home was added. This availability factor of the EV showed whether the EV was available at home to either supply the demand or generate revenue by feeding energy back to the grid. From [76], it was observed that the EV was at the office during the hours 09:00-17:00. It was assumed to be at home for the remaining hours. Thus, it can be assumed that the EV was not available between the hours of 08:00-18:00. It was assumed that the EV battery provides a distance efficiency of $15kWh/100$km [77]. A single trip was considered to be 30 km, which leads to a reduction of $9kWh$ per trip. However, these were only estimations and might not always be true practically. $EV_{av}(t)$ shows the EV availability at any instant.

$$P_{EV}^{pos}(t) \le P_{EV}^{max}(t) \qquad ,\forall t \tag{3.15a}$$

$$P_{EV}^{max}(t) \le P_{EV}^{rated} \qquad ,\forall t \tag{3.15b}$$

$$P_{EV}^{max}(t) \le \frac{P_{EV}^{rated}}{1 - D_{ch}} \left(\frac{E_{EV}(t)}{E_{EV}^{max}} - 1 \right) \qquad ,\forall t \tag{3.15c}$$

$$P_{EV}^{neg}(t) \le P_{EV}^{min}(t) \qquad ,\forall t \tag{3.15d}$$

$$P_{EV}^{min}(t) \le P_{EV}^{rated} \qquad ,\forall t \tag{3.15e}$$

$$P_{EV}^{min}(t) \le \frac{P_{EV}^{rated}}{D_{dis}} \frac{E_{EV}(t)}{E_{EV}^{max}} \qquad ,\forall t \tag{3.15f}$$

$$P_{EV}(t) = EV_{av}(t)\left(\eta_{ch}P_{EV}^{pos}(t) - \frac{1}{\eta_{dis}}P_{EV}^{neg}(t)\right) \qquad ,\forall t \tag{3.15g}$$

SoC (SoC_{EV}) and the energy content ($E_{ev}(t)$) of the EV were also calculated similar to the BES. The user can define their preference for the available energy during departure, which ensures enough capacity was available during the use.

$$SoC_{EV}(t) = \frac{E_{EV}(t)}{E_{EV}^{limit}(t)}, \qquad ,\forall t \tag{3.16a}$$

$$E_{EV}^{limit}(t) = \begin{cases} E_{EV}^{max} & t = 1 \\ E_{EV}^{limit}(t-1)\Delta E_{EV}(t) & t > 1 \end{cases} \tag{3.16b}$$

$$E_{EV}(t) \leq E_{EV}^{limit}(t) \tag{3.16c}$$

$$E_{EV}(t) = \begin{cases} E_{EV}^{init} & t = 1 \\ E_{EV}(t-1) + (P_{EV}(t) - P_{drive}(t))\delta t & t \leq t_{depart},\ t > t_{arrive} \end{cases} \tag{3.17a}$$

$$E_{EV}(t) \geq E_{EV}^{depart}, \text{ for } t = t_{depart} \qquad ,\forall t \tag{3.17b}$$

$P_{drive}(t)$ represents the EV battery power while driving and is assumed to be constant. The value for $P_{drive}(t)$ was assumed to be 0.867 kW.

General power balance

From fig 3.1, it can be observed that two power balances exist in this system. One on the DC multi-port converter side and the other on the grid facing AC side. These balances were expressed in the equations 3.18a 3.18b.

$$P_{inv}(t) = P_{PV}(t) - P_{EV}(t) - P_{bat}(t) \qquad ,\forall t \tag{3.18a}$$

$$P_{grid}(t) = P_{inv}(t) - P_{load}(t) - P_{heat}(t) \qquad ,\forall t \tag{3.18b}$$

$P_{load}(t), P_{heat}(t)$ denote the household appliance and the heating load, respectively.

Inverter Constraints

Inverter constraints were denoted by the following equations. The inverter efficiency was assumed to be 96% [78], and the inverter power was split into positive and negative power. This was necessary to distinguish between the positive inverter power, which shows the power flow from inverter to the grid and negative power which shows the power flow from the grid to inverter.

$$P_{inv}^{neg}(t) \leq P_{inv}^{max} \qquad ,\forall t \tag{3.19a}$$

$$P_{grid}^{pos}(t) \leq P_{inv}^{max} \qquad ,\forall t \tag{3.19b}$$

$$P_{inv}(t) = \eta_{inv}P_{inv}^{pos}(t) - \frac{1}{\eta_{inv}}P_{inv}^{neg}(t) \qquad ,\forall t \tag{3.19c}$$

P_{inv}^{max} represents the maximum inverter power. $P_{inv}^{pos}(t)$ and $P_{inv}^{neg}(t)$ represent the positive and negative inverter power. Positive power represents feeding to the grid and negative power represents consumption.

Grid Constraints

Grid constraints were also modeled similar to the inverter constraints. The grid cable efficiency was assumed to be 99%. The splitting of grid power also allowed to differentiate between the grid feeding revenue and the grid consumption price. Considering the cable efficiency also ensured that $P_{grid}^{buy}(t)$ and $P_{grid}^{sell}(t)$ do not have non-zero values simultaneously. This differentiation was necessary because the buying and selling prices could be different.

$$P_{grid}^{buy}(t) \leq P_{grid}^{max} \qquad ,\forall t \tag{3.20a}$$

$$P_{grid}^{sell}(t) \leq P_{grid}^{max} \qquad ,\forall t \tag{3.20b}$$

$$P_{grid}(t) = \eta_{cable} P_{grid}^{sell}(t) - \frac{1}{\eta_{cable}} P_{grid}^{buy}(t) \qquad ,\forall t \tag{3.20c}$$

$P_{grid}^{pos}(t)$ and $P_{grid}^{neg}(t)$ represent the positive and negative grid power. Positive power represents feeding to the grid and negative power represents consumption. $P_{grid}(t)$ was the net grid power at any instance.

PV Constraints

Following constraint for the PV were used. This constraint also allowed for the curtailment of PV as a part of DSM, instances when the momentary FIT is negative, and for frequency regulation. It should also be noted that PV power can never be negative.

$$P_{PV}(t) \leq \eta_{MPPT} P_{PV}^{forecast}(t) \qquad ,\forall t \tag{3.21a}$$

$$P_{PV}(t) \geq 0 \qquad ,\forall t \tag{3.21b}$$

The efficiency of the Maximum Power Point Tracking(MPPT) algorithm (η_{MPPT}) and the converter is assumed to be 98%. The PV forecast ($P_{PV}^{forecast}$) was obtained from KNMI for the year 2018.

3.3.4. Optimal Sizing

The optimal sizing was determined by the algorithm presented by accounting for various parameters such as the retail prices and the cost of the components. In the previous section, the objective function was discussed. The resulting system for the various components were also discussed. The optimal sizing for the PV and the BES was obtained as the EMS tried to minimize the cost of operation, and as a result, the optimal power flow to reduce the costs were obtained.

For the calculation of the PV costs, equation 3.4 was considered. The LCOE of the obtained PV system size was calculated to determine whether the system size was optimal. The LCOE is the sum of the total costs of the system in its lifetime divided by the total energy supplied by it during the lifetime. Mathematically, this was represented as:

$$LCOE = \sum_{t=1}^{Life} \frac{Costs}{Energy} \tag{3.22a}$$

$$Costs = CAPEX + OPEX \tag{3.22b}$$

$$Energy = \int_0^t P_x(t)\, dt \qquad ,\forall t \tag{3.22c}$$

Where $CAPEX$ and the $OPEX$ are the capital investments and the operational cost of the system during its lifetime, respectively. Energy is defined as the product of the system power ($P_x(t)$) and time for all instances. The unit of LCOE is €/kWh.

LCOE is effective for sizing the components which do not decay over time. However, the BES, as explained, undergoes degradation. The BES operational costs C_{bat} and the remaining value of the battery V_{bat} (€/kWh) were determined in the equations 3.2a and 3.2b. As observed, these values depended on the degradation ΔE_{bat}^{tot} which was calculated in the section 3.3.3. This degradation showed that the total lifetime of the BES was not constant and was affected by the various parameters.

In this EMS, the degradation of both the EV and the BES batteries were taken into account. The costs which arose as a cause of the degradation were minimized and thereby minimizing the degradation. This allowed for the optimal operation of the BES and the EV and thus helped to prolong their lifetime. This also allowed to know the remaining capacity of the BES and EV at all instances.

3.3.5. Optimal power flow

The inputs to the EMS were the PV generation data, the hourly energy prices, user preferences in the form of time of EV departure, and SoC of the EV battery at the departure time. Based on these inputs, an optimal solution which minimized the total costs and thus generate the maximum revenue was selected. As the minimization of the costs resulted in optimal power flow, the factors contributing to the increase of the costs reduced.

3.4. Applications of the model in this work

The discussed EMS model was used in this research for determining the effects of market instruments proposed for energy transition on power flows of the household. These market mechanisms are discussed in the following chapters and the equations which denote these market mechanisms are defined in their respective chapters. However, the equations presented in this chapter remain relevant throughout this work and are always considered. Thus, the market mechanisms are built on top of this EMS model and their effects on the total system costs inadvertently affected the power flow as the EMS tries to determine the optimal power flow to minimize the costs.

The solver used to solve this optimization problem was Conopt which is a part of the Knitro solvers. The problem was solved using GAMS v26.1 on a Windows 10 operating system with a processor speed of 3.5GHz and a memory of 8GB.

3.5. Conclusion

The smart control algorithm which was be used in this work was discussed in this chapter. The algorithm used was a Non Linear Programming problem designed to minimize the total costs to the household. The various system costs considered were the operational costs of the various components, the investment costs, and the rates of interest. Equations which describe the characteristics of these devices were presented and explained. The corresponding inequalities which govern the power flow were also discussed. Device constraints, user preference and boundary conditions for the problem were also presented and commented upon.

4

Uncontrolled Scenario

4.1. Introduction

For comparing the effectiveness of any EMS on a power system, it is essential to consider how a power system behaves in the absence of the EMS. To this end, such a scenario where the power flows are uncontrolled was discussed. A system comprising the EV battery, PV system, and the inverter was considered for the uncontrolled scenario. This system was then simulated using the proposed EMS to determine its effectiveness. Half-yearly power flow for the uncontrolled system were considered. Thus, the power flow can be assumed to be an indication of seasonal variations in the load and prices. Furthermore, this uncontrolled system could also be considered as a base scenario for the residential building where the power system was assumed to be available. For the uncontrolled system, several assumptions were made as well. These were described in the methodology section. Equations relevant for this simulation were also discussed. After the methodology was discussed, the resulting power flows and the costs were explained. Finally, comments were provided.

4.2. Methodology

For the uncontrolled case, the system considered only consisted of the PV installation, EV converter, and the load. The PV installation at the building was considered to be a 30 kW_p system with an MPPT and converter efficiency of 98%. This PV installation was connected to an inverter with a maximum power of 16.4 kW. Thus, the grid feeding-in was curtailed by the inverter at a maximum value of 16.4kW. The load, as discussed, consisted of the household load and the heating load. But now, the EV is considered only to be a load as it was assumed that the EV was not capable of V2G for the uncontrolled case. The EV was assumed to charge upon arrival, and continued to charge until it was full, thus replicating uncontrolled charging behavior. Maximum power at which the EV could charge depended on the EV converter size, assumed to be 3kW. For the sake of simplicity, it was assumed that the EV always charged at this maximum rated power. Thus, under uncontrolled charging, the EV would charge always at 3kW. This charging occurred until the required set point of 50 kWh was reached. A daily discharge of 9 kWh from the driving trip was considered here as well. Thus, the EV charged with a power of 3kW for a period of three hours. The load was also assumed to be uncontrollable, i.e, not allowed to shift in time for DSM applications. Finally, it was assumed that the building does not have a stationary battery system (BES).

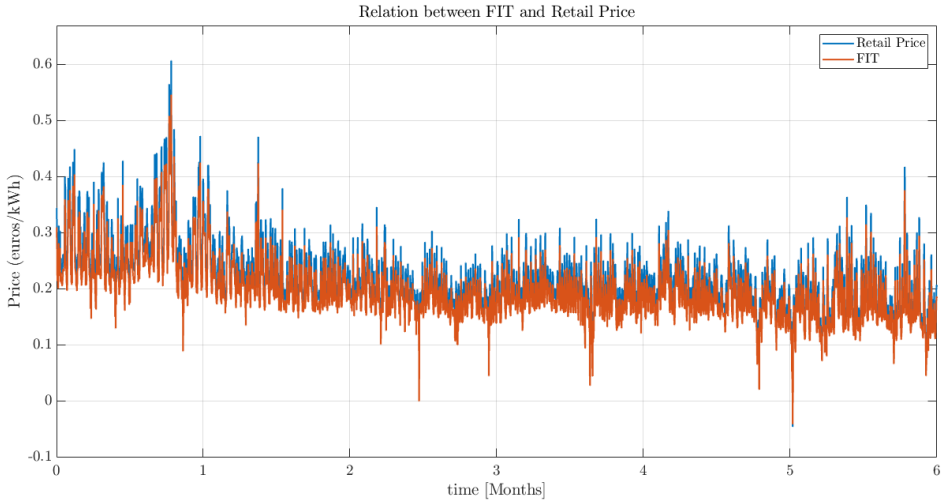

Figure 4.1: Price relation between the feeding-in tariff and the retail price (10% difference)

The associated costs to the system were the PV installation costs, Inverter costs, EV converter and degradation costs, consumption from the grid, and the revenue that would be generated under the situation when the system was feeding energy back to the grid. However, only calendar degradation of the EV battery was considered under the uncontrolled scenario. This was done for sake of simplicity. To this end, the percent difference between the retail price and the FIT was assumed to 10%. This was seen in 4.1. The retail prices assumed for this study were taken from APX for the year 2018 and were modified to reflect an average value of €0.20. The prices were dynamic in time and varied for each instance. This variation also meant that the FIT obtained at any instant varied. However, the absence of EMS meant that it was not possible to determine the optimal instances to feed energy back or consume energy from the grid. Thus, the positive energy difference after supplying the load via PV was fed back to the grid.

Table 4.1: System size for uncontrollable scenario

System Component	System Size used
Inverter (P_{inv}^{max})	16.409 kW
PV System (P_{pv}^{max})	30 kW_p
EV Converter (P_{ev}^{max})	3 kW

The relevant equations for the uncontrolled simulation were discussed as well. Grid costs were taken from equations 3.5b, 3.5a and 3.5c.

$$P_{load}^{total} = P_{load}^{appl}(t) + P_{load}^{heat}(t) + P_{load}^{EV\,Charging} \qquad \forall t \tag{4.1a}$$

$$P_{grid}(t) = P_{pv}(t) - P_{load}^{total}(t) \qquad \forall t \tag{4.1b}$$

$$P_{grid}(t) \leq P_{grid}^{max} \qquad \forall t \tag{4.1c}$$

Equation 4.1c ensures that the grid power consumption stays at a power level below the maximum grid power. In equation 4.1a, $P_{load}^{EV\,Charging}$ was considered to have a value of $3kW$. In equation 4.1b, if the resulting net grid power is positive, then it was the grid feeding power (P_{grid}^{sell}) at that instant. Otherwise, it was the grid consumption power (P_{grid}^{buy}).

$$P_{PV}(t) \leq \eta_{MPPT} P_{PV}^{forecast} \qquad , \forall t \tag{4.2a}$$

$$P_{PV}(t) \geq 0 \qquad , \forall t \tag{4.2b}$$

Where, MPPT is the maximum power point tracking algorithm designed to allow the PV operation at the max. power at that instant. PV forecast was taken from KNMI for the year 2018 and $P_{pv}(t)$ represents the PV power output at time, t.

The costs of the PV system were calculated by the equation 3.4, where P_{PV}^{max} was rated at 30 kW_p. V_{pv} was €1350/kW_p [72]. T_{sim} and T_{life} were 2 and 15, respectively, representing the times half a year fits in one year and the system's lifetime, respectively. The PV cost for the uncontrolled case was determined to be €1350

The costs related to the EV were calculated by 3.3a and 3.3b. Only calendar degradation was considered for the uncontrolled case. The EV battery degradation was calculated using the equation 3.10b. EV costs under the uncontrolled scenario were determined to be €691.27.

Inverter costs were also dependent on the maximum inverter power rating which was 16.409 kW. Costs were calculated by the equation 3.6 where V_{inv} was 200€/kW [73]. The inverter costs were determined to be €121.06.

Finally, the total cost calculated was the algebraic sum of all the costs.

4.3. Results

4.3.1. Power flow

For the uncontrolled scenario, it was observed that the load was supplied by the grid whenever PV was not available. There were no alternatives to supply the power during the instances of high costs and the power from grid was consumed at all times when the PV was not available. This led to increasing consumption from the grid and thus, the costs. This can be seen in the figure 4.2 below.

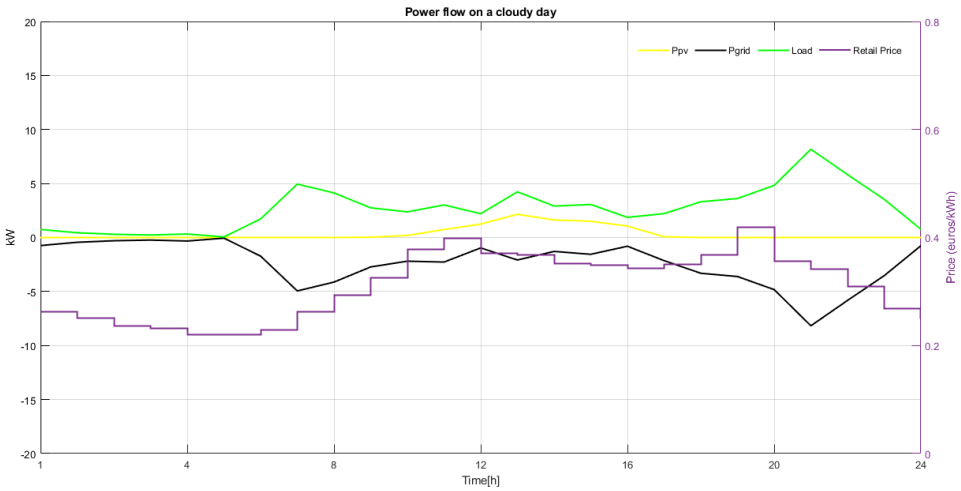

Figure 4.2: Power output of uncontrolled case on a cloudy day

On a sunny day, the PV output was large, but the load was low. This led to a significant generation in revenue during the days with high PV output and low load. This combination also helped the system generate significant revenue for offsetting the consumption costs. This can be seen in the figure 4.3 below.

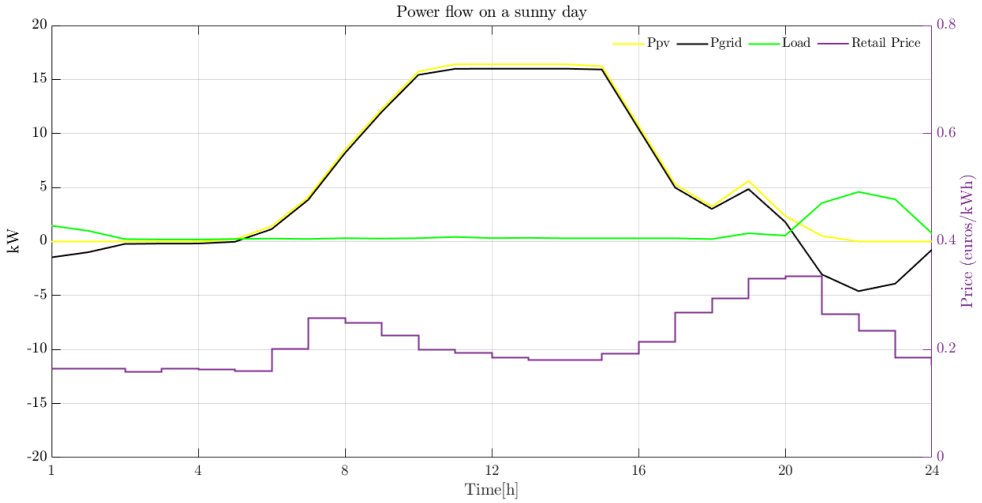

Figure 4.3: Power output of uncontrolled case on a sunny day

4.3.2. Costs

For the simulation period of 6 months, the total costs were calculated using the individual system cost components. Grid costs were negative which indicated that revenue was actually generated. The grid costs, $C_{grid}^{uncontrolled}$ were €-475.15. This revenue generation was significant and was attributed to the large PV size and the maximum allowable power for feeding in determined by the inverter size. However, the maximum PV generated could not be fed back to the grid and the excess power was curtailed as observed in 4.3. But this curtailment of power did not affect the consumption as the maximum consumption power was determined to be 9.2 kW.

The revenue generated was determined to be (C_{grid}^{sell}) €1663.5 and the consumption costs (C_{grid}^{buy}) were determined to be €1119.3. On subtracting the revenue from the costs, net revenue (C_{grid}) of €-544.203 was obtained. The PV costs(C_{pv}), as discussed, consists of the investment costs and was determined to be €1350 for a system of 30 kWp. The inverter costs (C_{inv}) were determined to be €121.06 and the PV the EV costs (C_{ev}) under uncontrolled scenario was determined to be €691.27.

The total system costs, which was calculated by adding all four cost components was determined to be a net total of ($C_{total}^{uncontrolled}$) €1618.1, for a period of 6 months. The system costs and the components have been summarized in the below table 4.2.

Table 4.2: System costs for uncontrollable scenario

Component	Cost (€)
Inverter ($C_{inv}^{uncontrolled}$)	121.060
Grid Costs ($C_{grid}^{uncontrolled}$)	-544.203
PV Costs($C_{PV}^{uncontrolled}$)	1350
EV Costs($C_{EV}^{uncontrolled}$)	691.27
Total Costs($C_{total}^{uncontrolled}$)	1618.27

4.4. Conclusion

The total system costs for a system with PV installed and uncontrolled load and EV charging was determined. The costs were determined for a PV system size of 30 kWp, inverter size of 16.40 kW and a EV converter of 3kW rated power. The revenue for feeding in was not zero and was a dynamic tariff, varying in time along with the retail price, with a 10% difference.

The total costs were determined to be €1618.27 and the total grid costs were determined to be €-544.203, which shows more energy was fed back (8.44MWh) to the grid than it was consumed (4.61 MWh). This

system size and the system costs served as the benchmark used for the cost comparison when the EMS was added to control the system, allow V2G and a BES was added. Additionally, total costs due to market mechanisms which were added in this work were also compared against this system cost.

5

Effects of FIT on system sizing and Power flow

5.1. Introduction

It was discussed that Feed-in Tariffs (FIT) have been widely used as a market mechanism. It was seen that the FIT were initially proposed to provide incentives for large suppliers to invest in renewable energy generation. But they were soon introduced for incentivizing end users to invest in their own decentralized generation. In an energy system which is getting increasingly decentralized with every year, it becomes necessary to determine the effects of supporting market mechanisms on the household power levels.

It is necessary for various actors involved in the energy ecosystem not only to determine the profits that were be made by investing in distributed generation and storage systems, but also to determine their effects on the grid power consumption, and thus, stability of the grid. Furthermore, with the analysis of power flows and exchange with the grid at different FIT, it is also possible to make an estimate as to how a prosumer household with this EMS is going to interact with the grid. Moreover, having a better understanding of the power flow also helps in determining what are some essential ancillary services that need to be prioritised. Using this knowledge, consumers can make decisions as to how to maximise their self-consumption or change their system sizing to suit their requirements. Finally, the knowledge can also be used by the system operators to help understand how prosumers with distributed generation and storage might use their network.

In this work, the analysis of FIT on the power flows and system sizing was performed using a non-linear optimization model. This model was explained in chapter 3. The optimization model is an Energy Management System (EMS) whose objective was to minimse the costs incurred by the prosumer household. The costs that have been considered were discussed in chapter 3.

5.2. Methodology

Percentage difference of retail price model was implemented where the FIT is a percentage difference of the retail price. The retail price was obtained from the day ahead market in the Netherlands (APX Prices from 2018). The wholesale prices were changed to reflect the retail price and they were designed in such a way that the average retail price over the period of simulation was 20 cents. This is the average retail cost of energy in the Netherlands. As explained, the spot market model of FIT leads to a FIT which is lower than the retail price (RP) by a certain offset (or a percent). This was seen in the figure 5.1. This percent value was varied to obtain the results for optimal sizing under different levels of FIT. Starting from a zero percent (FIT equals RP) difference to one hundred percent (FIT equals 0) in the increments of ten percent, the FIT was varied and the effects on system sizing and power flow were observed and recorded. It should be noted that the percent difference between retail price and FIT relates to the following equation

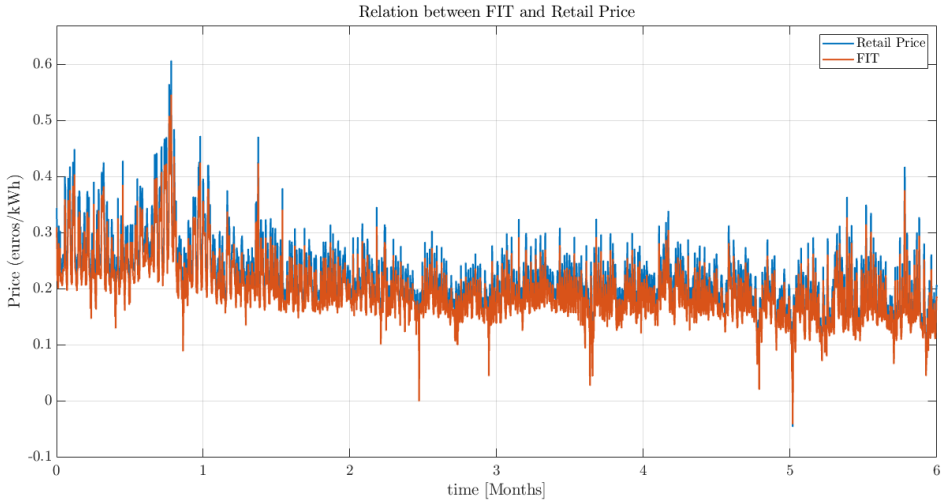

Figure 5.1: Price relation between the feeding-in tariff and the retail price (10% difference)

$$C_{grid}^{sell}(t) = C_{grid}^{buy}(t) \cdot (1 - \frac{x}{100}) \qquad ,\forall t \tag{5.1}$$

Where x is the percent difference between the prices. $C_{grid}^{sell}(t)$ represented the FIT and $C_{grid}^{buy}(t)$ reflected the RP.

The prices were one of the inputs to the optimization model along with the PV generation data, the household and the heat pump load. Optimal system sizes and power flows were obtained by running the model for different sets of prices and the results were recorded. For different iterations only the feed-in prices were varied. It should be noted that since the FIT also is dependent on retail price, with increasing difference, FIT reduced relative to retail price. In other words, when the difference increased, the revenue generation reduced and thus it can be said that the costs increased.

5.3. Results

The results of effects of different FIT on power flows within the household and the sizing of the system are presented in figure 5.2 and discussed in this section. Firstly, the effects of FIT on the BES system size and operational costs were discussed. After the comments on the BES system and costs, the effects of FIT on PV system sizing were presented and results were discussed. Finally, the effects on EV usage for V2G and EV costs are discussed. Following those discussions, conclusions are presented.

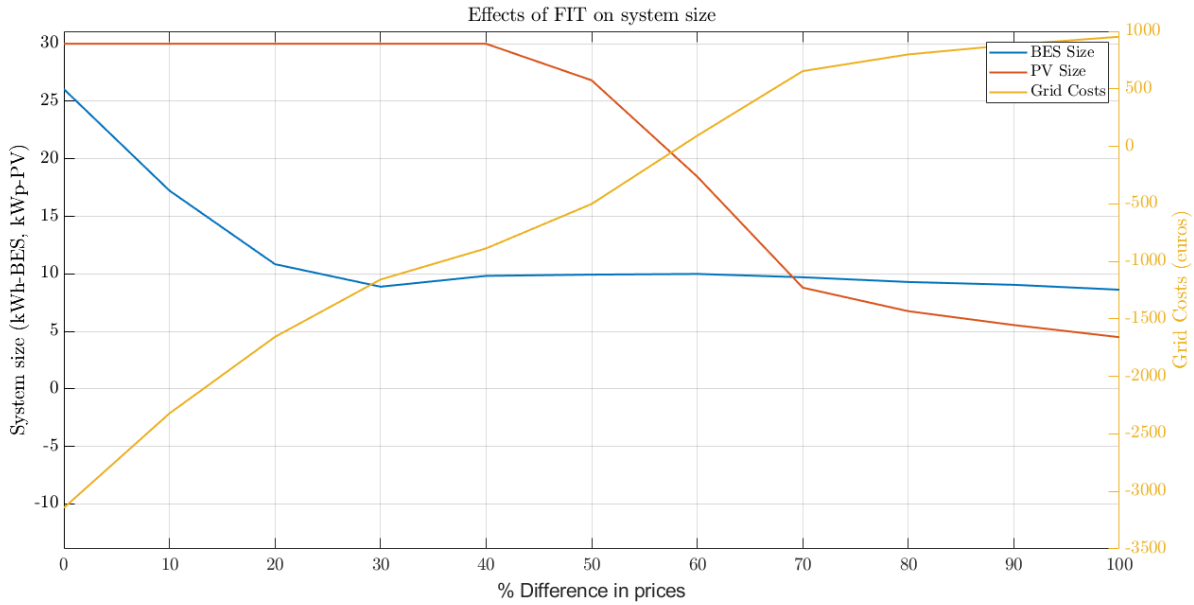

Figure 5.2: Effects of feed-in tariffs on system sizing

5.3.1. BES Sizing and Costs (E_{bat}^{max}, C_{bat})

From the plot 5.2, it was seen that the variations in feed-in tariff and the retail price have effects on the BES sizing. At large feed-in tariffs, it is noticed that the BES size (E_{bat}^{max}) is the largest at 26.05 kWh for zero difference. The values for different component sizes and the costs can be found in the table 5.1. The EMS charged the battery from the grid when the prices were low. Charging is solely done by grid consumption when the PV output was low or zero. However, when the PV output was large, the EMS also charged the BES using the energy produced by PV. This phenomenon was observed in the power flows in the figure 5.3. Table 5.1 represents the system sizing and costs for different levels of FIT.

Table 5.1: Table with sizing results for different FIT

Characteristic	0	10	20	30	40	50	60	70	80	90	100
BES Size (kWh)	26.057	17.237	10.840	8.882	9.824	9.933	9.991	9.702	9.291	9.046	8.620
BES degradation(kWh)	0.384	0.248	0.153	0.123	0.131	0.131	0.131	0.124	0.117	0.113	0.108
BES new value(€/kWh)	492.638	492.793	492.931	493.097	493.309	493.390	493.437	493.611	493.683	493.754	493.762
BES Costs (€)	461.376	302.073	193.477	153.658	162.204	159.719	158.915	148.796	139.888	134.387	128.109
PV size (kWp)	30	30	30	30	30	26.823	18.457	8.799	6.753	5.547	4.493
EV Degradation (kWh)	0.866	0.848	0.773	0.694	0.682	0.680	0.681	0.684	0.684	0.684	0.685
EV Costs (€)	1000	986.651	882.737	734.586	712.438	709.187	709.522	713.340	710.939	711.014	711.432
Grid Costs(€)	-3,142.526	-2,321.652	-1,656.455	-1,157.649	-887.179	-500.877	92.310	654.139	799.239	884.167	952.972
Tot. Costs(€)	-142.63	481.22	915.15	1221.06	1479.4	1715.71	1909.26	1981.31	2014.24	2036.4	2050.5

It was observed that the BES serves a dual purpose. They are: supplying the household load, which can be equated to avoiding grid costs in the form of retail prices and revenue generation in the form of feeding generated energy back to the grid. The revenue generated depended on the momentary feeding-in tariff, which varied over time. As explained, the FIT also varied similar the RP. Also, larger the BES size, larger the amount energy that could be stored for supplying the load and for feeding back to the grid. Arguably, as the energy fed in increased so did the revenue generated. Thus the optimization led to a larger BES size at high FIT to maximize the revnue. However, when the FIT start to reduce, the BES sizes also reduced. This happened because with the reduced FIT, it was no longer possible to generate the same level of revenue as the case under large FIT and so a large BES was not necessary and expensive. The total revenue generated by feeding energy back to the grid at zero difference between the prices was xx. The total revenue which was generated when feeding enegy back to the grid at 90% difference was determined to be xx. This represents a drop of xx % in revenue when the FIT started to reduce.

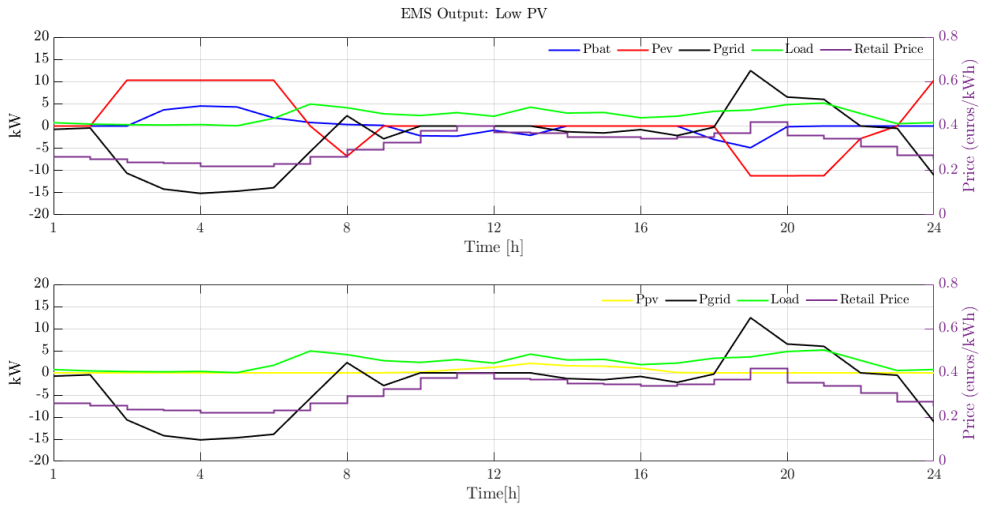

(a) Optimized power flows at 10% difference

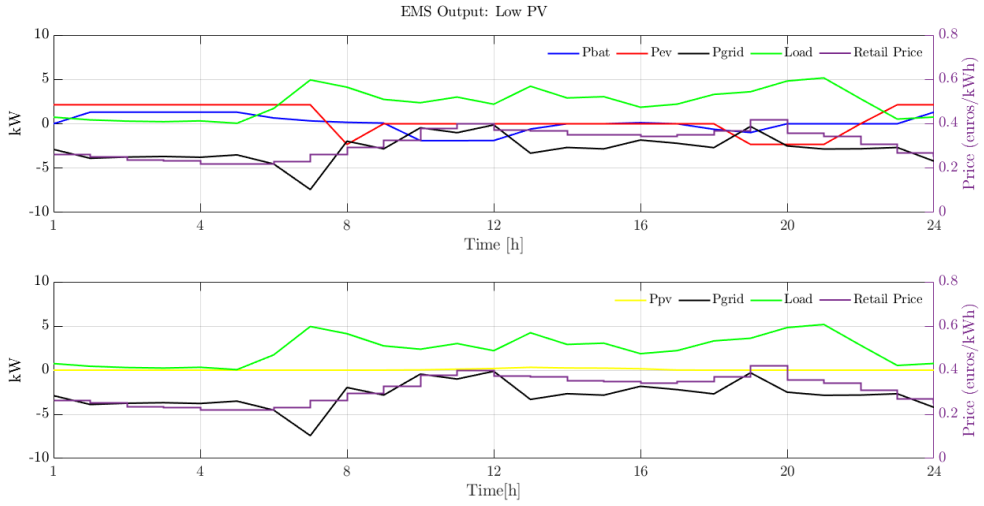

(b) Optimized power flows at 100% difference

Figure 5.3: EMS output for (different $E_{bat}^{max}, P_{PV}^{max}$) systems for a day with low PV output

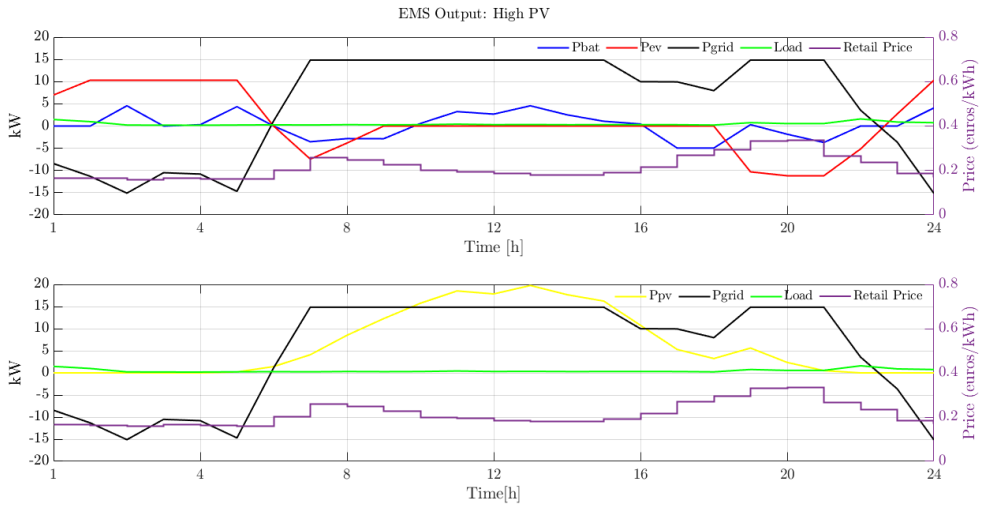

(a) Optimized power flows at 10% difference

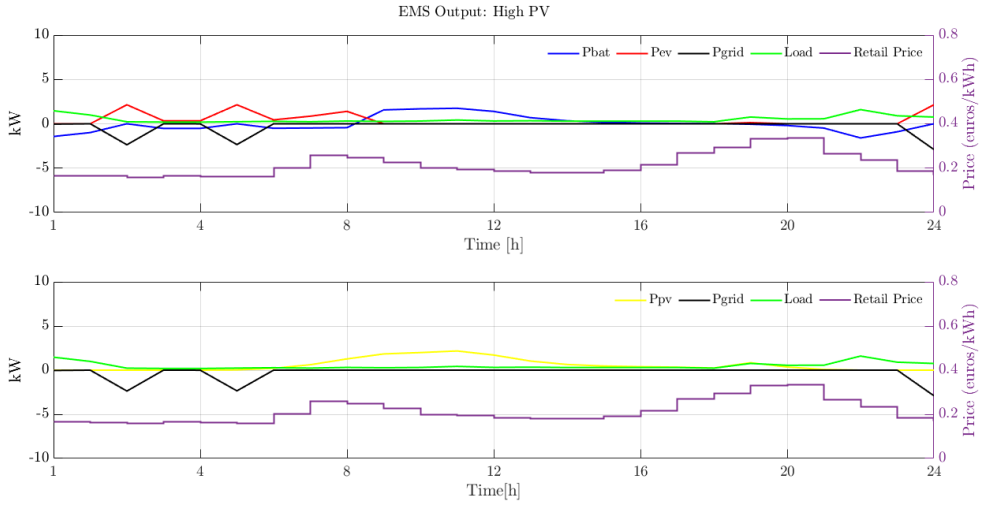

(b) Optimized power flows at 100% difference

Figure 5.4: EMS output for (different $E_{bat}^{max}, P_{PV}^{max}$) systems for a day with high PV output

Figures 5.3 and 5.4 showed the power flow of various components of different system sizes at high and zero FIT for days with varying PV output. These figures showed that the FIT had an impact on the size and the power flow of the system. Since a larger size was observed at high FIT, the power values observed were also larger. As the system size reduced, the power levels also reduced.

The use of BES also led to its degradation (ΔE_{bat}^{tot}) and thus a reduction in the value of the BES per kWh (V_{bat}). It also contributed to the operational costs of the BES C_{bat}. Equations 3.2a and 3.2b, show that the BES operation costs depend on the BES sizing and the degradation of the battery. At larger FIT, the battery degradation was comparatively larger than at lower FIT. This larger degradation was explained by the higher power levels observed when the FIT was high. This can be observed in figure 5.3. When the FIT dropped to zero, the power levels of the BES reduced as well which was observed in 5.4. This reduction was observed because the FIT was zero which meant that there was no possible way to generate revenue. Consumption from the grid was an increasing cost and thus if energy was consumed at high power, the costs would increase.

Interestingly, from the figure 5.2, it was observed that the BES size does not reduce to zero at zero FIT. This ocurred because of the dynamic Retail Price (RP) which were used. At instances when the grid price ($\lambda_{grid}^{buy}(t)$), was low, the energy was consumed from the grid and stored in the battery. Additionally, when

the PV output was available, the BES was also charged by using the PV power (refer figure 5.4). This charged energy in the BES was then discharged during the evening to supply the load or to charge the EV when it returned from the trip. Thus, excess consumption from the grid was avoided when there was an optimal BES size even at low FIT. This optimal value of the BES size was found to be between 8.5 kWh to 9.5 kWh based on the FIT used. Figure 5.5 showed the energy content of both, the BES and the EV battery for a day under large and small FIT respectively. It was observed from these plots that the BES use remained similar under both, high and low FIT. It was observed that around noon, when the prices were high, the BES discharged. This discharge occurred to supply the load, as observed in the plots in figure 5.3. In the figure 5.6, the energy content for the EV and BES were observed. Note that sizes of the BES were different for the different prices. But it was observed that under the high FIT, the charge and discharge of the BES followed the retail price. When the prices were high, the BES discharged. During the day, after 10:00, the BES started to charge via the high PV output and discharged again in the evening at 19:00 during high prices. This discharge of BES was not observed when the FIT was zero.

So, for any FIT, the BES size obtained depended on the investment costs, the retail prices, the FIT, and the operational costs due to the degradation. At high FIT the converter (which governed the rated power of the device) size obtained was also large, which led to higher power consumption. It was discussed in section 3.3.3 that the degradation of battery depended on the battery current which was directly related to the battery power. Thus, if the battery power increased, the battery current would increase as well. This increase in power thus leads to larger cyclic degradation. However, the converter size reduced along with the BES size when the FIT reduced. The reduction in the converter size also led to reduction in degradation at lower FIT.

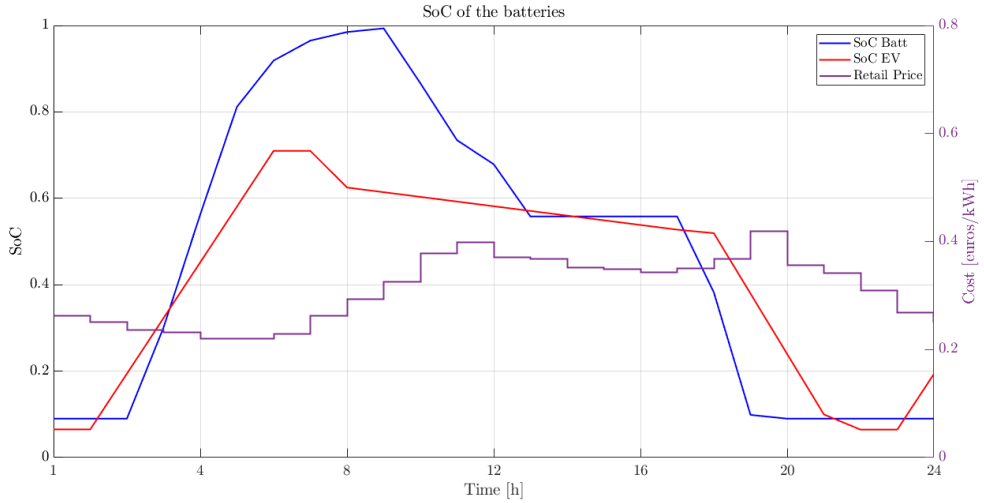

(a) SoC of BES and EV at high FIT

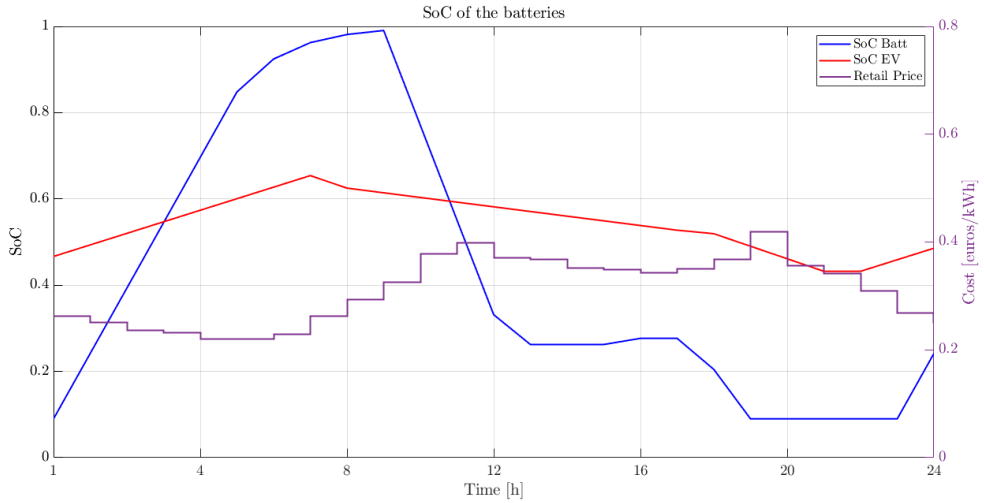

(b) SoC of BES and EV at zero FIT

Figure 5.5: SoC output for batteries of (different $E_{bat}^{max}, P_{PV}^{max}$) for a day with low PV output

Thus, for higher FIT, the degradation and the size were larger. This combination led to larger operating costs as well. From the table 5.1, it was observed that the BES operational costs at 10% difference in prices was €302.073. When the difference in prices was 90%, the BES operational costs was €134.387. This was a reduction of 55.5% in the BES operational costs. It was observed that the BES sizing at 30% difference in prices was 8.88 kWh while, the BES size at 40% difference was 9.82 kWh.

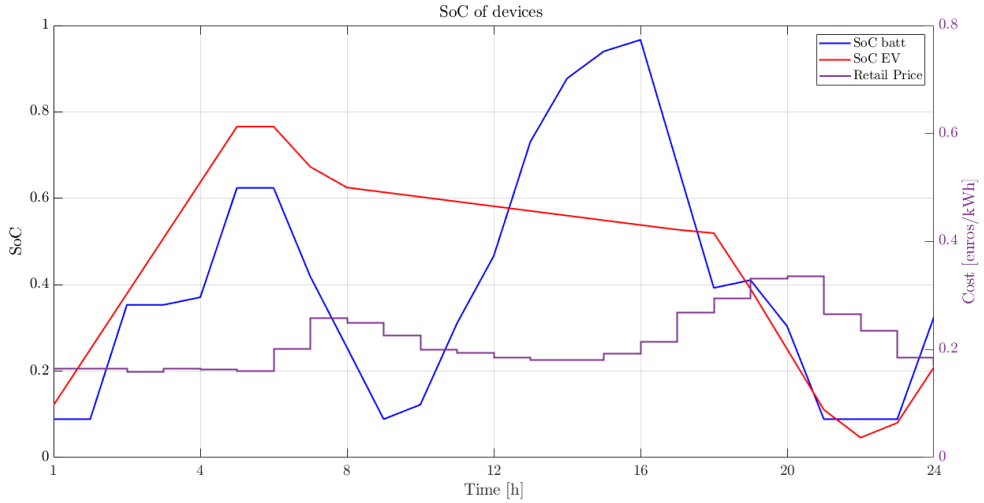

(a) SoC of BES and EV at high FIT

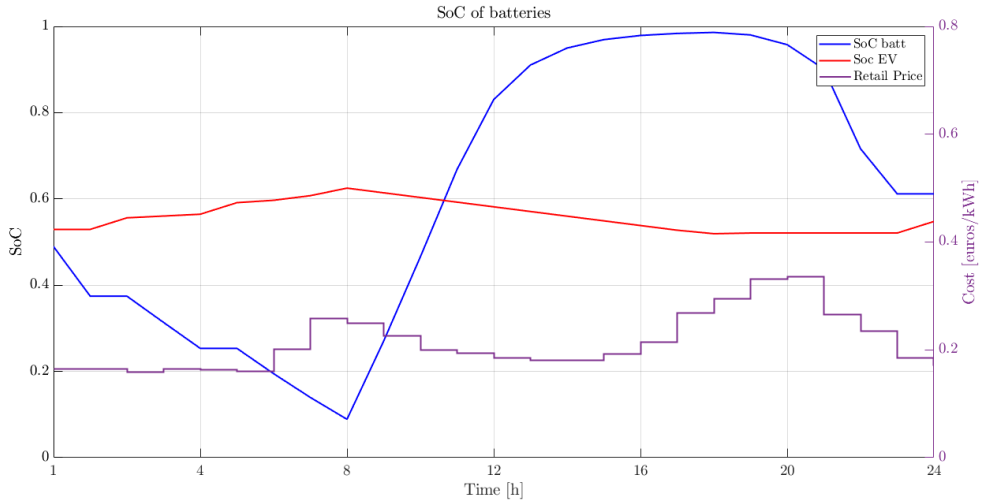

(b) SoC of BES and EV at zero FIT

Figure 5.6: SoC output for batteries of (different $E_{bat}^{max}, P_{PV}^{max}$) for a day with high PV output

This change in size occurred due to the increasing costs and reducing revenue as observed in this chapter. At higher FIT EV battery was preferred to supply the demand and feed energy back to the grid over the BES due to the larger size, relatively larger retention after degradation and capability to charge at higher power levels. This was observed in the resulting power flows as well (see fig. 5.3). But when the difference between FIT and RP reaches 40% it was observed that the EV power levels reduced. The average charging power for EV at 30% is 2.49 kW while at 40% it was found to be 1.66 kW (a difference of 0.83kW). Furthermore, there was also a reduction of average discharging power for EV from 1.8 kW to 1.3 kW (at 40%). Furthermore, the converter size for the EV battery reduced from 3.5 kW to 2.4 kW when the price difference changed from 30% to 40%. Thus, there was a reduction in EV power when the FIT reduced. However, the max BES converter power at 30% difference was determined to be 2.72 kW which reduced to 2.71 kW at 40% but saw an increase of 0.94kWh in its size. In other words, the average BES power did not change as much as the EV power did when the prices changed. The BES power reduced from 1.33 kW to 1.28 kW when the price difference changed from 30% to 40%. This difference was lower than the EV power difference at both prices and showed that there was not a significant change in BES use.

A factor which affected this change in BES and EV power 30% and 40% differences in prices was the availability of the EV. BES was always available and thus can be used to feed energy back during the times of high prices when the EV is not available (between 08:00-18:00). EV availability was same in both situations but

the FIT changed. Due to this reduction in FIT and the higher availability of the BES (compared to EV), the EMS preferred to use the BES over the EV at 40% difference. This energy from the BES was used to supply the demand and feed energy back to the grid, especially during winter when peak prices were observed during the day between 08:00-10:00 (refer section 5.3.8).

Less energy was consumed from the grid at 40% difference compared to 30% (3.08 MWh as compared to 3.84 MWh). However, this reduction in consumption was explained by the fact that more revenue could be generated by feeding in at 30% price difference and thus the larger consumption. But, the uncontrollable loads remained the same. The loads which varied include the BES and the EV charging. But, it was already observed that the EV charging had reduced. The EV charging energy at 30% difference was 2.47 MWh which reduced to 1.97 MWh at 40% difference. The BES energy consumed at 30% difference was 1.88 Mwh which increased to 1.90 MWh at 40%. As mentioned, a possible explanation for this increase in BES energy was to supply the household demand. To test this hypothesis, the grid costs were calculated for both the situations. At 30% difference, grid costs were found to be € 744.73 and at 40% difference, the grid costs were calculated to be €614.74. This was a reduction of 17.4% in grid costs at 40% difference in prices. The reduced grid costs showed that the BES size increased to supply the demand.

With the grid costs calculated at 40% difference in reference, the size of the BES was fixed at the value obtained at 30% difference and the simulation was done when the FIT was at 40% difference. It was observed that the grid costs increased to €633 from €614.74 (an increase of 3%). This shows that the increased BES size actually led to reduction of costs as the BES was also used to supply the demand and thus, the reduced consumption from the grid.

5.3.2. PV Costs and Size (C_{PV}, P_{ppv}^{max})

It was observed that after 40% difference in costs, the PV size reduced and led to lower PV costs. Since the PV costs are relatively larger than BES operation costs, the PV sizing therefore reduced when the opportunities to generate revenue decreased. At high FIT, the PV size was large because of the incentive to generate revenue. The PV costs can be effectively paid back with feeding energy back to the grid. Larger PV allows more energy to be fed in which means larger revenue. However, when the prices begin to reduce, it is noticed that the PV sizing also reduces. This reduction occurred due to the reduction in remuneration for the feeding-in of energy. At low FIT, there is less incentive to feed energy back to the grid. The PV costs are represented in the equation 3.4.

PV costs only depended on the rated kWp size that was obtained, and since no degradation was considered for the PV panels, the costs remained the same throughout the simulation period. As mentioned, relative to the BES and operation EV costs, the PV costs are larger (at high FIT). This led to the situation that if the PV sizing is kept the same, the system costs will increase significantly. The PV costs obtained at zero FIT was found to be €202.185. At very low price difference (i.e, high FIT), the PV cost was determined to be €1350, when the PV size was 30 kW_p. Thus, if the same size of PV was used for zero FIT, the total costs would've become €3198.31. This figure would represent an increase of 56% in total costs. Thus, due to the reduction in incentive to feed the generated energy back to the grid and the large costs for a big system size, the PV size reduced with reduction in FIT.

However, PV size does not drop to zero even when the FIT was zero. This was due to the reason that the PV served as a source used to charge the BES whenever available. This phenomenon can be observed in 5.7. This meant that charging the BES using the grid was avoided whenever the PV output was high. An analysis was done to determine the system costs when there was no PV and was determined to be €2196.5. This "no PV" system cost was compared to the system cost which was obtained when PV was considered available (€2050.5). The system costs when there was no PV was €146.5 larger than the situation when there was PV of 4.5kW_p for zero FIT.

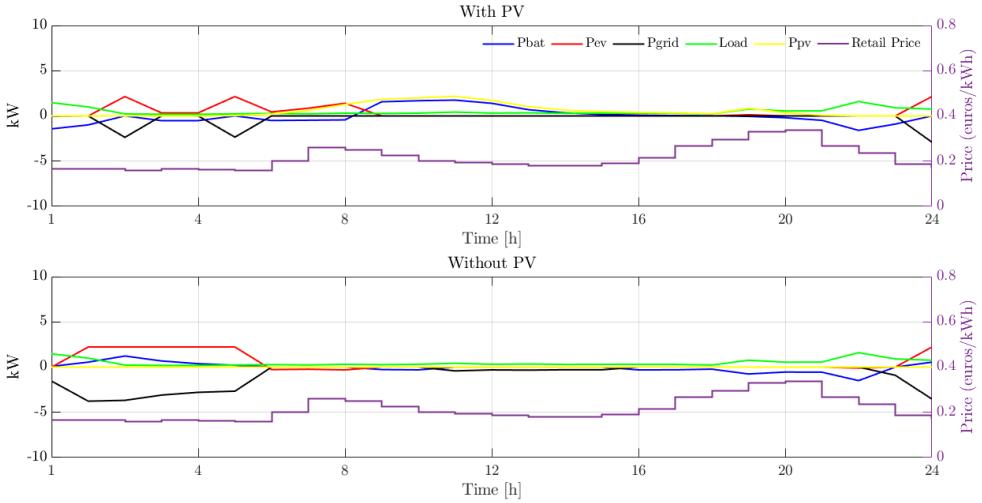

Figure 5.7: Comparison of the power flow output of the EMS at 0 FIT for a system with and without PV

Furthermore, it was observed that the PV was oversized with respect to the inverter at high FIT. For example, at 10% FIT, the PV size was $30kW_p$ and the inverter rating was 16.409 kW. This meant that the effective power which can be fed back to the grid via PV was limited by the inverter sizing. This can be explained by considering the LCOE of the PV system which was calculated in the equation 5.2.

$$LCOE_{PV} = \frac{V_{PV}.P_{PV}^{max}}{P_{PV}(t)\delta(t)T_{sim}^{life}} \tag{5.2}$$

On plugging the values of V_{PV} = 1350 euros/kW, P_{PV}^{max} = 30 kW_p, the energy generated by PV ($P_{PV}(t)\delta(t)$) during the time period of simulation, T_{sim}, the LCOE obtained was 0.08€/kWh which was lower than the average retail price of 0.20€. The lifetime of the PV system was assumed ot be 15 years.

Moreover, the oversizing of the PV allowed the EMS to charge the BES and EV by the PV as they were connected to the same DC link and these devices could absorb the part of the PV power. Furthermore, during the times of high prices in winter, large PV installation also had the benefit of feeding energy back to the grid to generate revenue. Larger PV at low irradiance produce relatively more power than a smaller PV installation. However, for this operations to be achieved, PV had to be curtailed during the periods of large PV output.

5.3.3. EV Costs (C_{EV})

A trend in changing EV costs was also observed. When the FIT were large, the FIT operational costs were also high. But as the prices reduced, the EV costs also reduced. At higher FIT, the EV battery was used for supplying the household load and feeding energy back to the grid by the V2G operation. This was observed in the relatively larger decays of the EV battery capacity at larger FIT (see table 5.1). This phenomenon is shown in the power flow plots in figures 5.3, 5.4. EV Costs are represented by the equations 3.3a and 3.3b and they were calculated in a similar method to BES costs.

Furthermore, the max observed power levels of the BES and EV are presented in the below table 5.2. It was also observed that maximum energy stored in the EV battery was also reduced and it can be concluded that the EV's use for V2G has further reduced. The reduction of EV's use for V2G is visible in figure 5.8. In the plot, it was observed that the SoC of the EV battery varied more when the FIT was high.

Table 5.2: Table with maximum BES and EV charging power for different FIT

	BES System			EV Battery		
Difference in prices(%)	$P_{bat}^{max}(kW)$	$P_{bat}^{min}(kW)$	$P_{bat}^{rated}(kW)$	$P_{EV}^{max}(kW)$	$P_{EV}^{min}(kW)$	$P_{EV}^{rated}(kW)$
0	6.62	6.92	6.95	9.96	10.51	10.52
10	4.56	4.82	4.85	10.32	10.7	10.74
20	3.4	3.54	3.54	8.18	8.52	8.52
30	2.63	2.72	2.72	3.12	3.38	3.38
40	2.61	2.71	2.71	2.38	2.58	2.58
50	2.41	2.51	2.51	2.27	2.47	2.47
60	2.35	2.45	2.45	2.27	2.47	2.47
70	2.11	2.29	2.29	2.34	2.44	2.44
80	1.91	2.07	2.07	2.17	2.26	2.26
90	1.82	1.89	1.89	2.14	2.23	2.23
100	1.74	1.89	1.89	2.14	2.23	2.23

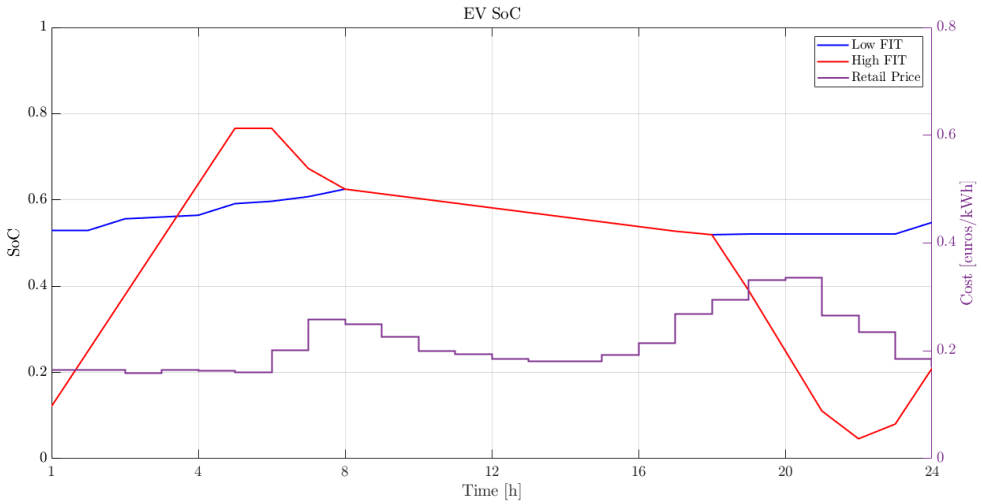

Figure 5.8: Figure showing the reduction of V2G operation at low FIT by SoC comparison of the EV

For a 10% difference, the obtained EV costs (C_{ev}) were determined to be €986.651.

5.3.4. Grid Costs (C_{grid})

Grid costs were calculated as the sum of the buying power costs and selling power costs as seen in section 3.3.2. Buying grid costs were determined by the product of the net energy being consumed from the grid with the retail price at that instant.

Selling grid costs refer to the revenue earned when the energy was fed back to the grid via the PV, BES or the EV. This cost is assined a negative as it signifies the revenue which is generated by feeding the energy back to the grid. This was also calculated in a way similar to buying grid costs, the difference being the energy fed back in is multiplied with the feed-in tariff at that instant.

Mathematically, they are expressed in equations 3.5a, 3.5b and 3.5c. It was seen that as the FIT reduce, the grid costs begin to increase. At larger FIT, grid costs are negative, implying under these conditions, the prosumers make a net profit. Naturally when the FIT reduced, the grid costs rose. It should be pointed out that the retail prices remain the same and do not change when the feed-in tariffs change. It was, however, due to the reduced FIT that the grid costs increase as the same amount of revenue cannot be generated anymore.

5.3.5. Inverter costs and Interest(C_{int}, C_{inv})

Inverter costs C_{inv} was calculated by using equation 3.6. For a 10% difference in FIT, the inverter costs was determined to be €121.06. This cost depended on the maximum inverter size obtained for a particular FIT.

Interest costs were calculated on the investment of BES and depended on the rate of interest, (assumed to be 1%) and the size of the BES (E_{bat}^{max}). Interest was calculated using equation 3.7. For a BES size of 17.237 kWh, the interest was determined to be €43.092. Interest depended on the obtained BES size and the interest rate.

5.3.6. Comparison of the system at 10% FIT with uncontrolled case

The system costs for the system size at 10% FIT was compared with the system costs for the uncontrolled scenario described in the previous chapter. Additionally, the average grid power was also compared.

For the system size obtained at the 10% FIT 5.1, the system size had a PV size of 30 kW_p, inverter size of 16.409 kW and a BES was added, of capacity 17.237 kWh (refer 5.3). The differences between the system costs for this sizing under optimal power flow algorithm and the uncontrolled case include the additional BES costs in the form of investment and operational costs. Another additional cost was the cost due to the degradation of the EV battery due to V2G, which was assumed to be absent in the uncontrolled case. Finally, the interest due to the acquiring the BES was also considered as a part of the system costs.

It was seen that the grid costs for the system under optimal power flow and sizing by the alogrithm was -€2321.65. The grid cost under the uncontrolled case was -€544.203. This represented a significant drop in the grid costs which was 326.6% lower than the costs under the uncontrolled case. This meant that significant revenue was generated when the V2G operation and a BES under the optimal control was considered.

Table 5.3: System size obtained for 10% FIT

System Component	System Size used
Inverter (P_{inv}^{max})	16.409 kW
PV System (P_{pv}^{max})	30 kW_p
EV Converter (P_{EV}^{max})	10.74 kW
BES Size (E_{bat}^{max})	17.237 kWh
BES Converter (P_{bat}^{max})	4.75 kW

Additionally, the EV costs were found to be €986.65 under the optimal control. The EV costs for the uncontrolled situation was found to be €691.27. However, under the V2G operation, the costs of EV operation also considered the cyclic degradation effects and the V2G operation. This was an increase of 29.93% in EV operation costs under the controlled case. Moreover, the BES costs under the controlled case was determined to be €302.073 which was €0 under the uncontrolled case as there was no BES considered.

The costs of the PV installation and the inverter costs were, however, the same for both the cases, controlled and uncontrolled and were €1350 and €121.6 repsectively. These costs were calculated using the cost equations presented in chapter3.

Furthermore, the introduction of the BES and the V2G under the control of the EMS also brought noticeable changes for the peak grid consumption power. For the uncontrolled situation, the peak consumption power was 9.27 kW, with the average consumption power being 1.9 kW. For the system under the control algorithm, the maximum grid consumption power was 15kW and the average grid consumption power of 8.8kW. Maximum feeding-in power of 15 kW remained same for both the situations. This showed that the grid power peaks increased under the control algorithm which was explained by the incentive to feed energy at high power to generate large revenue, offered by high FIT. The FIT for both the situations remained the same.

Table 5.4: Comparison of system costs between controlled and uncontrolled cases for the same system size

	Uncontrolled	Controlled under the algorithm
Inverter Costs(C_{inv}) (€)	121.06	121.06
PV Costs(C_{pv}) (€)	1350	1350
BES operational costs(C_{bat}) (€)	-	302.073
EV Operational costs(C_{ev}) (€)	691.27	986.651
Grid Costs (C_{grid}) (€)	-544.20	-2321.65
Total Costs(C_{total}) (€)	1618.27	481.22

The total system costs reduced by 70.26% for the controlled case, under the EMS smart control algorithm as opposed to the situation where there was no control.

5.3.7. Effects of V2G on costs and power flow for different tariffs

To further quantify the effects of V2G, simulations were performed on the same system size (refer table 5.3) which was obtained for the scenario of 10% difference between FIT and RP. Prices were varied for the same system size and the results were recorded for the situation when the maximum EV discharge power($P_{ev}^{min}(t)$) was set to zero. When this power was set to zero, V2G operation was not possible.

The prices used for this analysis were 10% difference between prices, 0 FIT and time of use (ToU) prices (refer table 2.1). For the different prices mentioned, the costs were compared and the resulting power flows were analysed as well.

Under 10% difference in prices

Under 10% difference in prices, the resulting power flows were already discussed in the previous sections. It was observed that the energy was consumed from the grid during the times of low RP and was fed back to the grid when the FIT was high. This difference in prices was plotted in the figure 5.1 and the resulting power flow were observed in figures 5.3a and 5.4a.

However, there were significant changes in the power flow when the V2G operation was prevented. The power flow for the same day under the cases with and without V2G were presented in the figures below.

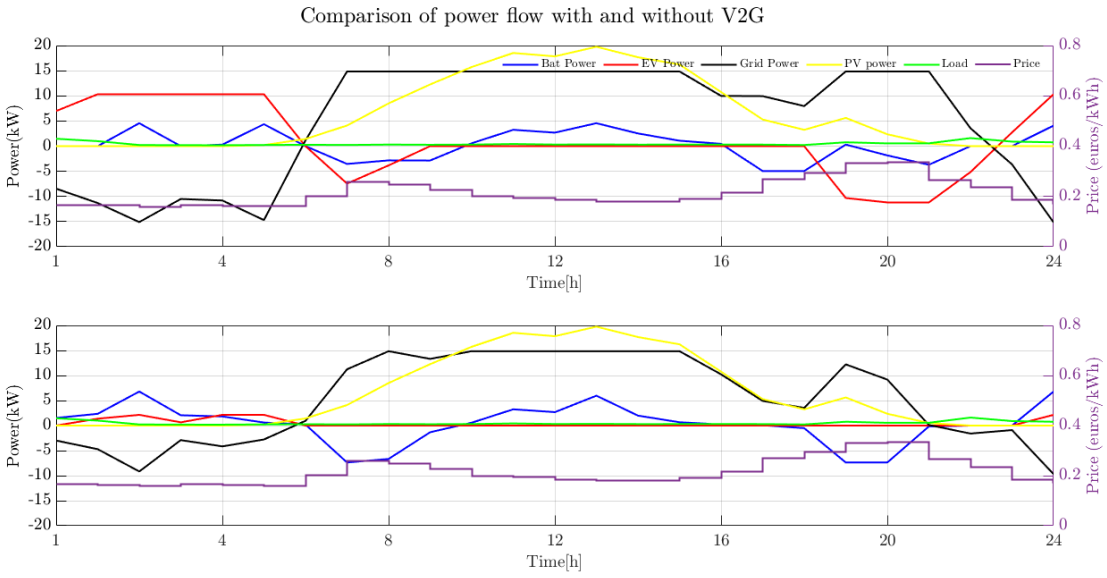

Figure 5.9: Comparison of BES, EV and grid power for high FIT with (top) and without (bottom) V2G

In the figure 5.9, the power flow was presented for a day with high PV output. The top plot represents the

power flow when V2G was considered and bottom plot represents the power flow when it wasn't considered. Since the FIT was large and the PV output was also high, most of the generated PV power was fed back to the grid. This explained the high feeding-in grid power ($P_{grid}(t)$) during the day. However, there were differences observed. Between 07:00 and 09:00, under no V2G, the grid feeding power was not as large as when the V2G was considered. This was explained by the inability of the EV battery to supply energy back to the grid in the morning hours as seen in the top plot.

Furthermore, it was observed that the charging power for EV under no V2G was lower than the situation when V2G was considered. This reduction happened because the EV could not be discharged to either supply the demand or to feed power to the grid. Thus, there was no requirement to charge the EV battery at high power and the only necessity to charge the battery was to have the required amount of set energy content (50 kWh) for the following day. This charging of the battery did not occur at a large power as opposed to the situation when V2G was considered. The high charging and discharging power for the EV battery under V2G occurred because apart from driving, stored energy was also fed to the grid to generate revenue. This energy could only be available if the EV power increased. Under V2G, the maximum power observed in the plot was around 10kW, both for charging and discharging. However, when V2G was removed, the discharging power reduced to zero and it was observed that the charging power did not exceed even 5kW.

Due to this reduction in the EV charging power and its incapability to discharge for supplying (demand or to feed power back to the grid) under no V2G, the BES power changed. The BES power increased on an average when the V2G operation was not allowed. This occurred because at this level of FIT, significant revenue could still be generated. Thus, to compensate for the loss of V2G capability, the EMS decided to charge and discharge the BES at a higher power. When V2G was considered, the BES charging or discharging power did not exceed 5kW during the day plotted in the figure 5.9. However, when V2G capability was removed, the BES charging and discharging power increased beyond 5kW, reaching to 7kW.

Figure 5.10 represents the situation when the PV output was low on a winter day. Here too, it was observed that the EV discharged during the evening when the price was high. It was again observed that the grid consumption was reduced as the power to charge the EV battery was low and the BES charging and discharging power increased when no V2G was considered.

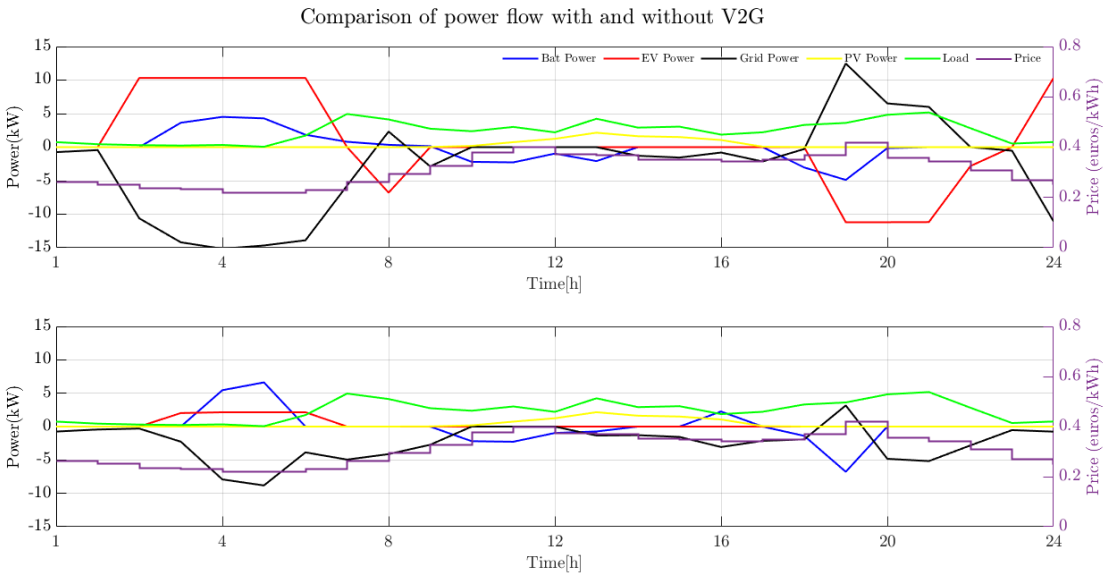

Figure 5.10: Comparison of BES, EV and grid power for high FIT with (top) and without (bottom) V2G (low PV)

The total costs (C_{total}) when V2G was considered was €481.22. This number increased to €638.03 when V2G was restricted. This represents a 45.16% increase in total costs when V2G was restricted. The total BES (C_{bat}) under V2G was determined to be €302.073 which rose to €349.10 when V2G was not allowed. This represented an increase of 15.51% in the BES operational costs. The EV costs (C_{ev}), on the other hand, reduced to

€698.51 from €986.65 when V2G was not allowed, representing a reduction of 29.2% in EV operational costs. The grid costs reduced from -€2320.94 to -€1891.5. This represents an 18.51% increase in grid costs when V2G was not allowed.

The changes in the power flow of BES and EV also led to changes in their battery degradation. The total degradation in battery (ΔE_{bat}^{tot}) caused during the period of six months was determined to be 0.24 kWh when V2G operation was allowed. But this degradation increased to 0.27 kWh when V2G was not allowed. This represented an increase of 12.5% in degradation. This increase occurred due to the higher power values of the BES when V2G was absent, to generate revenue. Conversely, the absence of V2G led to a reduction in EV battery degradation (ΔE_{EV}^{tot}). Under no V2G, the EV battery degradation was determined to be 0.67kWh, a reduction of 20.2% from 0.84kWh under V2G. Thus, absence of V2G led to a reduction in the degradation of EV battery degradation. These values are summarized in table 5.5.

Under zero FIT

When the FIT was reduced to zero, for the same system size, the changes in power flow were quite significant. All the power values had reduced because the FIT was zero which meant that revenue generation by feeding energy back was also null. This inadvertently led to increase in total costs to the system and to reduce the costs, the energy consumed reduced. Thus, the power at which energy was consumed also reduced. Thus a general reduction in power was observed. The power flow for the case when V2G was available and for the case when V2G was absent was presented in the figure 5.11.

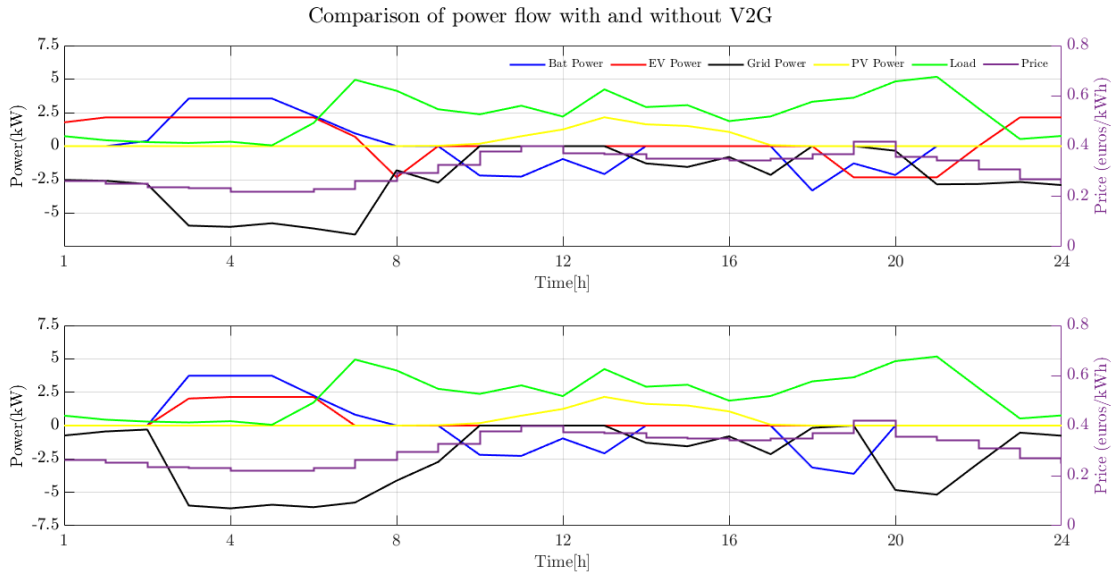

Figure 5.11: Comparison of BES, EV and grid power for 0 FIT, with (top) and without (bottom) V2G (low PV)

On comparison with the case with high FIT, it was observed all the power level during the day are significantly lower. Energy was consumed from the grid during the time of low prices, during the night. This energy was stored in the BES and EV which were later discharged during the period of high load in the evening (at time of high prices). It was also observed that the EV discharged in the evening (around 19:00-21:00) to supply the demand as the energy prices at that instant ($\lambda_{grid}^{buy}(t)$) were high. However, when V2G capability was removed, it was observed that during the evening hours, the demand was instead met by consuming power from the grid. BES was also discharged under both the scenarios to meet the demand. Furthermore, most of the power consumed from the grid during the night was used to charge the BES and not the EV under both cases, with and without V2G. This behaviour was different compared to the case when FIT was high and V2G was active where it was preferred to charge the EV instead of BES.

As observed in the figure 5.11, there are indeed differences in the grid and BES power flow and values.

However, these differences are not stark. The use of EV for V2G was already reduced, which dropped to zero when V2G capability was removed. The reduction in V2G at zero FIT occurred because the using EV for supplying demand would mean more energy would be required from the grid to meet the user preferences and supply demand at the same time. This would result in higher costs. Also, it would add the costs due to cyclic degradation of the EV battery. Presence of V2G operation meant more energy could be stored and supplied for meeting the demand and thus reducing the costs. Moreover, it was also observed that the PV output was curtailed and was used to charge the BES during the day. Overall, it was observed that at zero FIT, there was not much difference in the costs or degradation of the batteries with and without V2G.

The total costs (C_{tot}) under the situation when V2G was active, was determined to be €2860 while the total costs when V2G was not active was determined to be €2867.4. This represented a total increase of 0.25% when V2G capability was removed. The BES costs under the situation when V2G was active was determined to be €246.536, which increased to €249.882 when V2G was restricted. This represents an increase of 1.37% in BES costs (C_{bat}). EV costs (C_{EV}) also didn't show a significant change. With V2G capability, the EV costs were determined to be €702 while they were equal to €698.472 when V2G was restricted. This represents a reduction of 0.5% in costs when V2G was restricted. Grid costs (C_{grid}) were €418.19 when V2G was allowed and increased to €423.96 when V2G capability was removed. This was an increase of 1.36% in grid costs.

There were similar changes observed in BES and EV battery degradation. BES degradation (ΔE_{bat}^{tot}) under V2G was determined to be 0.2046 kWh whereas it was determined to be 0.2058 kWh when V2G was not available. This represented an increase of 0.58%. Similar values were also obtained for EV degradation. EV degradation (ΔE_{EV}^{tot}) was determined to be 0.6715 kWh without V2G which increase of 0.6751 kWh when V2G was active. This represented an increase of 0.53%. These values are summarized in table 5.5.

Under ToU prices

Time of Use prices were discussed in chapter 2 (see table 2.1). These prices did not vary during each time step, but rather varied depending the time of the day: day price and night price. The time of use prices for the day (considered from 09:00-20:00) were 0.2202 €/kWh, between 00:00-09:00 and 20:00-00:00 were 0.2061 €/kWh. The FIT was a constant of 0.092 €/kWh for all the hours.

Figure 5.12 represents the power flow of components for a day with low PV output under the ToU tariffs with and without V2G. It was observed that more energy was consumed from the grid during the time of low prices, i.e, during the night.

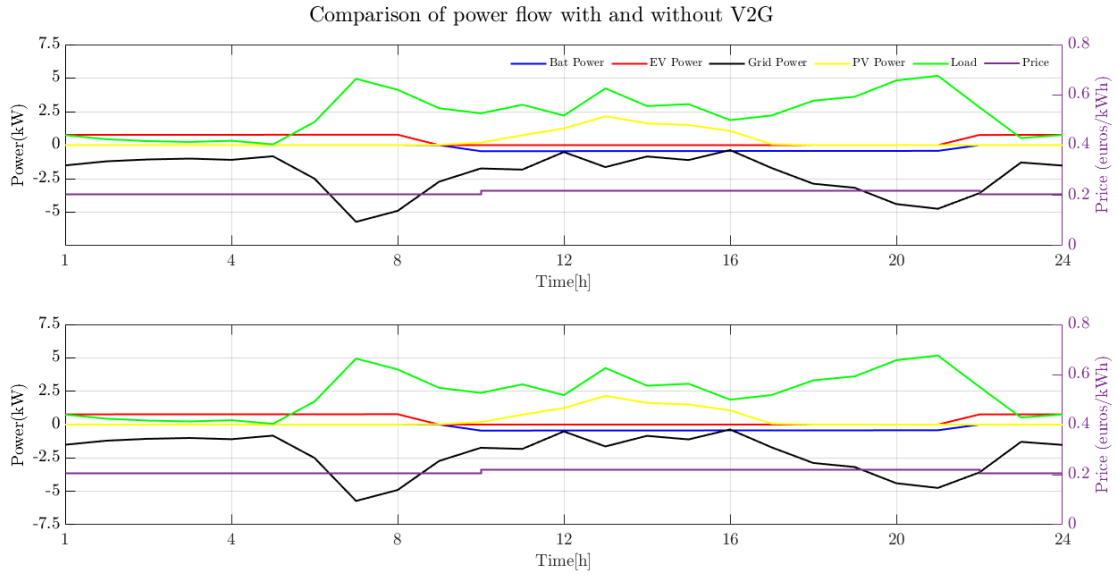

Figure 5.12: Comparison of BES, EV and grid power for ToU prices, with (top) and without (bottom) V2G (low PV)

Furthermore, it was observed from table 2.1 that the FIT was always lower than the retail price. Thus, feeding energy did not generate the same revenue observed under the 10% difference between FIT and RP under dynamic prices. Having the FIT much lower than the RP at all instances made feeding in only profitable when PV output was high. Thus, it was observed that neither the BES nor the EV battery were charged and discharged at high power. It should be noted that supplying the demand using the battery or through V2G would have been cheaper than using the grid during the evening (just before 20:00). However, this does not happen as the EV arrives back after 18:00 and has an hour to supply the load before the retail prices reduce. But since the charging of the EV has to happen later (for the trip next day), through grid, which results in shifting of costs rather than significant reduction. When the prices reduced after 20:00, the consumption from the grid increased to supply the load and charge the batteries.

Furthermore, it was observed that the BES discharged steadily throughout the day at a power of 0.4kW. This occurred to supply a portion of the load during the day, at the time of high prices. However, when the PV output was hig, the BES was also charged by the generated PV power. In figure 5.13, power output for different devices were observed for a day with high PV output with and without V2G available.

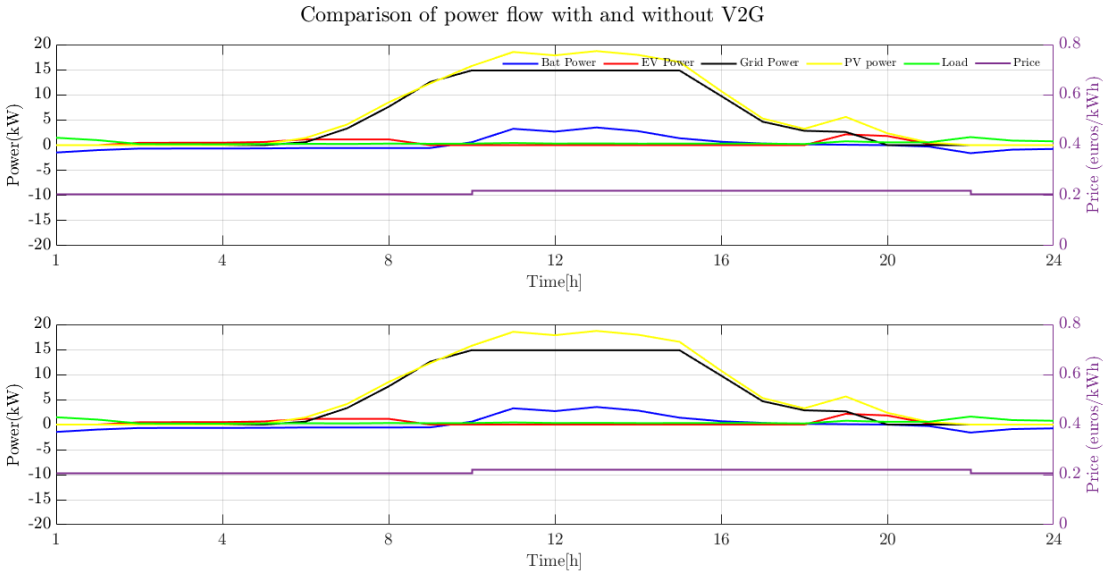

Figure 5.13: Comparison of BES, EV and grid power for ToU prices, with (top) and without (bottom) V2G (high PV)

As mentioned earlier, it was feasible to feed power back to the grid when the power output from PV was high. Furthermore, it was also observed that the BES was discharged to charge the EV during the night hours. Furthermore, it was observed that for both cases, with and without V2G available, there were no significant changes in power flow. This led to conclusion that V2G does not make a big difference in costs when ToU prices were considered. This conclusion was proved by considering the various costs involved.

The total costs (C_{total}) when ToU with V2G was considered was determined to be €1778.7, which rose to €1784 when V2G was not allowed. This represents a 0.3% increase in costs. The EV costs (C_{EV}) when V2G was considered under ToU prices were determined to be €698.83 which decreased to €698.4 when V2G was not allowed. This represents a 0.06% decrease in EV costs. The BES costs ($Cbat$) under ToU with V2G were determined to be €237.08 which increased to €237.10 when V2G was restricted. This is an increase of 0.008% in BES costs. The grid costs were negative for both the cases, with and without V2G. With V2G, they were determined to be -€650.204, which decreased to -€646.966 when V2G was restricted. This represents an increase of 0.5% when V2G was restricted and thus concludes that V2G does not lead to a significant change in costs at ToU tariffs.

Similar results were also found for the BES and EV degradation $\Delta E^{tot}_{bat}, \Delta E^{tot}_{EV}$. EV battery degradation was determined to be 0.6719 kWh when V2G was active which reduced to 0.6715 kWh when V2G was restricted. This represented an reduction of 0.059% in degradation. The BES degradation was determined to be 0.1955

kWh for both the cases from which it was concluded that the BES use did not change much between the two scenarios. These values are summarized in table 5.5.

Table 5.5: Variation in costs when V2G is allowed and not allowed under different prices

	High fit		Low Fit		ToU Prices	
Characteristic	With V2G	No V2G	With V2G	No V2G	With V2G	No V2G
EV Costs (C_{EV}, €)	986.64	698.51	702	698.5	698.83	698.5
Bat. Costs(C_{bat}, €)	302.07	349.10	246.53	250	237.08	237.10
Grid Costs(C_{grid}, €)	-2320.94	-1891.5	423.96	418.19	-650.204	-647
Total Costs(C_{total}, €)	481.2	638.03	2860	2867.4	1778.7	1784
Batt. degradation(ΔE_{bat}^{tot}, kWh)	0.24	0.27	0.2046	0.2058	0.1955	0.1955
EV degradation(ΔE_{EV}^{tot}, kWh)	0.84	0.67	0.6751	0.6715	0.6719	0.6715

5.3.8. Seasonal Analysis of FIT on power flows at 10% difference

Additional to the results presented in this section, a seasonal analysis was also done to determine the system behaviour over the period of simulation (half year). This was done on the system size mentioned in table 5.3.

For the seasonal analysis, it was assumed that the difference between the FIT and RP was 10%. Moreover, the starting date for the simulation was assumed to be 01/01/2018, starting at 00:00 hours. Winter season was assumed from 01/01/2018 to 28/02/2018, spring from 01/03/2018 to 30/04/2018 and summer from 01/05/2018 to 02/07/2018. The time steps for the analysis were one hour each and a total of 4380 hours (period for which the input data was also used) resulted in a period of time starting at 01/01/2018 00:00 to 02/07/2018 11:00.

For each month, the average hourly power of different components were obtained and were aggreagted over a single day. Thus, for example, all the power in the winter were averaged on a hourly basis and were plotted against a period of twenty four hours which represented a average winter day. Plots for the average winter, spring, summer and overall average powers were plotted against a period of twenty four hours. The plots and comments were discussed.

Grid Power

Figure 5.14 showed the variations in average grid power during the period of half year. From top to bottom, the subplots represent avg. power during winter, spring, summer and the overall period.

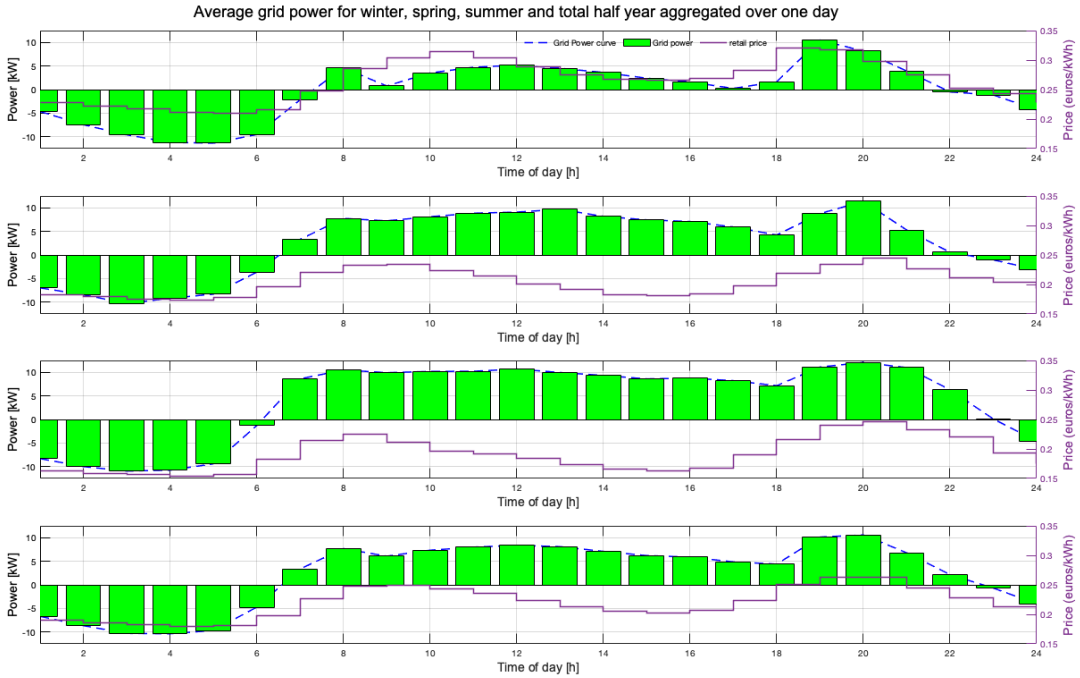

Figure 5.14: Average grid power during winter, spring, summer and overall period (from top to bottom) plotted against a period of twenty four hours

From the above figure, it was observed that the average grid power ($P_{grid}(t)$) was positive during the day (08:00-19:00) and in the evening (from 19:00 to 22:00) and negative during the night. Positive grid power meant feeding energy back to the grid and negative power means consumption from the grid. Considering the RP (C^{buy}_{grid}), it was observed that the grid power consumption occurred during the night, with a maximum average power greater than 10 kW. Feeding in occurred at similarly high power levels in the evening when the RP was high once again. Thus, in the night (early morning), peak consumption was observed and in the evening, peak feeding in was observed.

On comparison between grid feeding powers during winter and the other seasons, it was observed that the average grid feeding-in power during the day increased in spring and summer. This occurred due to the higher PV output during the spring and the summer season. Furthermore, it was seen that the number of feeding in hours in the winter were comparatively smaller than the number of feeding in hours during spring and summer. This was again due to the availability of the PV output. Moreover, the PV output was used to charge the BES which was then discharged into the grid between 17:00 and 18:00, until the EV was again available for feeding energy back via V2G. It should also be noted that during spring and summer, the PV output was first used to charge the BES and the remaining power was fed back to the grid.

EV Power

In the figure 5.15, averag EV power (P_{ev}) for winter, spring, summer and the total half year period was plotted after aggregating the averages for a period of twenty four hours.

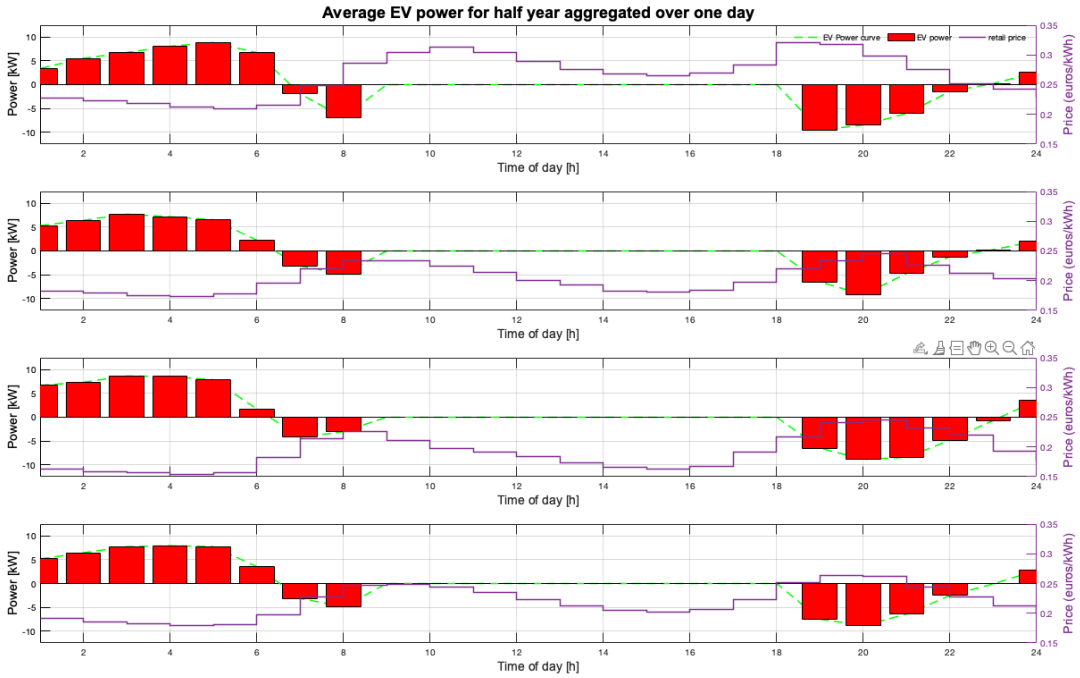

Figure 5.15: Average EV power during winter, spring, summer and overall period (from top to bottom) plotted against a period of twenty four hours

It was observed that the avg. EV power was positive during the night, with a peak of about 8.8kW during spring. A positive power related to charging while a negative EV power related to discharging of the battery, either to supply the demand or feed energy back to the grid via V2G. The EV charged at night during all the seasons, as observed, due to the low RP during the night. This charging was enough to supply the energy required for the driving use (for which a set point of 50 kWh was set to be achieved at 08:00) during the day. It was also observed that the during the period of increasing prices two hours before departure, the EV battery discharged to the grid to feed energy and generate revenue.

When the EV returned at 19:00 in the evening during the times of high prices, the EV battery discharged energy back to the grid to generate revenue before, finally, beginning to charge again. It was observed that the charging power, on average, increased during the nights of spring and summer. This happened due to the relatively lower RP as compared to the winter season. Furthermore, it was noticed that, in the evening, based on the hour the peak RP occurred, the peak average power shifted as well. This peak power shifted to coincide with the peak price which would be received for feeding energy back to the grid. EV was not available during the period 09:00-18:00 and thus zero average EV power was noticed between these times.

Battery Power

In the figure 5.16, averag BES power (P_{bat}) for winter, spring, summer and the total half year period was plotted after aggregating the averages for a period of twenty four hours.

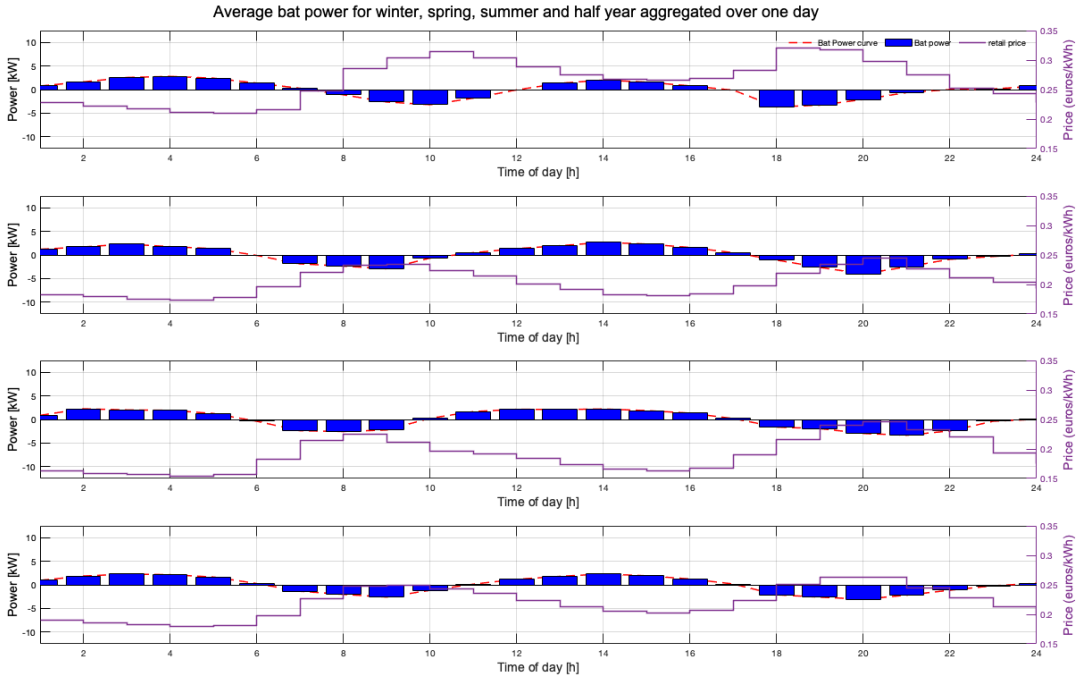

Figure 5.16: Average BES power during winter, spring, summer and overall period (from top to bottom) plotted against a period of twenty four hours

A behaviour similar to the EV power was also observed for the BES power. Charging of the BES occurred during the night at low RP and discharging during the times of high prices. However, since the BES was always available, frequent charging and discharging behaviour was noticed during the span of the day. The BES was discharged back to the grid to generate revenue during the periods of morning peak prices (between 08:00-11:00). It was then charged again during the time of low prices in the afternoon until the period of high prices during evening.

Compared to winter, there were noticeable differences in the avg. BES power during spring and summer. Firstly, it was noticed that the charging of the BES happened for a longer duration during spring and summer. This was due to the high PV output during spring and summer. Overall, it can be said that the BES usually charged through PV and then either discharged back to the grid to generate revenue or was used to supply the demand. Secondly, it was noticed that the average discharge power was higher in spring and summer compared to winter scenario as the available PV output meant that the BES could be charged for a price lower than the RP at a later occasion.

This is also the reason why the average BES charging power during winter night hours was higher than the average BES charging power during spring and summer night hours. During spring and summer, the BES was charged by the high PV output during the day and thus charging at comparatively higher RP during the night was avoided. From figures 5.14, 5.15, and 5.16, it was seen that the maximum and minimum powers correspond to minimum and maximum retail prices, respectively, during the day. It was observed that when this peak prices shift, the consumption/feeding-in also shifted along with the prices. For example, in 5.16, it was observed that the peak discharging power was at 18:00 during winter, which shifted to 20:00 during spring. The peak price for winter was also observed at 18:00 while the peak power for spring was observed at 20:00. This showed that RP could be used to change the consumption and the feeding-in behaviour. Thus, dynamic retail prices could potentially be used to manage the grid loading and help in solving grid issues.

PV Power

In the figure 5.17, average PV power (P_{pv}) for winter, spring, summer and the total half year period was plotted after aggregating the averages for a period of twenty four hours.

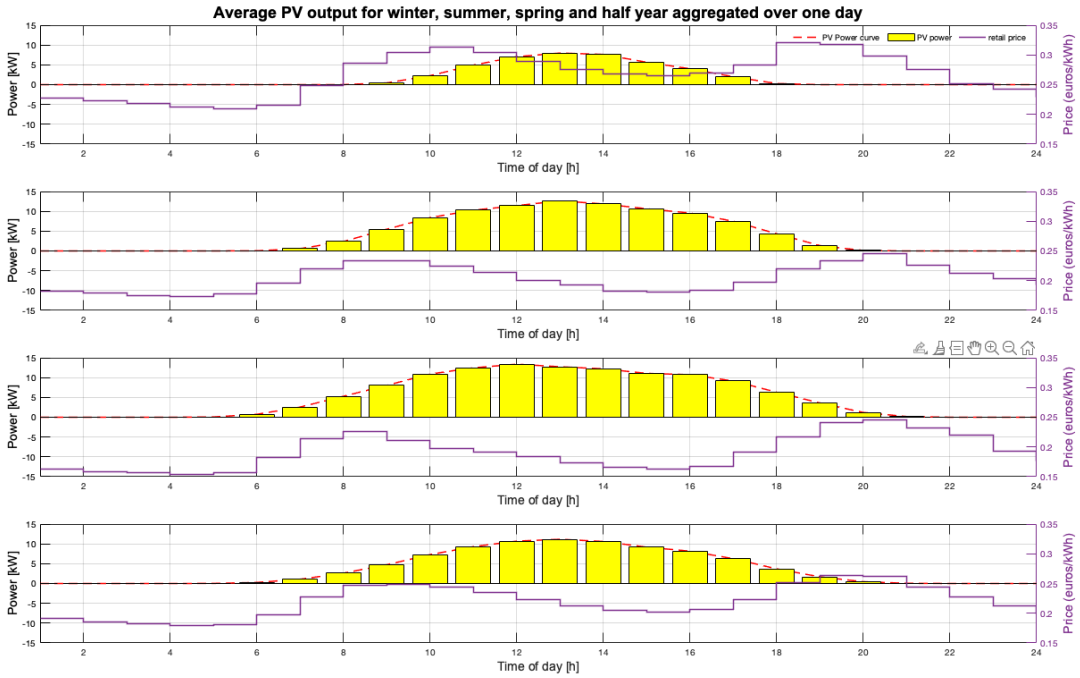

Figure 5.17: Average PV power during winter, spring, summer and overall period (from top to bottom) plotted against a period of twenty four hours

PV power depended on the solar irradiance available during the months. This meant that the avg. PV output for winter was lower than the avg. PV output for summer and spring. This was also observed in the plot. As the average PV power increased, feeding energy to the grid also increased. This was observed in figure 5.14 during the day hours in spring and summer when the feeding in increased compared to the winter hours. Also, as discussed, the increasing PV power during spring and summer was also used to charge the BES along with feeding energy back to the grid. Moreoever, during summer, the PV output is larger compared to PV output during spring due to higher irradiance. Furthermore, it was also observed that when the PV output was large, the retail prices reduced. This showed the advantages of having a storage system for revenue generation.

Table 5.6: Seasonal variation in the average grid, BES, EV and PV power under 10% difference in RP and FIT

	Grid P_{grid} (kW)		Battery P_{bat} (kW)		EV P_{ev}(kW)		PV P_{pv}(kW)
Season	Feeding in	Consumption	Charging	Discharging	Charging	Discharging	Average
Winter	10.49	11.34	2.79	3.66	8.85	9.55	7.97
Spring	11.36	10.28	2.67	4.01	7.73	9.12	12.64
Summer	12.07	10.92	2.26	3.34	8.67	8.84	13.4
Total	10.56	10.36	2.30	3.03	7.94	8.84	11.16

5.4. Discussion

The effects of FIT on the power flow for the house were observed and explained in this chapter. It was seen that the larger FIT lead to higher peak power for the devices and the grid. More energy was being fed in at large FIT which resulted in larger degradation of the BES and the EV batteries. It was also observed that under large FIT considerable amount of energy consumed from the grid was fed back at instances when the FIT was larger than the instantaneous retail price to generate revenue to offset the consumption costs.

Despite the situation with large FIT being beneficial to the household in minimizing the costs, there can be negative effects. These effects appear in the form of large grid peak. For a single household, this situation

might not pose a problem, but if multiple similar households are placed on the same feeder, the distribution grid has a possibility of being overwhelmed and congested for longer periods of time. If this situation continues, chances of a breakdown occurring can increase. Additionally, grid congestion would occur which can lead to voltage and frequency issues and thus lead to a drop in the quality of power. Thus, the FIT has to be designed carefully and should consider the penetration of distributed energy generation sources at any point before any changes are made to it.

However, FIT still remains an attractive incentive for prosumers to invest in renewable energy sources. As a result, the share of installed rooftop PV panels have increased and it has given the households a new means of revenue generation [79]. Having such a PV/BES-EV system also creates opportunities for consumers to participate in ancillary services markets or flex markets. P2P markets are also becoming relevant as a result of increasing amount distributed energy sources in the distribution grid as the traditional process of transmission over long distances can be avoided.

But the issues of grid voltage, frequency and harmonics still remain relevant [13]. To this end additional incentives in the form of market mechanisms are required to prevent the grid issues. Grid expansion can also help solve these issues but are expensive and is a slow process. To better understand the issues at a grid level, further research needs to be done where multiple houses with the system used in this research are being used under the same situation on a low voltage feeder level.

5.5. Conclusion

It was observed that the larger feed-in tariffs incentivise larger BES storage and larger PV installation. As a consequence, the power levels, on average, are larger as compared to the case when the FIT are lower. It can be said that larger FIT incentivise distributed generation and are an effective market mechanism for this purpose. However, large FIT can lead to consumers oversizing their generation and storage systems and might lead to congestion in the networks if energy flows are not regulated properly. In this study, the optimization was done to minimize the costs of a prosumer household. But when multiple households in a same feeder are considered, the optimization might need to be changed due to the reason that the grid constraints (such as maximum network capacity) also begin to play a significant role. Moreover, when multiple houses are considered, it might be interesting to maximize the social utility rather than minimizing the cost.

6

Capacity Mechanism

6.1. Introduction

One of the mechanisms proposed to overcome generation scarcity was capacity subscription [26], [42]. Apart from generation scarcity, capacity subscription also helped reduce the peak power in distribution grids. However, the mechanism proposed by de Vries and Doorman [26] was modified for this work. Capacity subscription was described as the capacity mechanism under which a consumer chooses to subscribe to a particular capacity level for a household based on their demand preferences. de Vries and Doorman [26] proposed this mechanism as a means to prevent supply interruption by curtailing excess consumption during generation scarcity. Thus, this method is also helpful in avoiding large energy prices during the times of scarcity. An important point to be noted is that de Vries and Doorman proposed that activation of Load Limiting Devices(LLDs) must only occur during the times of scarcity or congestion. The main aim of implementing this mechanism in this thesis, however, was to test the hypothesis that implementing capacity subscription will lead to stable grid power consumption and lower power peaks.

The capacity mechanism was first described along with the intended outcomes of this mechanism. The method of determining the optimal power subscription and the penalty mechanisms are described. Results of the simulation of capacity mechanism for two different capacity prices (and their variations) were also discussed. Power flow within the household and the grid power were discussed and compared with the situation when the system was behaving under the influence of the FIT alone. However, the system sizing used was not varied and kept constant. The sizing used was the sizing obtained when the difference between the retail price and FIT was 10% (see chapter 5).

Discussions related to the challenges and the opportunities in using this capacity mechanism were then made and the conclusions are then presented.

6.2. Methodology

In contrast with the method proposed by the authors [26], the current thesis implemented the mechanism in a way proposed by Bjarghov and Doorman in [42] (see 2). This was done to simulate the effects of the power flow when a subscribed capacity level has to always be respected regardless of the capacity. This has been termed as the static method for the capacity subscription. Surpassing the capacity limits subscribed lead to penalties. However, Bjarghov and Doorman's [42] primary objective was to determine the differences in the energy costs of the household under capacity subscription with and without a BES to comment on its effects in reducing the costs.

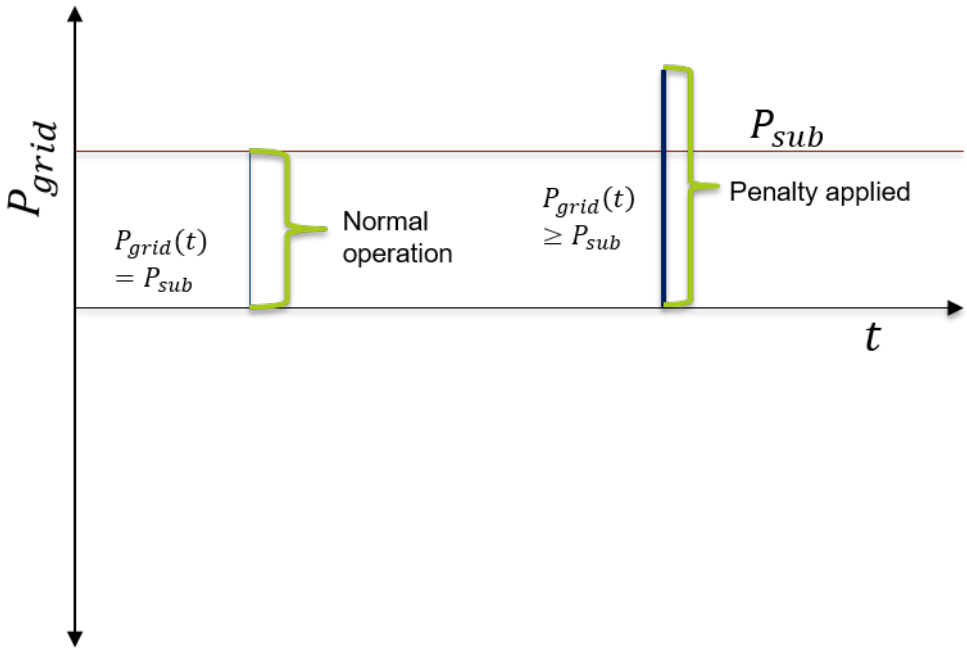

Figure 6.1: Schematic of the Capacity Mechanism implemented

In this study, however, the BES was already considered as an energy storage as described in chapter 3. All the system components described so far were considered. Moreover, to effectively compare the effects of the capacity mechanism, the system size obtained at 10% difference between the retail price and FIT was used for all the capacity prices considered in this research (see table 5.3). The uncontrollable load remained the same and it is assumed that they are not flexible. Furthermore, the effectiveness of the mechanism to reduce the peak grid power was also determined and the costs were compared with the uncontrolled case.

The capacity cost was introduced which was a price in terms of €/kW. Thus, larger the capacity consumed at any instant, larger the cost. This price was multiplied with the grid power at any instant t. Since the objective was to reduce the grid power, only changes in grid power led to changes in capacity cost. A new variable called the capacity subscription (P_{sub}) was introduced with the objective that the EMS would decide to determine the optimal connection capacity for the household based on the load and the capacity price. To ensure the optimal capacity was selected, a penalty mechanism was also added. The penalty was applied whenever the grid power exceeded the subscribed limit. This penalty incentivized the EMS to manage the load and power flow in such way that the grid power was either equal to the subscribed power or lower. The capacity prices were taken from the local DSO and from the Norwegian regulatory authority provided in [42], [80]. The prices were 0.0015 €/kW/h and 0.0123 €/kW/h. These prices were multiplied by 1 to 5 to get a range of capacity prices which were used to determine how the subscribed capacity changed with changes in capacity cost.

A penalty of 10x the capacity price was added whenever the grid power exceeded the subscribed capacity. This factor was also taken from [42] and the authors regard it to be a generic level of penalty. Thus, for example, if the subscribed capacity was 10 kW and the capacity price was 0.0015 €/kW/h, the penalty price would be 0.015 €/kW/h whenever grid power ($P_{grid}(t)$) was greater than 10 kW. These penalties were added cumulatively and the total capacity cost was the sum of the basic capacity cost and the penalties. This total cost was then added to the objective function described in chapter 3.

The following equations were implemented to reflect the capacity mechanism. Equation 6.1a describe the normal capacity cost and equations 6.1b - 6.1c describe the penalty costs

$$C_{cap}^{std}(t) = P_{sub} \cdot C_{sub} \qquad ,\forall t \tag{6.1a}$$

$$C_{cap}^{pen}(t) \geq C_{cap}^{std}(t) \qquad ,\forall t \tag{6.1b}$$

$$C_{cap}^{pen}(t) \geq (x_1 - m_1(P_{sub} + 0.1)) + m_1 P_{grid}^{X}(t) \qquad ,\forall t \tag{6.1c}$$

P_{sub} denoted the optimal subscribed capacity and C_{sub} was the cost per kW per hour. For the prices obtained from the Dutch DSO, the value of C_{sub} was €0.0015/kW/h and for the prices obtained from NVE, the value of C_{sub} was €0.0123/kW/h. These equations ensured that the optimal capacity was chosen by the EMS based on the load and the prices. The equations **??** - 6.1c were modelled using the linear equation for a line, $y = mx + c$ where m is the slope of the line and c the intercept formed at the point of intersection with the y-axis (fig 6.2). The value of m and c depended on the capacity prices being used. These inequalties ensure that the grid power remains below the subscribed capacity or the penalty is applied for exceeding that power level. The addition with 0.1 represents the sensitivity of the system in determining when the penalty was to be applied.

To prevent excess consumption beyond the subscribed capacity, two limits were placed. A financial incentive and a physical limit. When the grid power at any instance exceeds 1.5x the subscribed capacity, a penalty equal to 50 times the capacity price was added. The physical limit was a hard constraint which would ensure that the grid power would never exceed 1.5x the subscribed capacity. These two can work independently or together. They are represented by:

$$P_{sub} \leq P_{grid}^{max} \qquad ,\forall t \tag{6.2a}$$

$$P_{grid}^{X}(t) \leq 1.5 P_{sub} \qquad ,\forall t \tag{6.2b}$$

$$C_{cap}^{pen}(t) \geq 50 C_{sub} P_{sub} \qquad \forall t \tag{6.2c}$$

$$C_{cap}^{pen} \geq (x_2 - m_2(1.5P_{sub} + 0.1)) + m_2 P_{grid}^{X}(t) \qquad ,\forall t \tag{6.2d}$$

x_2 and m_2 were also calculated in a similar way to x_1 and m_1 however, the values used to calculate them would have a difference of a factor of 50. Furthermore, it should be noted that the representation P_{grid}^{X} signify both the feeding-in and the consuming power. Thus, this mechanism also ensures that excess feeding-in power was penalized as well along with excess consumption power.

Table 6.1: Table explaining the parameters used for the penalty calculation for the low price from the Dutch DSO

Symbol	Quantity	Value
x_1	Y-intercept obtained from the penalty line ($10C_{sub}$)	0.015
m_1	Slope of the penalty line	0.135
x_2	Y-intercept obtained from the excess penalty line ($50C_{sub}$)	0.075
m_2	Slope of the excess penalty line	0.6

The cost and the penalty curves were shown in the following figure 6.2. m_1 and m_2 were calculated for the different cases using this image, where $m_2 > m_1$. x_1 and x_2 were the different costs and also, $x_2 > x_1$. From the below figure, mathematically, $m_1 = \frac{10C_{sub} - C_{sub}}{P_{sub} + 0.1 - P_{sub}}$. m_2 was also calculated but for the higher power(1.5xP_{sub}) and price (50xC_{sub})

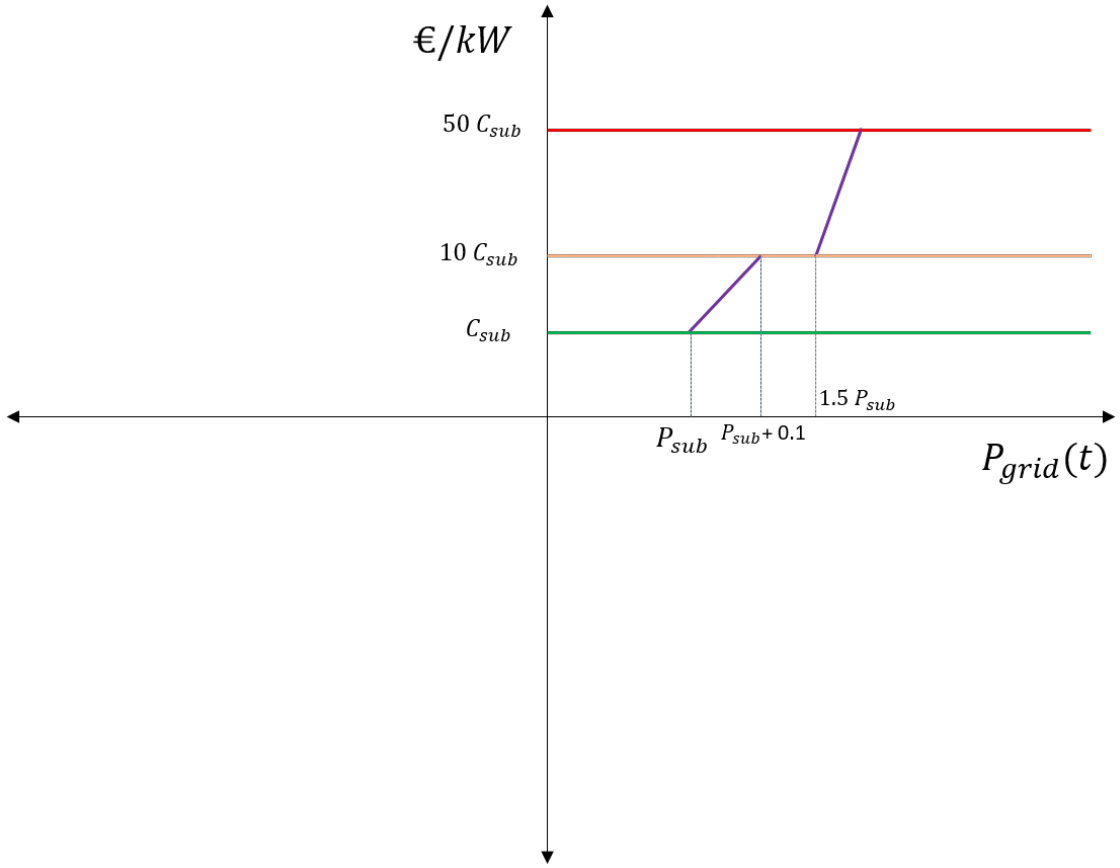

Figure 6.2: Representation of penalty calculation

The total capacity costs were calculated using the equation 6.3.

$$C_{cap} = \sum_{t=1}^{T} \left(C_{cap}^{std}(t) + C_{cap}^{pen}(t) \right) \qquad , \forall t \tag{6.3}$$

The modified objective function will then become

$$min(C_{total}) = min(C_{bat} + C_{EV} + C_{PV} + C_{grid} + C_{int} + C_{inv} + C_{cap}) \tag{6.4}$$

6.3. Results

In this section, the observed outputs of the impemented capacity mechanism were discussed and presented. Firstly, the effects on the power flow were discussed and then the effects on total costs were discussed.

6.3.1. Effects on power flow

As discussed, The capacity tariffs (CT) were increased up to 5 times their original value (from local DSO: € 0.0015/kW and from NVE: € 0.0123/kW). It was seen that when the capacity tariffs increased, the subscribed capacity reduced. The subscribed capacity is chosen by the EMS. When the capacity costs were € 0.0015, the capacity subscribed was 14.9 kW. The resulting power flow was the same as that was obtained when there was no capacity costs present. The revenue generated was same but total costs increased by a value equal to the capacity costs.

However, when the prices/kW started to rise, the subscribed capacity also reduced. This was due to the increasing costs per kW. Larger the capacity subscribed, larger the payment that needs to be made. Since the EMS minimizes the total cost, the capacity subscribed reduces. This was observed in figure 6.3

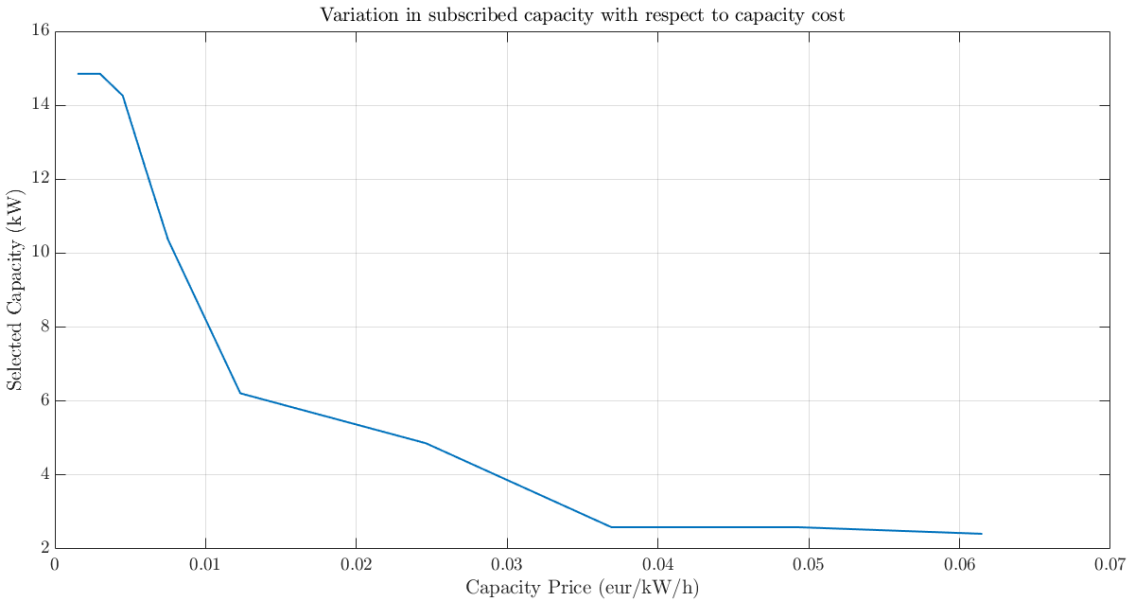

Figure 6.3: Influence of the capacity prices on subscribed capacity

Due to reduction in capacity subscribed, the peak grid power also reduced. This reduction happened to minimize the total costs. Exceeding this power would lead to large fines and thus, the Capacity mechanism leads to reduction of the grid power levels. The average power levels reduced as well. When prices from the local DSO were considered, average grid power grid fell (P_{grid}^{buy}) from 7.5 kW to 5.9 kW. While the average grid feeding in power (P_{grid}^{sell}) fell from 7.5 kW to 6.1 kW. This showed that the capacity prices influence the consumption and can be used to limit the power consumed and fed to the grid. Figures 6.4 and 6.5 showed the changes in power flow under low capacity and high capacity costs for the periods with low and high PV.

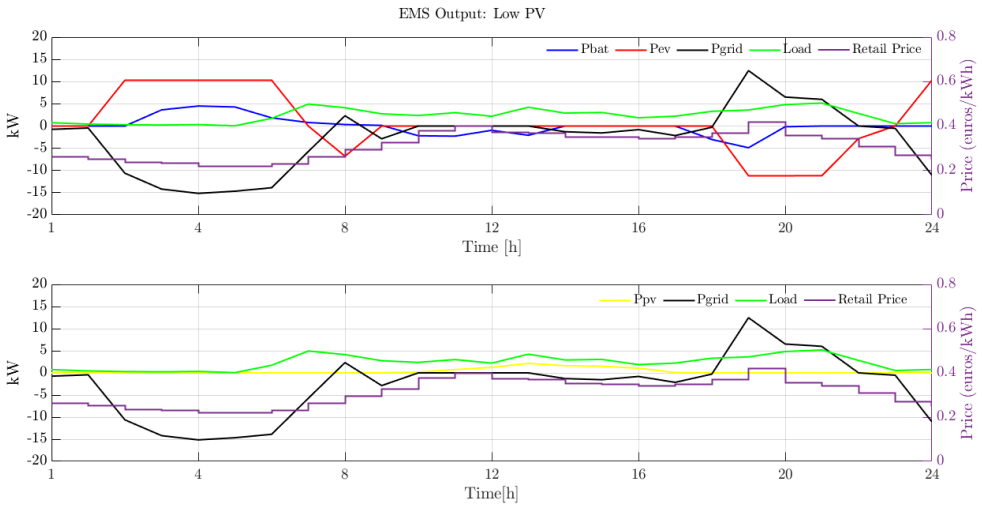

(a) Optimized power flows for a day with low PV output

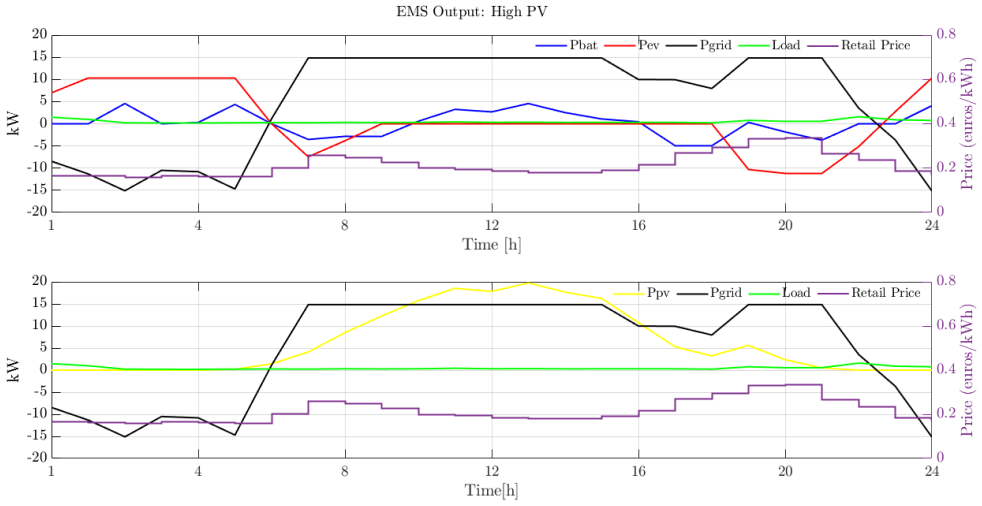

(b) Optimized power flows for a day with high PV output

Figure 6.4: EMS output for the system at low capacity tariff

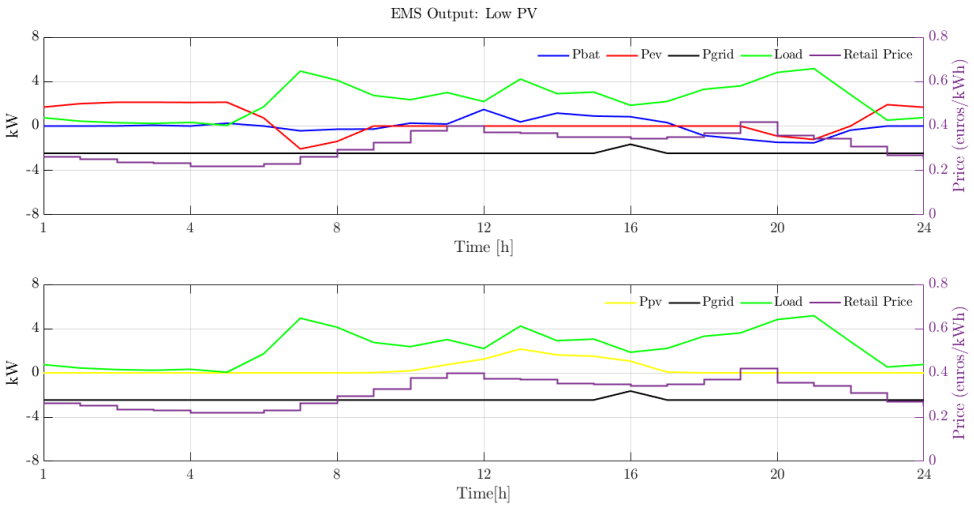

(a) Optimized power flows for a day with low PV output

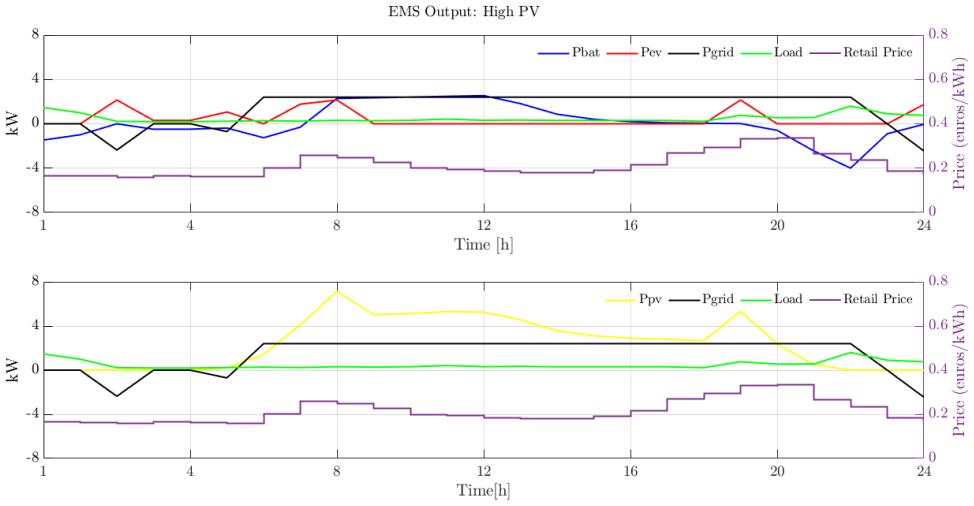

(b) Optimized power flows for a day with high PV output

Figure 6.5: EMS output for the system at high capacity tariff

From the figures 6.4 and 6.5, it was observed that there is a reduction in peak grid power when the capacity costs increased. In the figure 6.4, it was observed that the grid power had the maximum value of 14.9 kW and a minimum value of -14.9 kW. The subscribed power from 6.3 for this CT of 0.0015 €/kW/h 14.9 kW. This showed that the grid power was either equal to subscribed power (P_{sub}) or lower. Under this capacity tariff, the maximum grid power never exceeded this value. Moreover, the BES and the EV charging and discharging power was also high. This happened because the devices could discharge (to the grid) at high power and the grid power would be still lower than the subscribed capacity value of 14.9kW. In the plot for the sunny day, figure 6.4b, it was also observed that the PV output was high and a considerable amount of PV energy generated was fed back to the grid.

However, the power flow changed when the CT was increased to the maximum value of 0.0615 €/kW/h as observed in the plot 6.5. At this capacity tariff, the subscribed power (P_{sub}) was determined to be 2.41 kW. It was observed that the grid power while consumption or feeding in was at this level. Furthermore, the power level for the BES and the EV also reduced. This reduction happened because of the CT applied. Since the EMS tried to keep the grid power either below or equal to P_{sub}, the maximum power at which the BES or EV could be charged from the grid decreased. This phenomenon which occurred due to the high CT explained the reduction in BES and EV charging power at this CT. The same was also true for grid feeding-in power. In figure 6.5b, it was also observed that the PV output was significantly curtailed. However, despite the curtail-

ment, the PV power was still larger than P_{sub}. This level of PV power is significant because the BES and the EV could be charged via the DC link which connected their converters. This connection on the inverter's DC side meant that it was not affected by the grid power requirements at any CT. However, since feeding-in was a direct interaction with the grid, the generated PV power had to be curtailed due to the implemented capacity mechanism.

Furthermore, the EV use for V2G also reduced as seen in figure 6.6, with the SoC plots of the EV battery under various capacity tariffs . This behaviour was explained by the large power required by the EV battery to be used in a similar way when there were no capacity costs added. Since charging and discharging at a lower power requires a longer time, it could lead to situation that the EV does not have the required SoC during the time of departure the following day. But this situation was avoided by reduction of EV's V2G operation. This was observed in fig 6.6.

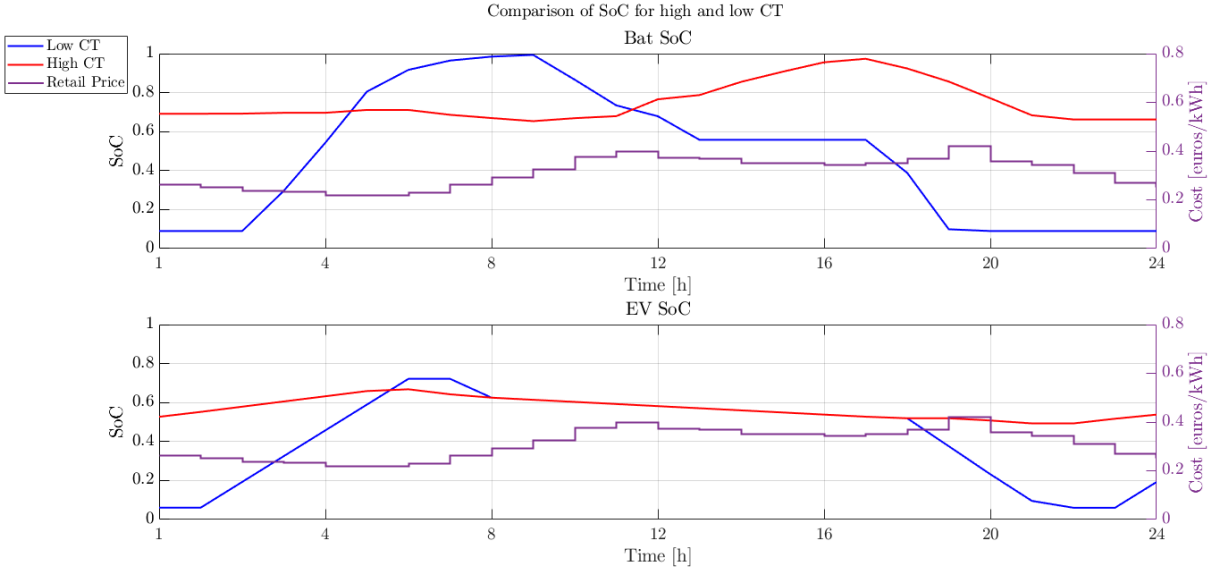

Figure 6.6: Comparison of Soc of the batteries under low and high CT

The effect of capacity costs on BES and EV SoC was observed in figure 6.6 It was observed that as the prices increase, the trajectory of the curve changed and the SoC values differed for different prices. Under large costs, instances were observed where the SoC did not reduce as much as under lower costs. These can be explained by considering the charging and discharging power of the BES during that week. Since the charging and discharging power was low, the same amount of energy would not be charged or discharged in the same duration.

It was observed that the $P_{grid}(t)$ did not exceed the subscribed levels for the various capacity prices. Thus, the capacity mechanism was able to reduce the peak grid power to lower levels. Furthermore, this reduction also led to increased use of BES for supplying energy to the load.

6.3.2. Effects on Cost

As the capacity mechanism was added, the revenue generated decreased and the grid costs increased due to the lower amount of energy that was fed back to the grid. Less energy is consumed from the grid as the capacity costs increase which leads to low cost, but also less energy is fed back to the grid meaning lower revenue. Grid costs reduced from -€2332.18 to -€317.21 when the CT increased. This happened because the capacity subscribed decreased when the tariffs increased. Since the capacity subscribed reduced, the max power at which energy can be consumed also reduced.

Table 6.2: System cost changes at different capacity tariffs

Parameter	0.0015	0.003	0.0045	0.006	0.0075	0.0123	0.0246	0.0369	0.0492	0.0615
Battery Costs (C_{bat}, €)	303.03	303.03	302.32	300	301.21	292.51	258.291	250.44	250.44	251.13
EV Costs (C_{EV}, €)	993.31	993.31	985.01	943.72	889.48	768.64	716.70	716.47	716.48	709.6
Capacity Costs(C_{cap}, €)	292.61	585.23	843.56	969.93	1022.36	1003.56	1618.58	1269.55	1692.74	2066.90
Grid Costs (C_{grid}, €)	-2332.18	-2332.18	-2290.8	-2110.41	-1886.45	-1215.18	-827.06	-370.21	-370.21	-317.21
Total Costs(C_{total}, €)	776.45	1069.07	1359.8	1622.91	1846.28	2369.21	3286.18	3385.93	3809.12	4230.1
Subscribed power(P_{sub}, kW)	14.9	14.9	14.1	12.3	10.37	6.21	4.86	2.59	2.59	2.41

Table 6.2 showed the various system component costs at different capacity tariffs. It was observed that the capacity costs increase quickly with changes in price. With the increasing capacity costs, the system costs also increased significantly. The FIT was still at 10% difference and it was seen that the grid costs (C_{grid}) are negative for all the different capacity tariffs used. This showed that the EMS still reduced the costs by feeding energy back to the grid. But, since grid feeding in also incurred a cost now, the power at which the feeding in occurred reduced quite significantly and the revenue reduced. At the lowest capacity tariff of € 0.0015/kW/h, the system costs (C_{total}) were lowest at €776.45 and at the highest capacity tariff of €0.0615/kW/h, the system cost was the largest at €4230.1. At this level of capacity tariff, the capacity costs formed around 48.88% of the total costs. Thus, this also underscores the importance of determining an efficient capacity tariff and a penalty mechanism.

The BES and the EV operational costs (C_{Bat}, C_{EV}) also reduced when the capacity tariffs increased as the power required to charge these devices at the same levels was no longer available due to the lower value of P_{sub}. A suitable capacity tariff would be between €0.006/kW/h - €0.0075/kW/h, but the reduction in grid power is not quite large and the costs are still significant. With these observations and the changes in power flow, it can be concluded that the capacity mechanism used in this study can be used as an effective DSM method to reduce the peak power for a household. However, the effectiveness of this method to reduce peak power in distribution grids should be studied with this EMS model implemented on multiple houses on a distribution grid feeder level.

6.3.3. Comparison with the uncontrolled case

The results obtained for the capacity mechanism at the current capacity tariff of €0.0015/kW/h was compared with the uncontrolled situation and the FIT results. The total system costs and the power levels were compared. Additionally, the costs obtained at CT of 0.0123 €/kW/h were also compared with the uncontrolled case.

The results for the uncontrolled case (see table 4.2) show a total system cost, C_{total}, of €1618.27. The total cost under the low capacity tariff was €776.45 which represent a 52.02% reduction in costs. The BES costs remained the same as they were under the system with FIT only, with C_{bat} = €303.03. However, in the uncontrolled case, there was no BES and thus, C_{bat} was considered to be zero. The EV operation costs C_{EV} increased to €993.31 representing an increase of 43.69% as compared to the uncontrolled case.

The costs of PV installation and the inverter costs were, however, the same for the capacity mechanism and the uncontrolled case as the system size used were the same. For low capacity tariffs grid costs, C_{grid} was found to be -€2332.18, this represent a 328.5% drop in the grid costs under the presence of the control mechanism. As a result, significant revenue was generated under the low capacity tariff as well.

However, when the capacity tariffs (CT) were equal to 0.0123 €/kW/h, the total system cost was (C_{total}) €2369.21 which is larger than the total system costs under both, the uncontrolled case and absence of CT. At this CT, the total system costs were 46.4% higher than the system costs under uncontrolled case and 392.33% higher than when there was no CT. EV and BES costs at high CT, however, reduced compared to when only FIT was considered. As explained, this happened due to the reduction in power levels which led to a reduction in power consumption and thus, the degradation. The BES degradation (ΔE_{bat}^{tot}) reduced from 0.25 kWh to 0.20 kWh and the EV degradation (ΔE_{EV}^{tot} reduced from 0.85 kWh to 0.68 kWh. Degradation was not considered for the uncontrolled scenario. Compared to when there was no CT, the reduction in C_{EV} and C_{BES} was 22.1% and 3.46% respectively. Compared to the uncontrolled case, the EV costs increased from €691.27 to €768.6 at

high CT. This represented a 11.19% increase.

PV and the inverter costs remained the same at high CT as well due to them only depending on size, which remained constant. However, there were significant changes in the grid costs. The grid costs (C_{grid}) under high CT was found to be €-1215.18. Compared to the uncontrolled case where the grid costs were €-544.20, the total change was a reduction of 55.2% in the case of high CT. Compared to the case when CT was absent, the total change was a reduction of 91.05% under the situation when no CT was present.

Finally, at low CT, there was no noticeable affect on grid power levels and they remained the same as when CT was absent. However, when the CT increased the grid power levels began to reduce. At high CT, there was significant reduction in grid power and the maximum grid power at any instance was 6.41kW (which was in the acceptable limits). Feeding-in power also reduced significantly and the maximum feeding-in power was found to be 6.41kW. This also led to curtailment of PV during the case of high CT.

These different costs are presented in table

Table 6.3: System cost comparsion for uncontrolled and controlled scenarios

	Uncontrolled case	FIT Only with control	FIT with low CT and control	FIT with high CT and control
Inverter Costs (C_{inv}, €)	121.06	121.06	121.06	121.06
PV Costs (C_{pv}, €)	1350	1350	1350	1350
EV Costs (C_{EV}, €)	691.27	986.651	993.31	768.64
BES Costs (C_{BES}, €)	-	302.07	303.03	292.51
Grid Costs (C_{grid}, €)	-544.20	-2321.65	-2332.18	-1215.18
System Costs (C_{total}, €)	1618.3	481.22	776.45	2369.21

6.3.4. Seasonal analysis of CT on power flows

As performed in section 5.3.8, similar analysis was also performed for the same system under the same conditions (i.e, 10% difference in prices) for the low capacity tariff (CT) obtained by the Dutch DSO and the high CT obtained from the Norwegian regulator (NVE).

The system size for analysing the effects of CT on power flows during different seasons of the year was the same as mentioned in table 5.3. However, additional CT were also considered. The CT considered for this analysis are €0.0015/kW/h and €0.0123/kW/h called as low CT and high CT respectively.

First, the effects of the CT on grid power were discussed. Then the effects of the low and high CT were discussed on EV power, following which the effects on average BES power were discussed. Finally, the effects of low and high CT on avg. PV power were discussed. The method in which the analysis was performed remained the same as discussed in section 5.3.8. The mean power flow for various devices over the seasons were aggregated and plotted against a period of twenty four hours.

Grid Power

Figure 6.7 figure showed the variation in average grid power during the period of half year under the influence of low CT and FIT. From top to bottom, the subplots represent avg. power during winter, spring, summer and the overall period of simulation of half-year.

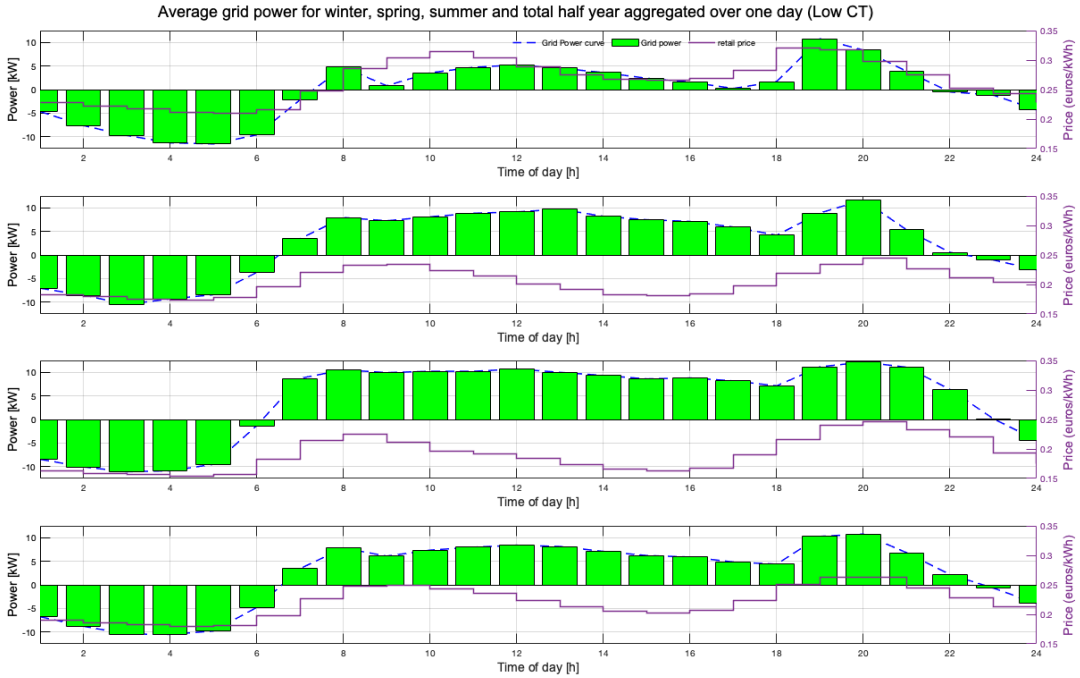

Figure 6.7: Average grid power during winter, spring, summer and overall period (from top to bottom) plotted against a period of twenty four hours at low CT

The average grid power (P_{grid}) under low CT had a similar behaviour to the situation under the case when no CT were applied. This low CT led to a subscribed capacity (P_{sub}) of 14.9 kW, which was the maximum that the grid power reached. Thus, higher the value of P_{sub}, larger the average grid power. As observed in section 5.3.8, feeding in occurred during the times of high retail price and consumption occurred during the times of low RP. However, as compared to the FIT only case, the maximum average grid power (in summer) increased when the low CT was introduced.

This increase in maximum average grid power was marginal and occurred because power was being fed back to the grid at a higher level compared to the FIT only case. A possible reason for feeding energy at a higher power could be to try and offset the additional costs C_{cap} incurred by the presence of the CT. Another possible explanation could be that the number of hours when feeding in occurred at high power, during summer, increased.

Figure 6.8 showed the avg. grid power under high CT. It should be noted that when the CT was €0.0123/kW/h, capacity subscribed (P_{sub}) was determined to be 6.21 kW. Exceeding this capacity led to addition of penalties which increased the total system costs. Thus, the average grid power (P_{grid}) reduced under the situation when the CT was high. This can be seen in the figure 6.8.

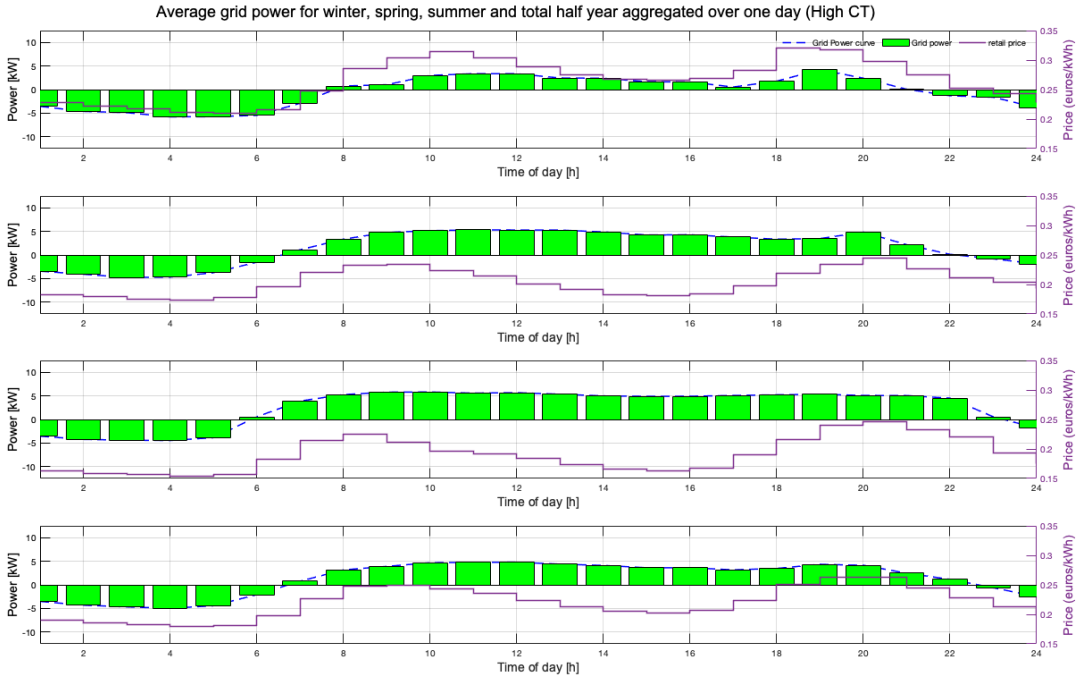

Figure 6.8: Average grid power during winter, spring, summer and overall period (from top to bottom) plotted against a period of twenty four hours at high CT

However, the consumption and the feeding in behaviour of the grid remained the same as the retail energy prices remained the same for both the cases (low and high CT). So, the feeding in and consumption pattern remain the same between the cases of low and high CT. This underscored the relevance of capacity tariff to reduce the grid power levels. On comparison between different seasons under high CT, it was observed that avg. grid feeding power was higher during a summer day compared to winter and spring. This was due to the higher PV availability during summer.

EV Power under low and high CT

In the figure 6.9, average EV power (P_{ev}) for winter, spring, summer and the total half year period was plotted after aggregating the averages for a period of twenty four hours under low capacity tariff.

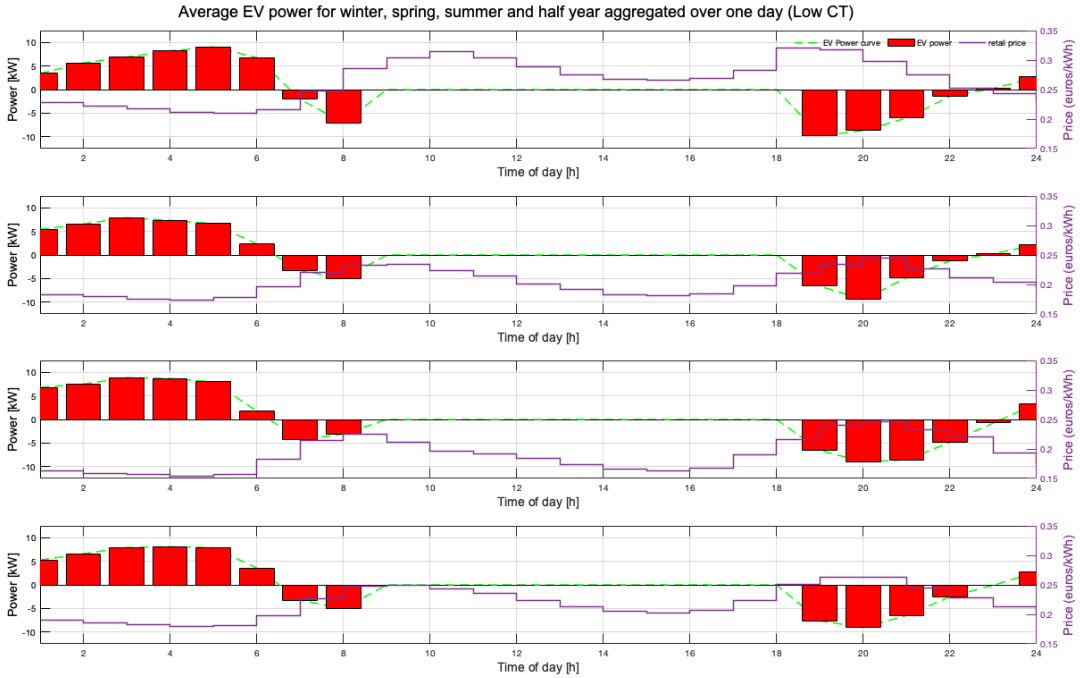

Figure 6.9: Average EV power during winter, spring, summer and overall period (from top to bottom) plotted against a period of twenty four hours at low CT

The avg. EV power (P_{grid}) under low CT had a similar behaviour to the situation under the case when no CT were applied. This was because the grid power for the low CT was high as the capacity subscribed, C_{sub} was 14.9kW. This allowed for charging and discharging of the EV battery at higher powers as seen in the case of FIT only. Charging of the battery occurred at night and discharging occurred during the evening hours of high prices. At times of peak prices, higher average discharge powers were observed.

Figure 6.10 showed the avg. grid power under high CT. As mentioned, when the CT was €0.0123/kW/h, capacity subscribed (P_{sub}) was determined to be 6.21 kW. It was seen that this reduction in subscribed capacity led to reduction in grid power. In figure 6.10, it was observed that the reduction in grid power also reduced the avg. power at which the EV charged and discharged.

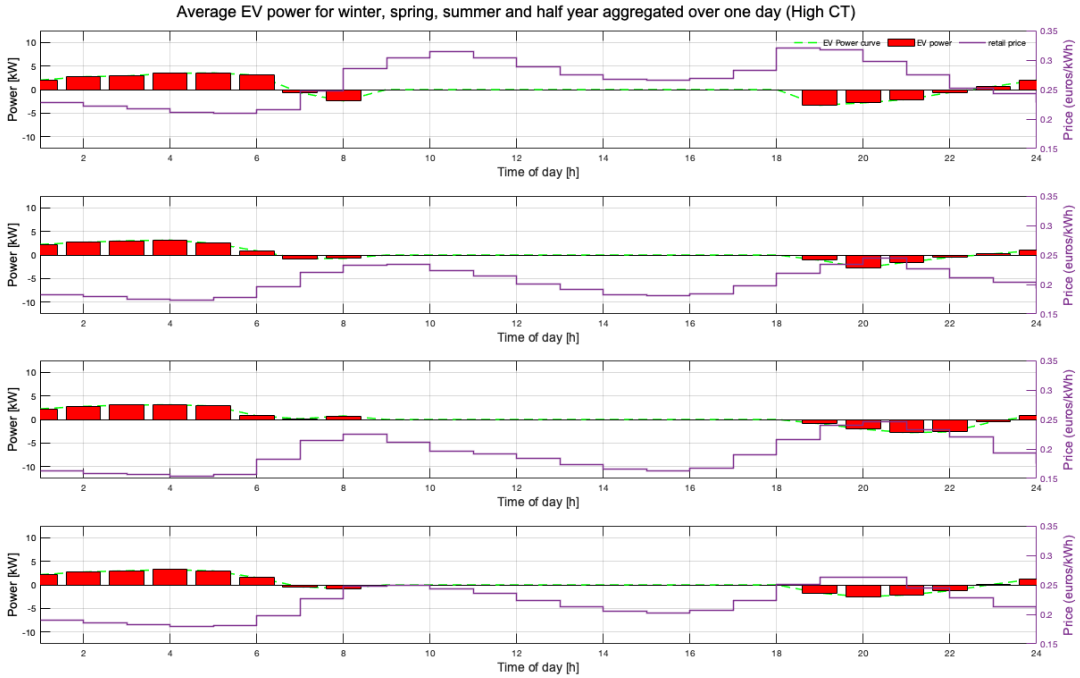

Figure 6.10: Average EV power during winter, spring, summer and overall period (from top to bottom) plotted against a period of twenty four hours at high CT

The EV charging and discharging behaviour under high CT remains the same across the seasons as observed under the case with low CT. Charging occurred at low RP during the night hours and discharging happened at times of high RP during the evening. The main difference being the average power at which these operations occurred.

Battery Power under low and high CT

In the figure 6.11, average BES power (P_{bat}) for winter, spring, summer and the total half year period was plotted after aggregating the averages for a period of twenty four hours under low capacity tariff.

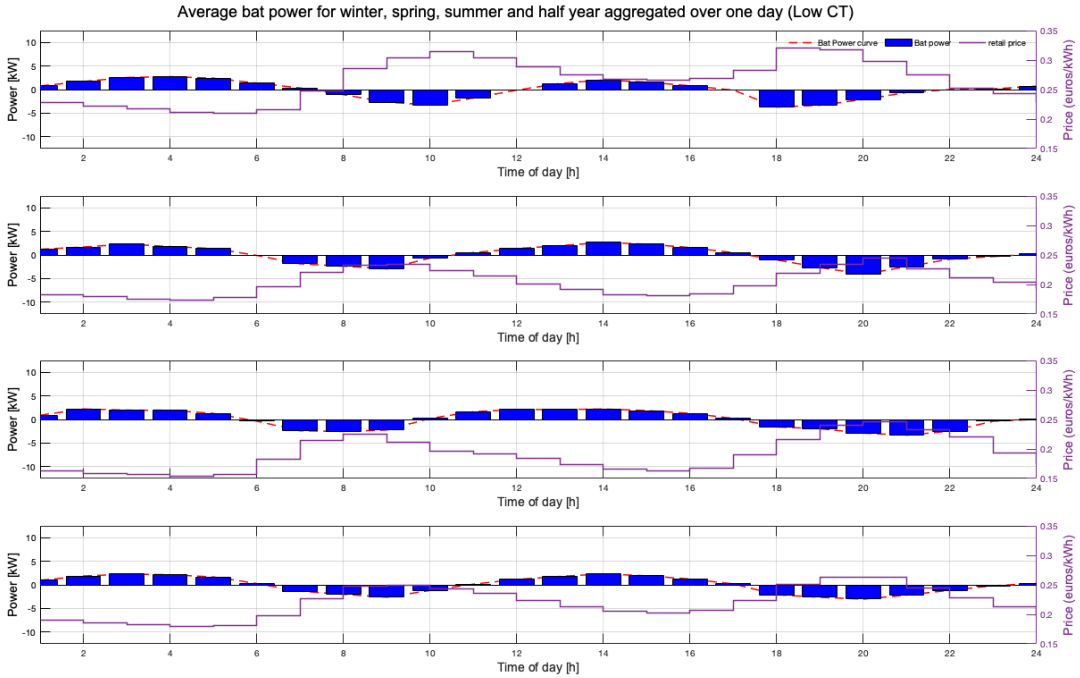

Figure 6.11: Average BES power during winter, spring, summer and overall period (from top to bottom) plotted against a period of twenty four hours at low CT

At low CT, the avg. BES power behaviour is similar to the situation of FIT only. This meant that the BES charging and discharging occurred sporadically throughout the day, depending on the prices and the PV output. Charging occurred during the middle of the day when the PV output was high and the prices were low. BES was discharged when the prices were high, during the morning hours between 08:00 - 10:00 and in the evening (between 18:00-20:00)

Figure 6.12 showed the behaviour of avg. BES power over different seasons for half a year under high CT.

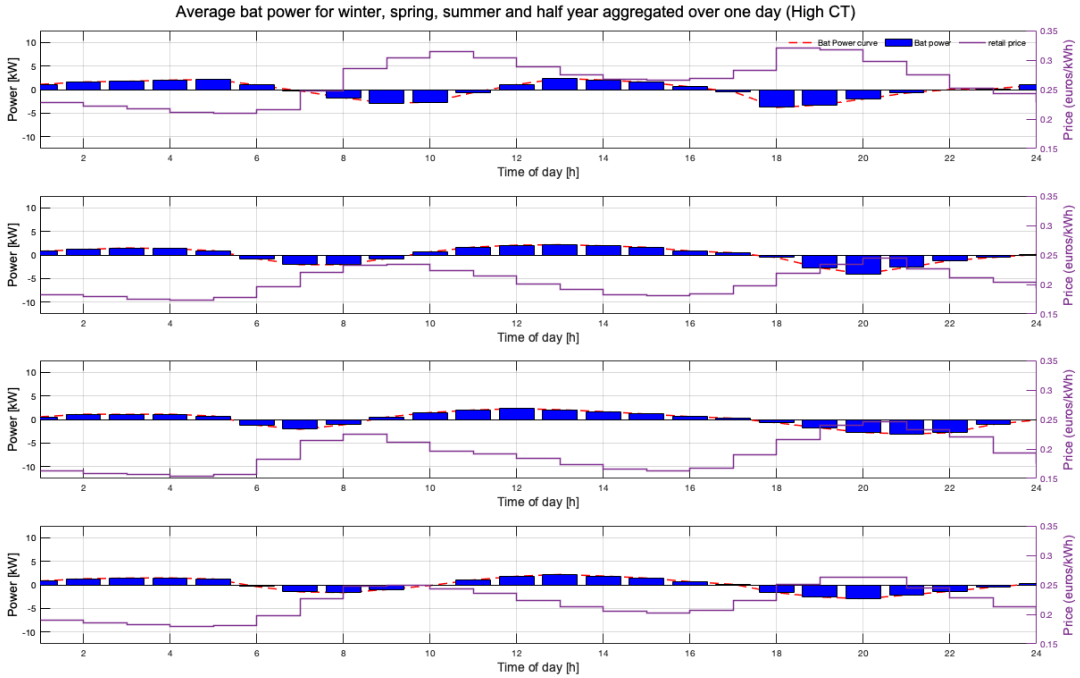

Figure 6.12: Average BES power during winter, spring, summer and overall period (from top to bottom) plotted against a period of twenty four hours at high CT

At high CT, the battery power behaviour was still similar to the case under low CT. However, certain differences were visible. The average power for certain duration reduced. The average charging power reduced during the night hours. This led to reduction in the average discharge power during the morning peak hours between 08:00-10:00. However, due to the availability of the PV power in the middle of the day and evening, the charging power during the middle of the day remained similar.

The reduction in the charging and discharging power of the EV and BES and the reduction in the average grid power level under high CT showed that the capacity tariffs were indeed able to reduce the peak grid power as desired. This reduction in the grid power, however, did not lead to any new significant changes in the behaviour of the system as the incentive to generate revenue by feeding energy back to the grid was still high. But, it proved that the capacity tariffs were able to reduce the power. It would also be useful to study the effects of such a mechanism on a grid feeder level with multiple prosumer houses described in this research with this mechanism implemented.

PV Power under low and hgh CT

In the figure 6.13, average PV power (P_{pv}) for winter, spring, summer and the total half year period was plotted after aggregating the averages for a period of twenty four hours under low capacity tariff.

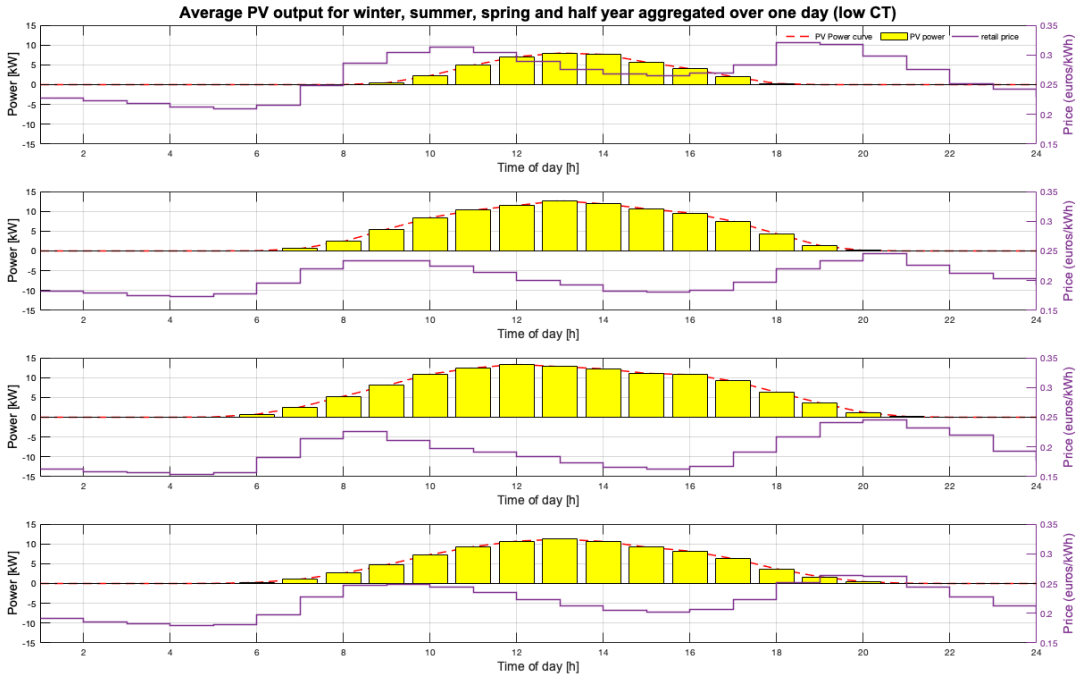

Figure 6.13: Average PV power during winter, spring, summer and overall period (from top to bottom) plotted against a period of twenty four hours at low CT

At low CT, average PV power remained the same as the case as when there was no CT implemented. This meant that the PV output was the highest during summer due to the higher solar irradiance, followed by the average PV output during spring and with average PV output being the smallest during winter. This large PV output during the periods of low load and higher irradiance allowed for feeding energy back to the grid and charging the BES simultaneously.

Figure 6.14 showed the behaviour of avg. PV power over different seasons for half a year under high CT.

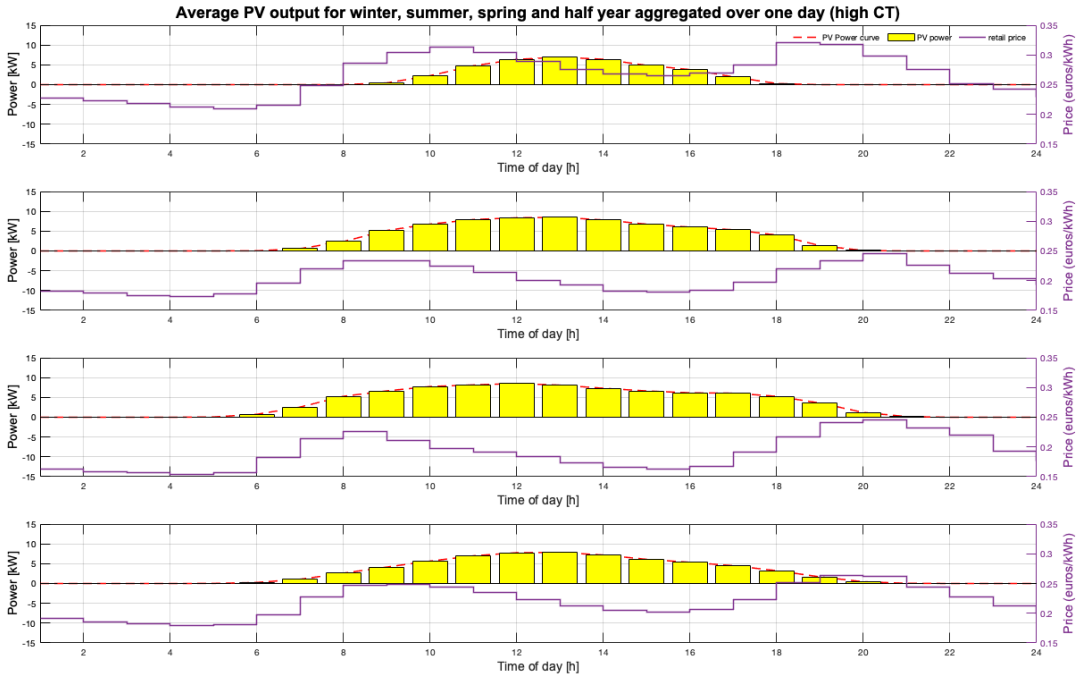

Figure 6.14: Average PV power during winter, spring, summer and overall period (from top to bottom) plotted against a period of twenty four hours at high CT

As mentioned, under high CT, the subscribed power P_{sub} reduced to 6.2 kW. This meant that surpassing this power while feeding-in or consuming from the grid would lead to penalties being added to the total operating costs. Due to this additional high cost, the PV curtailment was observed at high CT. However, it was still observed that despite this curtailment, the maximum avg. PV power was still larger than P_{sub}. This was because the PV output was used to charge the BES during the day, supply the demand and still have enough leftover energy to feed back to the grid to generate revenue.

Table 6.4: Seasonal variation in the average grid, BES, EV and PV power under FIT and low CT

	Grid P_{grid} (kW)		Battery P_{bat} (kW)		EV P_{ev}(kW)		PV P_{pv}(kW)
Season	Feeding in	Consumption	Charging	Discharging	Charging	Discharging	Average
Winter	10.76	11.51	2.73	3.70	9.02	9.80	7.97
Spring	11.65	10.44	2.67	4.06	7.88	9.43	12.64
Summer	12.15	11.07	2.32	3.32	8.85	8.99	13.4
Total	10.75	10.48	2.31	3.02	8.07	9.04	11.16

Table 6.5: Seasonal variation in the average grid, BES, EV and PV power under FIT and high CT

	Grid P_{grid} (kW)		Battery P_{bat} (kW)		EV P_{ev}(kW)		PV P_{pv}(kW)
Season	Feeding in	Consumption	Charging	Discharging	Charging	Discharging	Average
Winter	4.22	5.77	2.35	3.78	3.53	3.31	6.93
Spring	5.30	4.76	2.17	3.99	3.14	2.68	8.47
Summer	5.82	4.45	2.29	3.05	3.10	2.78	8.52
Total	4.79	4.95	2.19	2.93	3.22	2.51	7.88

Tables 6.5 and 6.4 present the various power values observed during different months.

6.4. Discussion

The results of the capacity mechanism were presented. Effects of the capacity prices on the power flow were observed. It was observed that on the basis of the prices, the subscribed capacity varied which led to changes in the total system costs. Thus, for the capacity mechanism to produce the desired results, two required parameters are the selected power level and the capacity tariff per kW per time step.

In literature, it was observed that the proposed mechanisms carry the assumption that the households have the information about their loads. de Vries and Doorman in [26] present the argument that households can determine their own optimal capacity to have under the situation of scarcity. This assumption is also seen in [42] where Bjarghov and Doorman again consider the household to know their peak consumption. However, in practice, this might not be true. As found by Mulder et. al. [2], in the Netherlands, the competition in the retail markets is present on the basis of product innovation rather than prices (of homogeneous products). This gives less incentive to keep track of consumption per household as switching suppliers would not make a big difference. Additionally, this also shows that if the consumers decide to determine their own capacity, it would lead to sub-optimal results as the variation can be quite stochastic. Furthermore, the studies do not consider EVs and BESs as an additional load requirement for the household as they are considered flexible and are charged only when the prices are low. This charging of the devices may not be always suitable for the household.

Steen in [40] propose to charge the consumers based on their peak capacity consumed from the grid. They propose distribution tariffs based on the average of the maximum consumption calculated hourly over a period of a month. The selected capacity then becomes the average of the peak values and remains valid for the entire month. The consumer is made aware of their consumption and can determine to reduce the consumption as higher peaks lead to higher costs. But a penalty mechanism is not discussed as they assume consumers to be responsive to price signals. This assumption was adopted by them because the retail electricity prices in Sweden reflect the wholesale day-ahead price and are dynamic in time. However, they assume certain household loads to be flexible and their operation can be delayed to a point in time with lower electricity costs. The loads are moved in time by manual intervention, by the residents. Moreover, they do not provide details about the EV battery such as the battery capacity and assume that the EV has to be completely charged by the departure time. V2G operation is also ignored. A control strategy is not provided and assumed that consumers will respond to price signals.

This work determined the optimal capacity which needs to be selected in order to minimize the costs to the household. This determination also took into account the revenue that was generated by discharging of energy storage devices into the grid and thus selected a capcity which allowed charging/discharging of the BES and EV for revenue generation at the lowest cost. Additionally, this control also meant that the manual intervention required by the household is quite low as the smart control determined the optimal power flow to minimize the costs. Finally, the grid power peaks were lowered using the capacity tariff rather rather than changing the consumption pattern.

There are additional methods which can be used to determine the capacity for a household. However, it is not sure if they are able to determine the optimal capacity for the household with such a system.

6.5. Conclusion

In this chapter, capacity subscription as a mechanism to reduce peak power for households was discussed. The primary reason to choose this mechanism was its capability to ensure the optimal selection of the required capacity for a particular capacity tariff. Also, this mechanism was proposed as an incentive to keep the distribution grid power levels relatively stable. As observed from the results, this mechanism led to lower grid power levels while consumption as well as feeding-in, thus ensuring the grid power peaks were reduced. It was concluded that the capacity tariff was crucial to the functioning of the mechanism and should be designed carefully.

7

Frequency Regulation

7.1. Introduction

It was seen in the literature that there exist multiple possibilities for performing frequency regulation by using distributed energy sources such as EVs and PV. In this chapter, frequency regulation using the available energy sources, namely BES, EV, and PV at a prosumer residence, was performed. The objective is to reserve optimal power for frequency regulation and provide the required power in either direction when the FCR is called. The constituent power flows are studied, and it is determined how the EMS supplies the power for the required regulation. Revenue generated by reserving power for FCR is also calculated, and the variation in the costs are also presented. From the results, conclusions on supplying power for FCR are drawn, and finally, recommendations are made.

First, the methodology and the implementation was explained. Additional constraints were added to the EMS model, which was discussed in the previous chapters. Once the method has been discussed, the simulation method is described. The implementation results are then presented, and discussion on power flows and costs are then made. Next, a discussion on the FCR process in the Netherlands, and a pilot project is done. In this discussion, challenges to prosumer households participating in FCR were also presented, and suggestions are made to overcome these challenges. Furthermore, the technical aspects of power electronic devices and Lithium-ion batteries necessary for FCR are discussed. Conclusions and further research are presented after the discussion.

7.2. Methodology

The EMS model, described in chapter 3, has been used for frequency regulation with new additions. The additional constraints are required for reserving the power by different devices capable of delivering up and down-regulation. Up-regulation refers to feeding power back to the grid to increase the frequency back to the nominal value. Up-regulation may be necessary when many local loads are suddenly connected to the grid. Down-regulation is reducing the grid frequency when excess energy fed in causes an increase from the nominal frequency. This situation can occur during instances of high FIT, leading to an increased feeding in or on a sunny day with low loads. Thus, it is essential to differentiate between the power reserved for up and down regulation as the current household loads directly impact the power that can be reserved. BES and EV can provide up and down-regulation depending upon their current, maximum, and minimum power. However, PV can only provide down-regulation power as the PV output cannot be increased beyond the current maximum power point. The FCR concept was shown in figure 7.1.

The following expressions denote the up-regulation by EV and BES.

$$P_{Up}^{EV}(t) \leq EV_{av}(t)\left(P_{EV}(t) + P_{EV}^{rated\,min}\right) \tag{7.1a}$$

$$P_{Up}^{EV}(t) \geq 0 \tag{7.1b}$$

$$P_{Up}^{bat}(t) \leq \left(P_{bat}(t) + P_{bat}^{rated\,min}\right) \tag{7.1c}$$

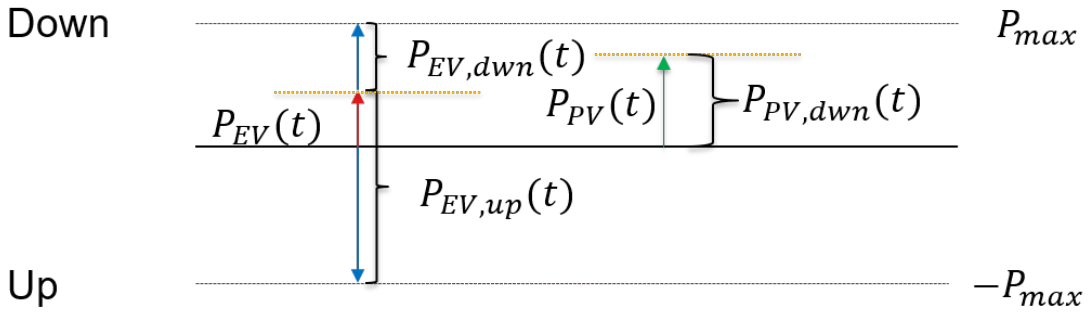

Figure 7.1: Schematic representation of FCR using PV and EV as example

$$P_{Up}^{bat}(t) \geq 0 \tag{7.1d}$$

These equations were taken from [69]. The total up-regulation is the sum of up regulation by the battery, $Pbat_{up}(t)$ and up regulation by the EV through V2G $Pev_{up}(t)$, as shown below. $P_{bat}^{rated\,min}$ represents the maximum power at which the battery can charge and the total up-regulation provided by the battery would be equal to the sum its current power and the rated power (see eq. 7.1c and fig. 7.1). Same holds true for the EV as well. It should be noted that the EV can only provide power for up or down-regulation when it is available, and the parameter $EV_{av}(t)$ denotes whether the EV is available or not at that instance. The value for $EV_{av}(t)$ is either 0 or 1, where 0 indicates the EV is not available. η_{inv} considered was 0.98.

$$P_{Up}(t) \leq \eta_{inv}\left(P_{Up}^{bat}(t) + P_{Up}^{EV}(t)\right) \tag{7.2a}$$

$$P_{Up}(t) \leq P_{inv}^{max} - P_{inv}(t) \tag{7.2b}$$

$$P_{Up}(t) \leq P_{sub} - P_{inv}(t) + P_{load}(t) + P_{heat}(t) \tag{7.2c}$$

The up regulation ($P_{up}(t)$) also depends on the current inverter ($P_{inv}(t)$) power and the max inverter power (P_{inv}^{max}). FCR beyond the capability of the inverter cannot be provided. From eq. 7.2b, it was seen that the up regulation depended on the difference between the current inverter power and the maximum inverter power. This difference represents the power that can still be supplied by the inverter. However, the current load at that instant ($P_{load}(t) + P_{heat}(t)$) also limit the power for FCR if the inverter is supplying power to these loads. But these loads can be supplied by the PV or the energy stored in the BES and EV. A final limit to be also considered was the presence of the capacity subscription (P_{sub}), exceeding which led to addition of penalties. This requirement was represented in 7.2c and acts as the grid balancing mechanism for up regulation in FCR.

The following expressions denote the down-regulation provided by the BES, EV and PV. These expressions were reproduced from [69]

$$P_{Dwn}^{EV}(t) \leq EV_{av}(t)\left(P_{EV}^{rated\,max} - P_{EV}(t)\right) \tag{7.3a}$$

$$P_{Dwn}^{EV}(t) \geq 0 \tag{7.3b}$$

$$P_{Dwn}^{bat}(t) \leq \left(P_{bat}^{rated\,max} - P_{bat}(t)\right) \tag{7.3c}$$

$$P_{Dwn}^{bat}(t) \geq 0 \tag{7.3d}$$

$$P_{Dwn}^{PV} \leq P_{PV}(t) \tag{7.3e}$$

Like up regulation, the total down-regulation offered is also the sum of the devices' individual down-regulation power. It should be noted that the PV can only provide a down regulation from the MPPT output at that instant (see eq.7.3e). Furthermore, the rated power $P_{bat}^{rated\,max}$ represents the maximum power at which the battery can discharge and thus the down regulation offered would be the difference between the rated power and battery power at that instant (see eq. 7.3c). This also holds true for the EV. Expressions 7.4a - 7.4c signify

the total down regulation and the associated grid and inverter balance.

$$P_{Dwn}(t) \leq \frac{1}{\eta_{inv}} \left(P_{Dwn}^{bat}(t) + P_{Dwn}^{EV}(t) + P_{Dwn}^{PV} \right) \tag{7.4a}$$

$$P_{Up}(t) \leq P_{inv}^{max} + P_{inv}(t) \tag{7.4b}$$

$$P_{Dwn}(t) \leq P_{sub} + P_{inv}(t) - P_{load}(t) - P_{heat}(t) \tag{7.4c}$$

Like Up regulation, the total down regulation ($P_{dwn}(t)$) also depends on the current inverter power (in eq. 7.4b). However, as stated, for consumption from grid, the inverter power $P_{inv}(t)$ was denoted with a negative sign, which explained the addition with the maximum inverter power P_max. Furthermore, the logic used for the grid balance (in eq. 7.4c) was the same as the total consumption at that instant subtracted from the subscribed limit P_{sub}.

The total costs for regulation are calculated as follows [69]

$$C_{reg} = (1 - \epsilon_{fc}) \eta_{inv} \eta_{ch} \sum_{t=1}^{T} \left(P_{Up}(t) \cdot \lambda_{Up} + P_{Dwn}(t) \cdot \lambda_{dwn} \right) + Comp \tag{7.5}$$

Here, ϵ_{fc} was assumed to be zero and it represented the forecasting error between actual and reserved capacity. λ_{Up} and λ_{dwn} represent the revenue obtained for reserving powers $P_{up}(t)$ and $P_{dwn}(t)$ respectively. However, ϵ_{fc} will not be zero in practical applications and to offset these errors, $Comp$ was introduced. Since the value of ϵ_{fc} was assumed to be zero, $Comp$ was also zero.

The resulting regulation costs need to be subtracted from the total costs as revenue is generated when the power is being reserved. In certain regulation markets, including in the Netherlands, the power reserved for FCR needs to be symmetric. This constraint means that the power reserved for up-regulation should be the same as the power reserved for down-regulation during an auction period. The following expression does this:

$$P_{Up}(t) = P_{Dwn}(t) \tag{7.6}$$

Thus, the objective function now becomes

$$min(C_{total}) = min(C_{bat} + C_{EV} + C_{PV} + C_{grid} + C_{int} + C_{inv} + C_{cap} - C_{Reg}) \tag{7.7}$$

It should be noted that the FCR markets are real-time markets, but the auction for FCR happens similar to the day-ahead markets, and the BSPs have to submit their bids on a day-ahead basis. Thus, the EMS should provide the power it intends to reserve for FCR a day before the actual FCR delivery date (Ideally, it should happen by forecasting the generation on the next day). In the FCR market set up in the Netherlands, the BSPs also receive remuneration for reserving the contracted power for FCR even if they are not called to deliver the power. TenneT creates a merit order of BSP assets for FCR based on the bids, and the BSPs are called to provide the power based on this merit order. Remuneration for FCR is based on the highest marginal price of all awarded bids, if this price is higher than the cross-border FCR cost. If the cross border marginal cost is higher, then the remuneration is set to that value. The cost of providing FCR, however, has to be borne by the BSP. Thus, the BSP obtains the FIT if the energy is fed back to the grid to deliver up-regulation or pay the retail price for consumption in case of down-regulation.

Once the EMS provides the information about the reserved power to the aggregator, the aggregator decides which assets to use for FCR provision on the following day. The aggregator can divide the power for FCR between various assets and provide setpoints on the day of delivery. These setpoints are an additional input to the EMS system and can be considered additional grid supply and demand. Since the required regulation has to be reflected on the grid power levels, the EMS decides optimal BES, EV, and PV power values for providing the up and down-regulation. This operation also ensures that the power flow obtained after frequency regulation is also optimal, and the costs to the household are minimized. Finally, it should also be noted that up, and down-regulation cannot be provided simultaneously.

7.3. Results

From the simulation results, it was seen that the EMS reserves the power at different time steps. This power is reserved day ahead of the intended day of FCR delivery. It was seen that the reserved power depends on the current BES, EV, PV, uncontrolled load, and grid power levels. Since the demand and the PV generation vary hourly, the reserved power also changes in line with these variations.

Since the day considered for frequency regulation was sunny, much of the generated PV power was being fed back into the grid. For this simulation, the difference between FIT and the retail tariff considered was 10EMS chooses the minimum value between up and down reserve power and that value becomes the reserved power for that instance. The symmetric constraint is being used so that the net FCR power is zero, which is a requirement in certain FCR markets [51]. Furthermore, the symmetric constraint led to picking up the lowest value among the up and down-regulation and assign it for both.

Power flows for when the FCR is reserved compared (figure 7.3) to when FCR is not reserved (figure(7.2)) also showed differences. These differences occur due to the role of FCR in revenue generation and minimizing the costs. When FCR is not considered for minimizing the costs, it was seen that the power is fed back to the grid whenever profitable based on the FIT at that instant. The energy was consumed from the grid whenever the retail price was low. However, this behavior changes when the revenue generated from reserving power for FCR is also considered to minimize operational costs. Now an additional revenue component is added to the objective function. This addition resulted in EMS determining the optimal consumption from the grid at any instant so that the total cost was minimized. These changes in grid consumption consequently also affect the BES and the EV power flow as well, and the observed changes are visible in the power flows. The differences in power flow when power was reserved for FCR compared to when power was not reserved for FCR can be seen in the following plots.

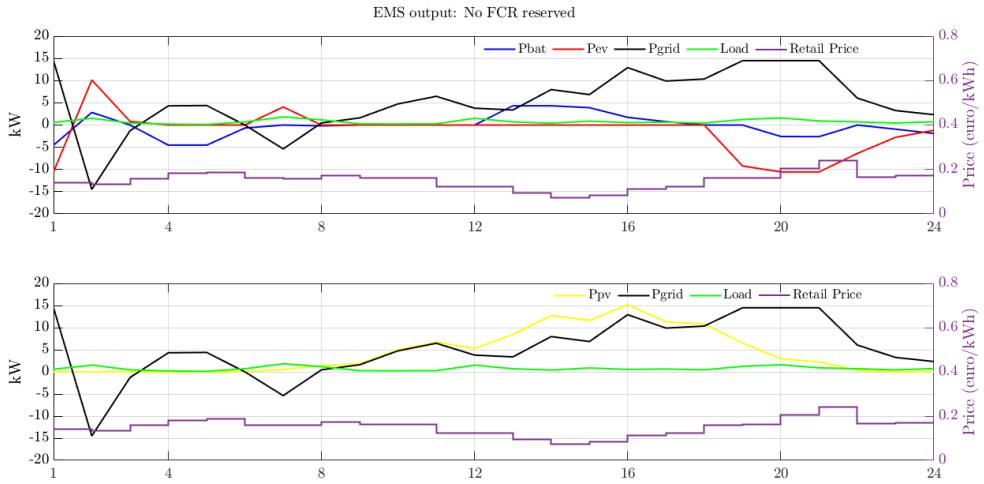

Figure 7.2: Power flow when power for FCR was not reserved

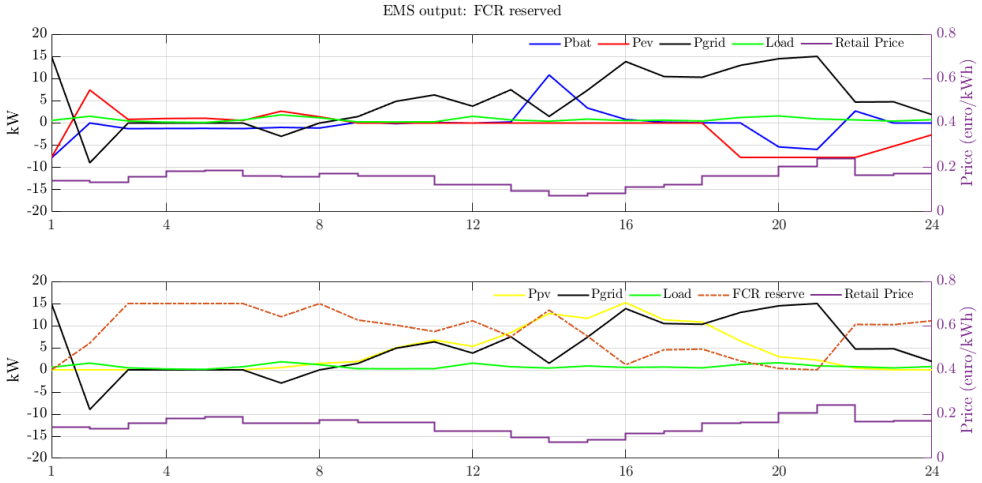

Figure 7.3: Power flow when power for FCR was reserved

It should also be noted that if the symmetric constraint is not used, the revenue generated by FCR would be even higher. Furthermore, up-regulation is more profitable than down-regulation because the energy needs to be fed into the system for up-regulation. This feeding of energy leads to additional revenue generation in the form of FIT. However, down-regulation can also be cost-effective if the excess grid power is being used to charge the BES and the EV, which are then discharged to the grid during the period of high FIT.

Finally, different load and generation situations can affect the power reserved for FCR in various ways. The generation and the load data were already known in this work, but the practical applications could be more complex.

7.3.1. Comparison with uncontrolled case and other controlled cases

For the comparison with the uncontrolled case, FIT only, FIT with capacity mechanism, the FCR reserve was calculated over a period of six months and the prices taken for FCR calculation were obtained from (cite: german FCR citation here) for the year 2018. The effects of FCR on the system costs, grid costs, EV cost, BES costs and the power consumption level were considered. The sizing used for FCR can be found in table 5.3, but the addition was the presence of the CT which was considered to be €0.0015/kW/h.

Addition of the FCR mechanism led to significant changes in the costs of the system. FCR being a revenue generating mechanism, provided the EMS incentive to reserve the optimal amount of power at any instance to reduce the costs. This also meant reduced feeding power or consuming power from the grid at times when it was more profitable to reserve the power for regulation. This behaviour of not feeding energy back or consuming energy from the grid at certain instances where the EMS would have fed back/consumed energy under the absence of FCR mechanism led to the changes in power flow which were visible in the figure 7.2 and figure 7.3.

The total grid costs C_{grid} for the system under FCR was determined to be €-1880.23. This is significantly lower than the grid costs under the uncontrolled case which was found to be €-544.20. This decrease in the grid costs between the uncontrolled case and the control with FCR was 245.5%. On comparison with the case when there was no CT and a low CT case, grid costs actually increased. This increase was of 19.38%. This was explained by the behaviour of the EMS not to consume/feed energy to reserve larger power for FCR and thus generate revenue at the instances when FCR was more profitable.

The inverter and the PV costs (C_{PV}, C_{inv}) remained the same as the system size does not vary for either of the cases. However, the BES and the EV costs under the FCR mechanism varied. The BES costs (C_{BES}) increased to €384.08 when FCR was implemented, up from a cost of €302.07 under FIT only and low CT. This was an increase of 27.1%. The EV costs (C_{EV}) under FCR reduced to €795.74 from €986.65 when there was no CT. This decrease was of 24%. The EV costs under FCR increased on comparison with the uncontrolled case

(from €691.27 to €795.74), which was an increase of 15.11%. These deviations in BES and EV costs from the FIT only and low CT cases occurred due to the incentive provided by the FCR market for reserving the power.

The total system costs (C_{total}), however, reduced for the case when FCR was added. The system costs were found to be €-146.44 for the FCR case. This was a reduction of 428.61% compared to the no CT case, 630.2% reduction compared to the FIT plus low CT case, and a reduction of 1205.07% compared to the uncontrolled system. The additional revenue due to FCR was determined to be €1256.01.

Furthermore, the grid power levels remained the same as for the case when FCR was added as FIT only and FIT with low CT cases. This was also explained by the decision of the EMS to reserve the maximum power to maximise the revenue FCR which required reserving higher grid power. Thus, the subscribed capacity, P_{sub} also remained at 15kW. The costs are summarized in table 7.1

Table 7.1: System cost comparison with the addition of FCR

	Uncontrolled case	FIT Only with control	Low CT and control	FCR with control
Inverter Costs (C_{inv}, €)	121.06	121.06	121.06	121.06
PV Costs (C_{PV}, €)	1350	1350	1350	1350
EV Costs (C_{EV}, €)	691.27	986.651	993.31	795.74
BES Costs (C_{bat}, €)	-	302.07	303.03	384.08
Grid Costs (C_{grid}, €)	-544.20	-2321.65	-2332.18	-1880.23
System Costs (C_{total}, €)	1618.27	481.22	776.45	-146.44
FCR revenue (C_{reg}, €)	-	-	-	1256.01

7.3.2. Seasonal Analysis of FCR

Seasonal analysis to understand how FCR affected the power flows during various periods of the half year was also performed. This analysis was similar to the ones which were observed in chapters 5 and 6. The system size used for the FCR study was the same as mentioned in 5.3. For the seasonal analysis, the simulation was performed over the period of half a year with dynamic prices. As mentioned earlier, the FCR prices were obtained from the German FCR market for the year 2018. It is also worth mentioning that the FCR was reserved on a weekly basis in 2018 which has since changed to a period of four blocks with varying hourly prices in July 2020. The FCR prices, however, used in this research varied weekly. Additional to the FCR prices, a FIT of 10% was considered and a CT of 0.0015 €/kW/h was also considered.

First, the effects of introducing the FCR prices were observed and discussed. The method in which the analysis was performed remained the same as discussed for FIT only case and FIT with CT case.

Grid Power

Figure 7.4 represents the grid power when FCR mechanism was added.

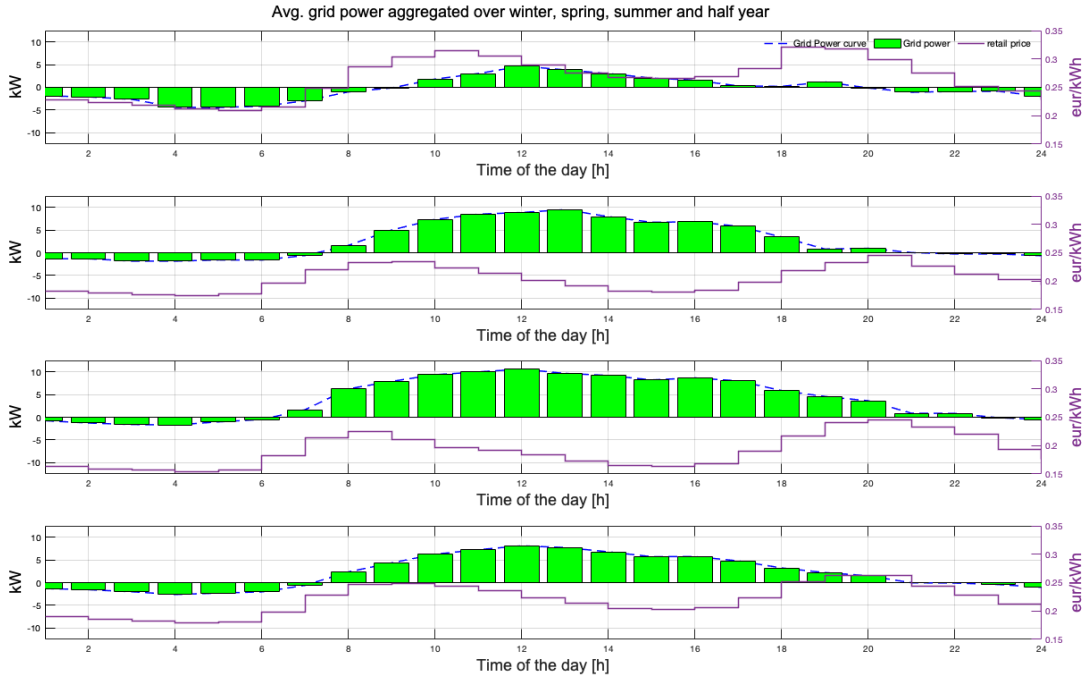

Figure 7.4: Average grid power during (top to bottom) winter, spring, summer and overall period plotted against a period of twenty four hours

Compared to the cases of FIT only and FIT along with low CT (refer figures 5.14 and6.7), significant changes were observed in average grid power when the FCR mechanism was introduced. The average grid consumption and feeding in power had reduced significantly. This was because less energy was consumed from the grid to charge the BES and the EV battery. Since less energy was consumed from the grid to charge the batteries, the feeding in observed was also lower.

Feeding-in and consumption of power from grid does occur at the times of high and low RP (and thus FIT) but the average power had reduced. The power in winter does not exceed 5kW when FCR mechanism was introduced but exceeded upwards of 10kW when only FIT and low CT were considered. Furthermore, it was observed that the feeding in power had reduced significantly during the evening hours. This feeding in behaviour reduced because just reserving power resulted in revenue generation. Largest feeding in grid power were observed during the summer period. This happened because of the large PV output which was sufficient to charge the BES and the remaining power was fed back to the grid to generate revenue. Therefore, in conclusion, presence of FCR mechanism also led to reduction in the grid power level without addition of extra costs.

EV Power

Figure 7.5 showed the resulting average EV power over different periods when FCR was introduced.

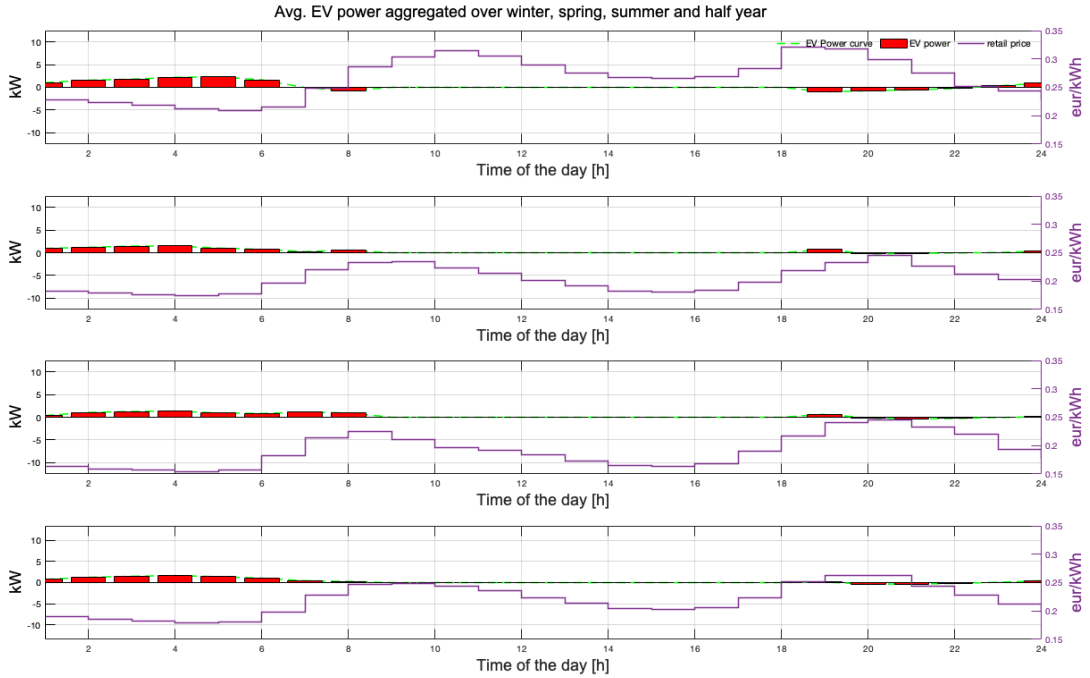

Figure 7.5: Average EV power during (top to bottom) winter, spring, summer and overall period plotted against a period of twenty four hours

It was observed that on average, charging and discharging power of the EV had reduced. The charging and discharging power level were even lower than the average EV power (observed in the figure 6.10) under high CT. Thus, the introduction of FCR led to significant reduction in both the charging and discharging power of the EV battery. As discussed in the chapter, the total power that could be reserved for FCR depended on the current device ($P_X(t)$ where x = BES, EV and PV) power and their maximum rated power. If the current power output of the device was rather high, it would result in lower power being reserved for regulation in that particular direction. Thus, if the battery is being charged at a high power, it would result in lower power being reserved for up regulation while if it is discharging at a high power, it would result in lower power being reserved for discharging. Since equation 7.6 describes that the power reserved should be symmetrical, it is desirable to have a lower device power at all times to maximize the power being reserved. Larger the power reserved, higher the revenue that was generated as determined by the equation 7.5. To maximize this revenue and thus reduce the total costs, the EMS decides to reduce the charging and the discharging power of the EV.

Furthermore, as the average EV power under FCR was low, the battery degradation had reduced significantly when compared to the situation of FIT only and FIT with low CT. This reduction in battery degradation meant that the operational costs were also low. With this observations, it was concluded that having low power levels for EV was more profitable and reduced the costs. However, it should be noted that V2G operation did occur during the winter time when the FIT was high in the evening. But this was significantly lower than observed under previous cases. In spring and summer, it was observed that the V2G operation had reduced further. This occurred due to the high PV availability which meant that significant feeding in had already occurred during the day and EV was preferred to reserve power. EV degradation when FCR was introduced was determined to be 0.682 kWh, down from 0.84 kWh observed under the case with only FIT and low CT. Total EV costs had reduced to €715.59 when FCR was introduced, down from €985.

Battery (BES) Power

Figure 7.6 represented the average BES power for the period of six months when the FCR mechanism was implemented.

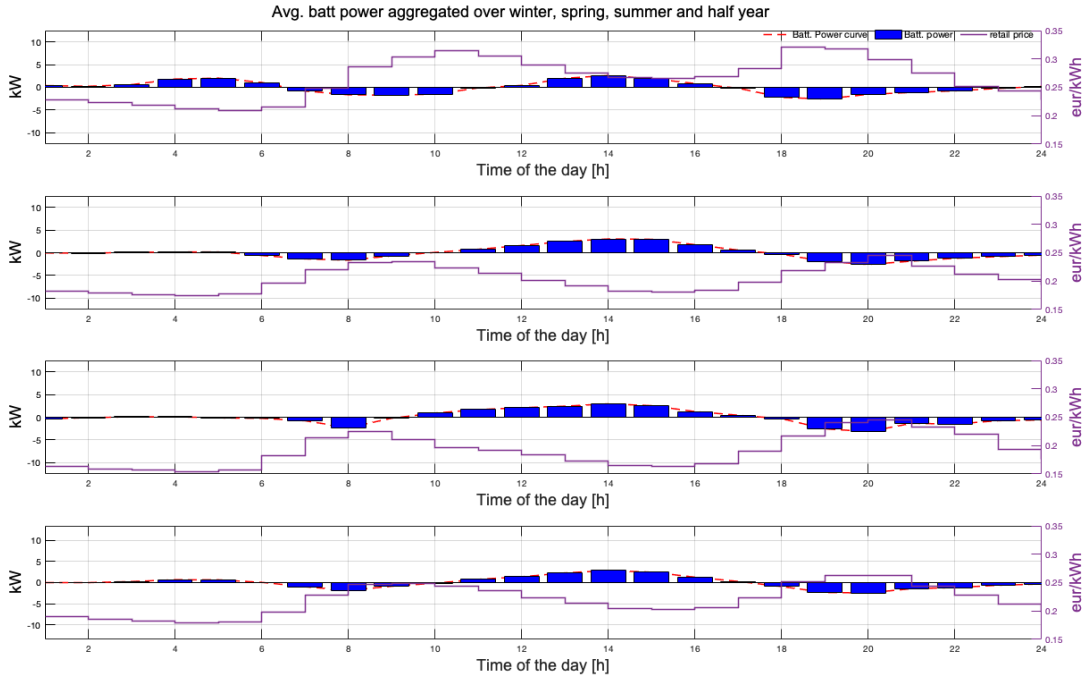

Figure 7.6: Average BES power during (top to bottom) winter, spring, summer and overall period plotted against a period of twenty four hours

Average BES power over the period of six months remained similar to the case when only FIT and FIT with CT were analysed. BES was charged during the time of low prices in the night and discharged during high prices in the evening during the winter months. BES was also charged during the day depending on the PV output available at that instant. However, during the periods of spring and summer, it was observed that BES was not charged by using the grid power during the night, but rather using the PV energy generated. The reason for this behaviour was to be able to reserve maximum power for FCR during those hours as explained in under the EV power flow.

Additionally, the reduction in charging power during the night also meant that there was lower BES degradation observed when FCR was introduced. The total degradation for the period of six months was observed to be 0.22kWh which was lower than 0.27kWh observed under the case of FIT with low CT.

PV Power

Figure 7.7 represents the average PV power over the different seasons for a period of six months.

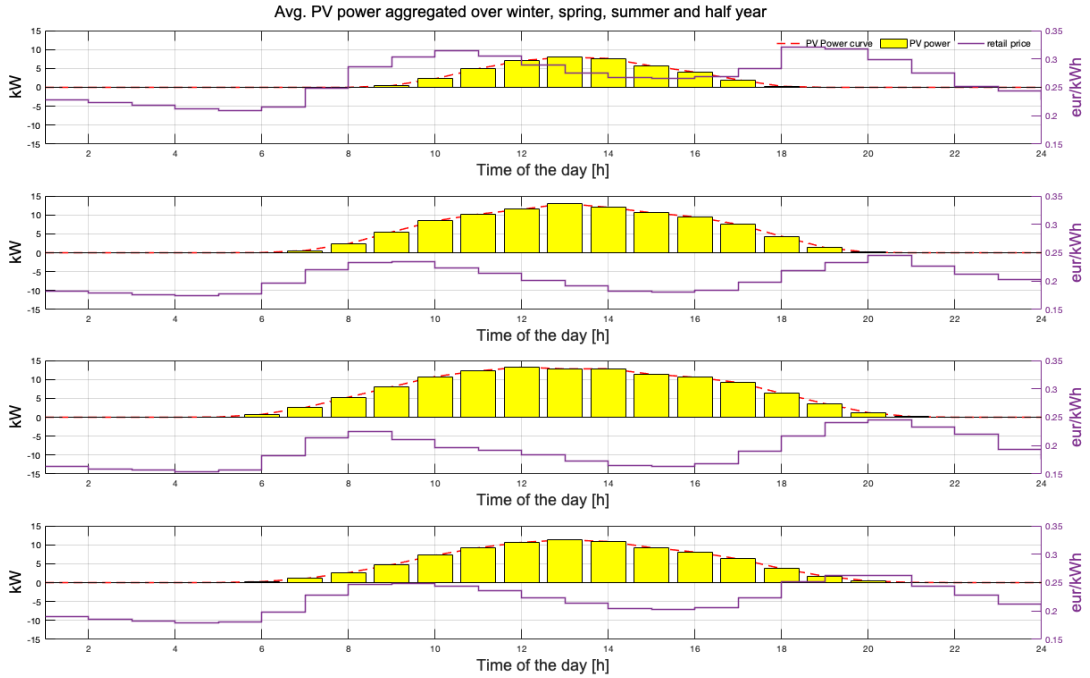

Figure 7.7: Average PV power during (top to bottom) winter, spring, summer and overall period plotted against a period of twenty four hours

PV output is not really affected by the addition of the FCR mechanism. This was because PV helped in reserving power for down regulation. Thus, larger the PV output available, larger the power reserved by the PV system for down regulation. This phenomenon was observed due to the equation 7.3e and thus, no curtailment occurs unlike the situation when high CT was applied. Seasonal variations observed were as expected with the summer average output being the largest and the winter average output being the lowest. The leftover PV output after charging the BES during the day hours was fed back to the grid to generate revenue, which could be observed in the average grid output power during spring and summer.

Reserved power variation

Figure 7.8 showed the variation in reserved power (both up and down) over different seasons during the period of half year. It was observed that the maximum power reserved was during the months of spring and summer with values reaching to almost 15kW. This is why the subscribed capacity (P_{sub}) chosen by the system was 15kW when FCR was introduced. The trajectory of the reserved power curve remained similar for all the seasons. The highest reserved power were observed during the early morning and the night hours. This phenomenon was observed because the PV output during those times was the least and thus the grid was not being used to feed energy back to the grid. However, as the PV output increased through the course of the day, the reserved power reduced with the maximum dip occurring between 12:00 and 13:00 during different months. It was observed that the dip during winter was not as prominent as observed during other seasons.

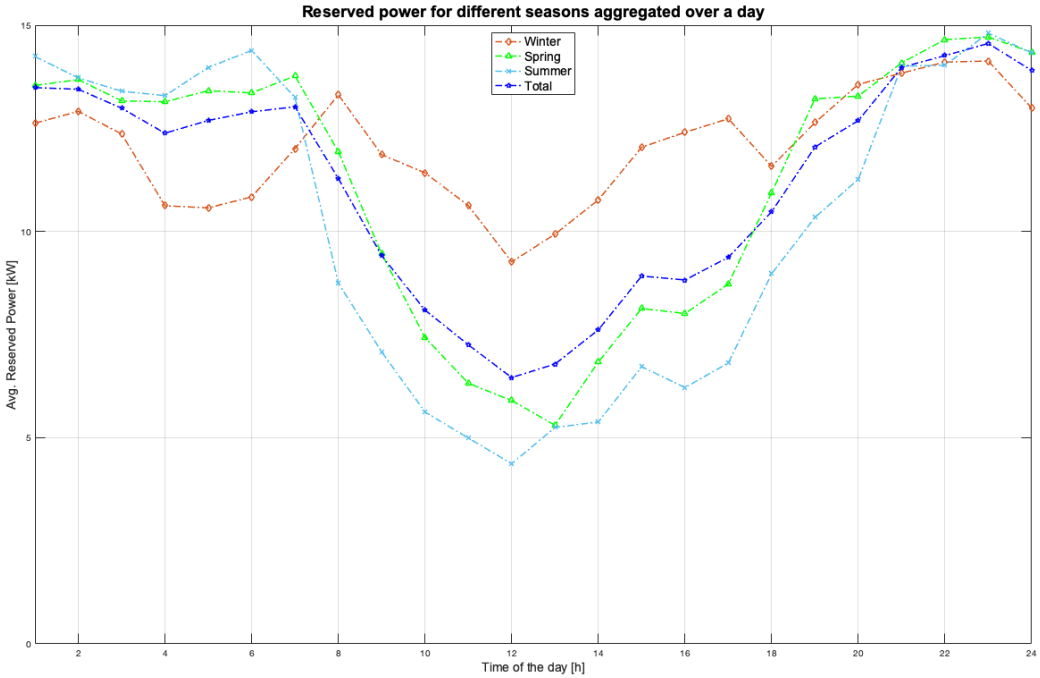

Figure 7.8: Average up and down power during (top to bottom) winter, spring, summer and overall period plotted against a period of twenty four hours

This was because the PV output was low on average during winter. Higher the average PV power, larger the feeding-in thus resulting in lower avg. reserved power at that instant. Furthermore, it was also observed that there was significant dip in reserved power at 04:00 during winter. This was because the average RP was low and as observed from figure 7.5, EV charging power was the highest on average at this time during winter. Thus, the lower reserved power. During spring and summer, from figure 7.6, it was observed that the BES charging had reduced quite significantly during the early hours and thus higher power on average was reserved during these months. Additionally, from figure 7.4, it was observed that the feeding-in was largest during the afternoon hours during spring and summer, and as already seen, this led to reduction in reserved power during the afternoon. It was also observed that during winter, the average grid consumption in the morning was higher than the average grid consumption during spring and summer and thus, lower power was reserved during the morning hours.

Table 7.2: Seasonal variation in the average grid, BES, EV and PV power when FCR was introduced

Season	Grid Power(P_{grid} kW)		EV Power(P_{EV} kW)		Battery Power(P_{bat} kW)		PV Power(P_{pv} kW)
	Consumption	Feeding in	Charging	Discharging	Charging	Discharging	Average
Winter	4.428	4.675	2.32	0.99	2.61	2.55	7.97
Spring	1.85	9.49	1.45	0.23	3.04	2.59	12.99
Summer	1.71	10.59	1.36	0.31	3.17	2.95	13.23
Total	2.61	8.11	1.67	0.37	2.45	2.87	11.29

7.4. Discussion

Up and down-regulation for a single day was observed in the results. It was seen that the grid power values change based on the time of provision of up or down-regulation. However, it is essential to discuss various FCR market requirements. As explained, FCR plays a critical role in grid stability and ensuring the power supply to consumers. Thus, the assets being used for frequency regulation need to deliver the contracted power within seconds. The requirements were discussed in the literature review and have been obtained from [51].

One of the essential requirements is that the asset should deliver the full contracted power within thirty

seconds after the FCR is called. The asset must deliver half of the contracted power within fifteen seconds and the power ramping between fifteen and thirty seconds should be linear. TenneT says that all the assets which are being used for FCR must meet this requirement. This requirement entails that the devices which are being used for FCR should have a high response time. The response time for a Tesla Power Wall, for instance, is 10 seconds, which allows for maximum power delivery within 10 seconds [71]. Therefore, commercial storage devices like Tesla Power Wall can effectively deliver the power required for FCR. Li-ion batteries have shown even shorter response times of magnitudes in the order of milliseconds. Thus Li-ion batteries can be used for frequency regulation. Research has also been done to prove their usability for FCR [55], [56]; however, their degradation remains a concern. But, it was observed that using this EMS, the degradation remained rather quite low compared to the case when FCR was not reserved.

Moreover, it is also crucial to determine the system's latency between the aggregator and the EMS. If a setpoint takes too long to be available to the EMS or if the EMS takes too long to respond, the FCR delivery gets affected as it is a time-critical process.

The minimum power that needs to be offered for the FCR by the BSP is 1MW. Additional power can then be offered in the steps of 0.1MW to a maximum total of 150 MW. This base power can either be obtained by a single RPU or multiple RPUs to form an RPG. However, the aggregator should prove that the assets can deliver this power. This can be challenging if there are numerous RPU assets, as the testing would be quite complicated. For example, if EVs are being used to provide frequency regulation, it should be shown that the fleet of EVs can supply the required FCR during the tests. Furthermore, it should also be shown that there would indeed be the necessary number of EVs when FCR is needed. If the EVs are not capable of V2G, only down-regulation would be possible, dependent on the maximum usable SoC of each vehicle.

Furthermore, TenneT also specifies that the BSP should have the entire FCR power available for the complete auction duration. The current auction duration lasts for 4 hours (as of July 2020). This requirement means that whether the BSP delivers the power or not, the assets must be available to supply the power for the entire auction period. The accepted bids are called based on the merit order created by TenneT, based on the marginal costs for delivering the FCR. The BSP gets paid for reserving the power based on the highest accepted marginal price. If multiple residences are being considered to be an asset for delivering FCR, this would mean that the aggregator would have to make sure that these households reserve the contracted FCR for the auction period. Depending on the delivery time, this might not be feasible due to the stochastic nature of household loads. However, this could be avoided if the pool of assets being used for FCR is large enough but can lead to higher operational costs.

The product specifications and requirements differ for energy-limited and energy unlimited sources. Energy unlimited sources are the sources that can continuously provide support without interruption and include baseload plants such as coal power plants. As the name suggests, energy-limited sources can only deliver power for a short duration before they need to be charged to supply power for FCR. Energy-limited sources include BES and EV in this research. TenneT states that the energy-limited sources must provide the full power in the events of a frequency deviation of 0.2 Hz for at least fifteen minutes. If the variation is smaller, then the energy-limited sources must provide the proportional FCR support for a proportionally longer period. Once the FCR has been supplied, energy-limited devices have two hours before they are required to have the contracted FCR once again. The aggregator may choose how to distribute the contracted FCR between their assets but has to note the individual preferences and household requirements. This allocation can be done using an optimization problem similar to the classical economic dispatch but with customer choices as additional constraints to reduce the costs.

Additionally, the real-time power values of assets during the contracted time of FCR provision also needs to be shared with TenneT. These values should have a refresh rate of at least 4 seconds or better, and the power value (in MW) with at least three decimal points must be shared. A maximum inaccuracy of 1% is allowed in the values. The data exchange can occur either via a dedicated leased line or via the web service setup by TenneT. The leased data line must exchange the value using the protocol IEC 870-5-101 or IEC 870-5-104. In using leased lines, two channels must be set up; one to exchange the data normally and the other as a backup in case of interruptions. The BSP needs to store the relevant asset FCR delivery and reserving data for at least six months after the date of delivery.

The bidding for FCR can begin up to two weeks before the intended date of delivery, and the bidding closes at 8:00 CET the day before the delivery. If the contract has been awarded to the BSP, the BSP must reserve the contracted power for the entire reservation period. As mentioned, the BSP can divide the FCR power among its assets. However, the individual assets should also be known to have qualified the pre-qualification tests. Allocation of the awarded power among the BSP assets needs to be shared with TenneT on D-1 before 17:00, where D is the day of delivery. Changes in the allocation are also allowed, but this has to be intimated to TenneT before actual delivery. This requirement means that the BSP must decide the assets that will be used for FCR delivery/reserving power well in advance. However, if, for some reason, the BSP chooses to change the assets to deliver FCR, the BSP must send a new allocation message with the updated details. Moreover, it is also possible for the BSP to subcontract the power in case the BSP is not able to deliver the reserved power for FCR. The minimum power that the BSP can subcontract is 100 kW, and the increments also need to occur in the steps of 100 kW.

From the discussion, it can be concluded that ideally, the BSP would require a large and technically diverse pool of assets for participation in the FCR market. Power electronic converters such as the multi-port converters, DC chargers for EVs, and inverters for PV integration make use of fast switching semiconductor devices such as IGBTs and MOSFETs. These devices have rapid switching times (in the order of ms), which allow the change of the power levels rapidly and thus can be used to provide the required FCR. However, it is also essential to identify their operational costs for FCR provision. Since the components might have different operational costs based on their operational behavior, the BSP needs to determine an efficient way to reimburse their services, which is also fair. It should also be noticed that while using dynamic prices that vary in time, for specific instances, it would be more profitable if the energy is being fed back to the grid rather than being reserved for FCR.

To test the suitability of using renewable energy and storage for FCR, TenneT performed a pilot study in 2017-2018 with various organizations that acted as aggregator BSPs [62]. This study's objective was to identify the challenges and the capability of an aggregated pool of sources, such as renewables and demand response, to provide FCR. Furthermore, the barriers to entering the FCR market were also investigated. To this end, several deviations were considered in the existing market for the pilot. Firstly, the minimum bid size for the pilot participants was reduced to 100kW from 1 MW. Furthermore, assets used for the project were already prequalified and were allowed to deliver the power for FCR. The FCR power allocation was done weekly by sending an email to TenneT, which is different now as the FCR allocation happens daily. Finally, all the participants' bids were accepted, which happens via an auction in the regular market. It should also be noted that for the pilot, participants were not penalized for non-conformity.

The pilot project's main conclusions were that the aggregated assets could provide the required power for FCR, but certain barriers were also found. One of the critical barriers was found in the form of relaying data in real-time to TenneT. Setting up a leased line for communication proved challenging when multiple technical installments are providing FCR. To overcome this barrier, TenneT decided to set up a web-based service to transfer the asset data to TenneT once or twice a day. However, it should be noted that web-based services are prone to errors and privacy issues, which should be carefully considered while participating in the FCR market. Another challenge was the dependency of the assets on third parties. The aggregator can control various remote sources via their control; however, the aggregators do not own the assets. This situation can cause dependencies on third parties for installing hardware for measurements and cause delays and errors.

It was also found that the pilot participants had challenges in meeting the minimum bid requirement of 1MW. However, after the pilot project, TenneT decided not to change this minimum power requirement to participate in the FCR market. This decision was taken due to transaction costs to TenneT and the lack of a positive business case for the BSP. Additionally, this was not done because of the changes applied to the bidding period (which has been lowered to 4 hours from a week) and the measurement requirements. But there are possibilities that TenneT would reduce the bid requirement from 1 MW in the future.

7.5. Conclusion

It was seen that the EMS was able to reserve the optimal power for FCR in this chapter. The optimal power to reserve was determined based on the instantaneous power of EV, PV, BES, Inverter power, and the maximum deliverable power. The power reserved for FCR leads to additional revenue generation, which leads to a decrease in system costs. Thus, it was observed that the larger the power reserved for FCR, the higher the revenue generation. This was reflected by comparing the total system costs when the FCR power was reserved against the same day when FCR power was not reserved. A trial simulation of FCR power delivery was also done by assuming that the instances and the amount of power required were known. It was observed that the EMS was able to deliver the required FCR power. The process for FCR delivery in the Netherlands and challenges to deliver FCR using aggregated sources were also discussed. Challenges mainly exist in the form of the minimum power requirement for FCR, data communication with TenneT, and reserving the contracted power for four-hour blocks if stochastic sources are used. Challenges also exist for the optimal allocation of resources, which can be solved by modified unit commitment problems. Pre-qualification of individual assets can also be a challenge; however, if there are multiple assets of similar characteristics, pre-qualification tests for one asset can be performed as the other assets would have similar behavior. Finally, a large pool of assets will be necessary for FCR provision and backup if they have a stochastic behavior. This can be solved by providing a baseline power delivery behavior and monitoring based on this baseline.

8

Discussion

8.1. Introduction

Different market mechanisms were discussed in this research. The effects of Feed-in tariff (FIT) on system sizing and power flow were discussed. Capacity Mechanism (CM) was discussed and its effects on power flow of the system was observed. Finally, the Frequency Containment Reserve (FCR) market in the Netherlands was also discussed and a method to reserve power in FCR market was also seen. However, these mechanisms would work concurrently in a future scenario. The costs arising due to influence of each mechanism should also be discussed. In this chapter, the influence of all the mechanisms on the system costs are discussed and discussion on certain aspects were made.

8.2. Costs due to the various mechanisms

In chapter 4, section 4.3.2, the costs of the uncontrolled system was determined. The total cost, C_{total} was €1618.3, the grid costs, C_{grid} were determined to be €-544.20 and the EV cost, C_{EV} was determined to be €691.27. The PV and inverter costs were the same for all the mechanisms as the same system size was considered for determining the effects of different market mechanisms. These costs were €1350 for PV and €121.06 for the inverter.

In chapter 5, section 5.3, the system sizes and system costs for various levels of FIT was observed. For a 10% system size, the total observed costs (C_{total}) were €481.22. Grid costs (C_{grid}) were determined to be -€2321.65. The BES(C_{bat}) and EV(C_{EV}) costs were €302.073 and €986.651, respectively.

In chapter 6, section 6.3.2, the system costs were determined for various capacity tariffs. The system costs at a tariff of 0.0015 €/kW/h were discussed. C_{total} was determined to be €776.45, C_{grid} was found to be €-2332.18, C_{bat} was determined to be €303.03 and C_{EV} was determined to be €993.31. The capacity cost, C_{cap} was €292.61. For the high CT of 0.0123 €/kW/h, there were variations in the costs as well. C_{total} was determined to be €2369.21, C_{bat} was equal to €292.51, C_{EV} was determined to be €768.64. Finally, the capacity costs had increased significantly to €1003.5

In chapter 7, section 6.3.3, the total costs when FCR was also introduced was observed. These costs were: C_{total} was -€146.44, C_{grid} was -€1880.23, C_{bat} was €384.08 and C_{EV} was €795.74. The capacity cost, C_{cap} was €295.65 when FCR was introduced. The breakdown of all these costs was plotted in the figure 8.1

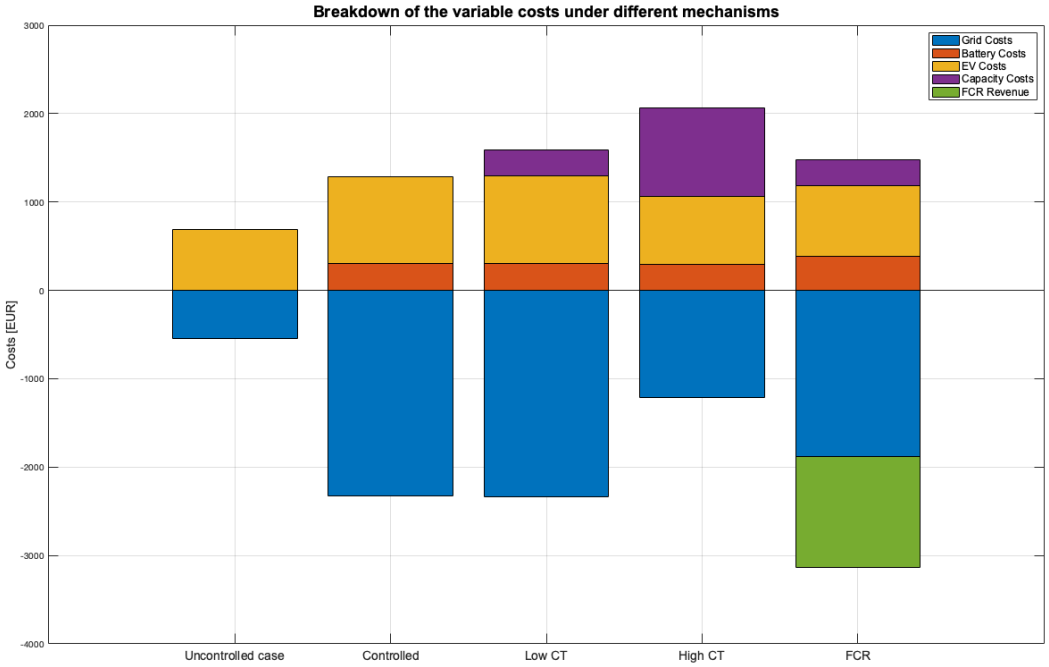

Figure 8.1: Varying cost components under different market mechanisms

It was observed that in the uncontrolled scenario, the grid costs were the highest. This was because there was no EMS to determine the optimal consumption from the grid low tariffs. The EV costs were low as only calendar degradation was considered. The total cost was high as there was no EMS to control the feeding in and neither was V2G allowed. However, under the control of EMS, the grid costs, which was already negative, started to reduce. With this reduction in grid costs, it was inferred that the EMS was able to reduce the total maximum costs even further by reducing the grid costs. This phenomenon was observed for all the mechanisms but when the high CT was applied, the capacity costs increased rapidly. The increase in capacity costs could be attributed to the large increase in CT which was charged at each instance. From 0.0015 €/kW/h to 0.0123 €/kW/h, there was an increase of 87.8% in the capacity tariff. The lowest total costs were observed when FCR market was introduced to the model. When FCR was added to the EMS model, along with the other market mechanisms, it was observed that the grid costs (C_{grid}) increased. But the total costs (C_{total}) reduced and was negative. As already discussed in chapter 7, this reduction was due to the revenue generated by reserving power for FCR. However, one important observation from 8.1 was that the sum of the variable costs was low. For uncontrolled case, the addition of EV and grid costs resulted in a value of €147.07. Under the EMS control, the sum of the variable costs was determined to be -€1032.92. When low CT was added, the sum of the variable costs was -€743 and when high CT was considered, the total variable costs were €849.7. The lowest total variable cost was determined when FCR was added and was found to be -€1660.77. This showed that the total investment costs formed the significant portion of the total costs.

In the literature review (see chapter 2), the various components of the retail energy price in the Netherlands was discussed [3]. This research tried to determine the costs due to certain future market mechanisms to a prosumer building. On comparison with the current retail price structure, it was observed the variable energy costs (or the grid costs, C_{grid}) was quite low due to the high FIT and the dynamic nature of prices. However, currently the retail prices used are ToU prices which as observed did not incentivize the use of BES or the EV for V2G. The network management costs in the utility energy bill reflect CT (C_{cap}). With the mechanism proposed in this research, it was observed that the capacity costs would not be a constant (which is the current situation) if such a mechanism is implemented by the government. Instead the capacity costs would increase and would incentivize the consumers to reduce their grid consumption and supply. Finally, FCR was also observed. With the introduction of FCR, it was observed that the prosumer household could generate significant revenue and thus reduce the costs. Equigy [63], a crowd balancing platform established

by various TSOs across Western Europe (including TenneT) showed the intent of TSOs to make use of the flexibility offered by prosumer households for grid balancing. However, it should be noted that for participation in FCR market, an aggregator is required. But it is also possible for various energy suppliers themselves to act as aggregators. In such a case, the FCR revenue would be visible on the utility bill. Finally, the remaining components of the retail bill included the taxes and the government subsidies which depended on the current regulation and policies put forth by the government. It should also be noted that a large part of the total energy costs (63%) was subsidised by the government for residents [3].

8.3. Power flow due to the various mechanisms

Apart from the costs, the power flow resulting by the addition of various mechanisms were also discussed in this research. Currently, the FIT for the prosumers who have a capacity size of 3x80A or less can receive the entire variable energy cost back when they feed energy back to the grid [3]. This high level of FIT is expected to continue at least until 2023 [81], [82]. Such high remuneration for feeding in power by the prosumers gives them incentive to invest in larger generation systems. For different levels of FIT, the resulting system sizes were also studied in this research. It was observed that at high FIT, the system was large and the resulting peak power was also significant. Thus, if this situation continues, it can be concluded that prosumers using this EMS have incentive to feed energy back at high power. This would lead high peak power for several hours during a day as seen in the seasonal analysis in chapter 5, section 5.3.8. If the increasing number of PV installations [5] and EVs [17] in the distribution grid continue, the problems discussed in chapter 2 (section 2.2) would continue to occur and as a result would lead to increasing grid reinforcement costs[35]. But actual grid studies are necessary to quantify the severity of these issues.

From literature, it was found that FIT were a good incentive to increase distributed generation [31], [29]. From the results of chapter 5, it was also observed that high FIT did lead to higher system size when controlled by this EMS. But as found out in [81], [82] that the FIT would reduce in the future. This would mean that the incentive to invest in a larger generation system and storage size would also reduce. However, with this EMS, it was observed that prosumers would be capable of reserving power in the ancillary services market for frequency regulation. Depending on the FCR prices, there would still be an incentive to invest in higher generation and storage systems. This should also be quantified with a specific study. Additionally, with increasing number of distributed generation, peer to peer markets have emerged as an interesting business case [83]. These markets are not just relevant for people with large energy production, but also promote localised generation and consumption. Additionally, [83] also mentions that peer-to-peer energy trading could also help in reduction of grid issues caused by the presence of distributed generation. It should be noted that when the number of distributed generation systems in the network increase, the revenue generated by the energy supplier would reduce [84]. This would force the supplier to increase the energy prices which would mean that the consumers who do not have their own energy generation systems would have to pay higher prices, which can be unfair. But with peer to peer markets, this issue could be prevented if the supplier has invested in the distributed energy generation [83]. Vandebron [85] is an energy supplier in the Netherlands which aggregates energy produced from independent prosumers and supplies it to their consumers. Lichtblick from Eneco[86] is another aggregator which is involved in supplying locally generated energy to their consumers.

In chapter 6, a capacity mechanism which incentivized prosumers to reduce their peak grid power was studied. This capacity mechanism required the consumers to subscribe to a particular power level based on a capacity tariff which was charged per kW. The consumers were incentivized to keep their grid power below the subscribed level by applying a penalty whenever this level was exceeded. Both consumption and feeding in were penalized if the grid power exceeded the subscribed limit. It should be noted that the current distribution network tariffs do not differentiate between the feeding in or consumption. A flat rate is charged irrespective of the current power level. This tariff does not incentivize the consumers to reduce their consumption. But from the results of chapter 6, it was observed that the implemented mechanism was able to reduce the grid consumption and the peak power. Moreover, for a particular CT, the EMS also determined the optimal subscription such that the demand was always met. From the methods which were studied in the literature ([42], [26], [40]), this determination of the optimal capacity was a new addition developed during this research. However, for reducing the grid power to desired levels and ensuring the costs do not increase,

capacity tariffs need to designed appropriately. This requirement was discussed in literature by [37], [38], [39] and [87].

With the availability of the energy generation and storage at the prosumer household and with research on using renewable energy sources for frequency regulation, it was studied how this EMS could be used to reserve power on the FCR market. From the results of chapter 7, it was observed that the EMS reserved power for FCR. For the simulation to determine the amount of reserved power, CT of 0.0015 €/kW/h was used. At this tariff, a maximum of 15 kW reserved power was observed. Also observed were significant changes in the power flow when FCR was introduced. Since, FCR was a revenue generating mechanism, there were instances when reserving power was more profitable than feeding in. Since feeding in or consuming power from the grid at any instant reduced the total power which could be reserved, the consumption and feeding in was reduced in comparison with the situation when there was no FCR. When the power flow for various seasons of the half year was determined under FCR, it was observed that the average grid power and EV had reduced signficantly. However, the peak power remained the same as the case when FCR was absent. This was an interesting outcome as it showed that prosumers using this EMS would be willing to reduce the consumption or feeding in based provided a remuneration is awarded. This behaviour should be further explored in detail and might be an interesting alternative for capacity mechanism.

The effects of V2G operation were also observed on the power flow, the total costs and battery degradation. The EV battery degradation (ΔE_{EV}^{tot}) when V2G was absent was determined to be 0.671 kWh. ΔE_{EV}^{cal}, degradation caused by calendar ageing, was determined to be 0.652 kWh. This showed that the significant proportion (97.16%) of the EV battery degradation was due to the passage of time, rather than the usage for charging. When V2G was allowed at high FIT, the EV battery degradation was determined to be 0.84 kWh. Even under this circumstances, the calendar ageing was the major component and accounted for 77.6% of degradation. Thus, it can also be concluded that degradation due to the charging operation and V2G operation was not as significant as calendar ageing. Moreover, the total cost reduction due to V2G was larger than the increased EV costs. However, it should be noted that there were few underlying assumptions considered for the calculation of battery degradation. Under those assumptions, it can be stated that V2G was profitable and played a significant role in supplying power to fulfil demand, feed energy back to the grid, and reserve power for FCR. Additionally, the introduction of FCR also reduced the degradation in the batteries.

9

Conclusion and Recommendation

9.1. Conclusion

This research used the provided EMS model and added equations of certain future market mechanisms to it to determine how these mechanisms would influence the power consumption behaviour and the system costs for a prosumer household. Using the half yearly data, simulations were made on GAMS and the results were studied.

In Chapter 3, the EMS model was discussed. Constraints for the devices which govern the power flow, the system size and the operational costs were studied. It was also observed that the EMS was simultaneously able to size the system and determine the optimal power flow which minimized the operational costs. The operational costs of BES and EV, grid costs, the PV installation costs, converter costs, and the interest were considered together considered to be the total costs.

Chapter 4.3.2, discussed the power flow and the costs for a distributed generation and storage system when there was no EMS to control the power flow. Total system costs comprised of the EV costs (without V2G), PV costs, grid costs and the inverter costs. This costs were then compared to the costs obtained when EMS was implemented.

In chapter 5, the EMS discussed in chapter 3 was used to determine the optimal size of the generation and storage system under different FIT levels. Percentage difference of retail price was the model which was used to calculate the FIT. In this model of FIT, the FIT is lower than the RP by a particular percent value. It was observed that when the difference between the RP and FIT was low, optimal system sizes were high. As the difference increased, the FIT reduced. This reduction in remuneration led to smaller optimal system sizes. Since the revenue that could be generated reduced, the operational costs increased and to reduce this cost, smaller system sizes were used. It was observed that BES size reduced from 26.057 kWh when FIT was equal to RP to 8.62 kWh when there was no FIT. PV size reduced from 30 kW_p at zero difference to 4.493 kW_p. These sizes of the BES and PV at zero FIT showed that despite having no remuneration, generation and storage systems are still required to obtain the minimal cost. For the system power flow at 10% difference between FIT and RP, it was observed that the maximum grid power observed was 14.85 kW and this value was seen for both, consumption and feeding in. Energy was consumed at low prices and fed back at high prices.

As the FIT started to reduce, the EV's use for V2G started to decrease as well. When EV was used for V2G, high charging and discharging power levels were observed. When the FIT reduced, the power levels reduced as well and it was observed that the energy stored in EV decreased. The effect of V2G on power flow and system costs was observed for ToU prices, high, and low FIT. It was observed that at high FIT, V2G was able to reduce the costs significantly by feeding more energy into the grid and generating revenue. An increase of 45.15% in total costs was observed when V2G was restricted at high FIT. Under no V2G, the BES costs and average BES power increased. But, V2G restriction at zero FIT and ToU prices did not make a significant difference in costs or the power flow. Total costs increased by 0.25% when V2G was restricted for zero FIT and increased by 0.3% for ToU prices. Seasonal variations were also discussed and it was determined that the PV

power was the lowest on average during winter which led to low average grid feeding power. However, with the increase in irradiance during spring and summer, the average PV output increased. When this PV power was fed back to the grid which increased the average grid feeding power. Additionally, the increased PV output led to more feeding in hours during spring and summer days. The maximum value of average grid power remained same during the different seasons.

Chapter 6 discussed a variation of a capacity mechanism introduced in the literature. The mechanism was modified to reduce the grid peak power for both consumption and feeding in. This was done by incentivizing the consumers to subscribe to a particular power level. Exceeding this power level led to addition of penalties. The capacity price per kW was varied and the effects on the costs and the power flow were observed. It was noticed that when the CT was low, the grid peak power was still high. However, when the CT started to increase, the grid peak power reduced. Moreover, the increasing CT also led to reduction in charging and discharging EV. Similar to increasing FIT, increasing CT led to reduction in EV's use for V2G. Finally, increasing CT also led to PV curtailment as the generated energy could not be fed back without exceeding the subscribed power. But increasing the CT led to increase in total costs. Moreover, the seasonal analysis of the various power level showed that as the CT increased, the average power level of different devices reduced. The implementation used in this research also led to selection of optimal power to subscribe based on the capacity tariff.

Chapter 7 discussed the use of EMS to reserve the power for FCR market in the Netherlands. It was observed that EMS was able to use the PV, BES and EV for reserving power. This also led to increase in revenue and thus, reduction in costs. Since reserving power generated revenue, it was always profitable to reserve power. Seasonal analysis of power flow when FCR was introduced showed that there was a general reduction in average grid power and average power across all the devices except PV. The average PV power generated remained the same and it was fed back to the grid to generate revenue. The total system costs were the lowest for the case when FCR was introduced.

Compared to the uncontrolled case, when the EMS was added and the BES was introduced, the total costs reduced by 70.26% under the EMS control. When low CT was considered, the reduction in costs was 52.02% under EMS control with low CT compared to the uncontrolled case. However, there was an increase of 46.4% in total costs when high CT was considered on comparison with the uncontrolled case. The total costs reduced by 1205.07% when FCR mechanism was introduced on comparison with the uncontrolled case.

9.2. Recommendations

This research determined the effect of power flow and the costs on the household level. Several observations were made about the effect of market mechanisms on the power flow and the costs. However, this research does not consider the effects of the market mechanisms on the grid. High grid power values were observed under high FIT. Thus, it would be interesting to design a grid model with multiple prosumer houses having variable system sizes under the control of the discussed EMS model. With this grid study, it can be determined what are the effects of high FIT on the grid parameters such as line loading, voltage, power loss, harmonics etc. It is also interesting to determine how the EMS would supply power for local consumption in the feeder in a scenario where a peer to peer market is introduced.

Furthermore, it was observed that the CT was able to reduce the peak grid power for both consumption and feeding in. Introducing the capacity tariff on the grid model would also help in determining the effectiveness of the EMS and the CM on reducing peak power in the grid. Again, effects on various grid parameters could be studied and conclusions could be made. Moreover, using the CM, it should also be studied how much grid expansion and reinforcement costs could be avoided. This would be really beneficial to a DSO and could help in making optimal expansions in the future. At the household level, it is also interesting to see how a variable capacity tariff signal can be produced and to determine its effects on costs and power flow.

Further research needs to be done in FCR mechanism as the current implementation does not reserve the same power for a period of four hours. This is a requirement set forth by TenneT and meeting this requirement would be a significant improvement for the provision of FCR if necessary. It should be checked if adding more

households equipped with this EMS can lead to a co-ordinated FCR reserve and delivery. Finally, the observed effects of FCR on average grid power for different seasons should be checked on a grid scale to see what effects does decentralized FCR on grid parameters.

Bibliography

[1] F. Tanrisever, K. Derinkuyu, and G. Jongen, "Organization and functioning of liberalized electricity markets: An overview of the dutch market," *Renewable and Sustainable Energy Reviews*, vol. 51, pp. 1363 – 1374, 2015. [Online]. Available: http://www.sciencedirect.com/science/article/pii/S1364032115006668

[2] M. Mulder and B. Willems, "The dutch retail electricity market," *Energy Policy*, vol. 127, pp. 228 – 239, 2019. [Online]. Available: http://www.sciencedirect.com/science/article/pii/S0301421518308061

[3] Eneco. (2020) Energy offer. [Online]. Available: https://www.eneco.nl/duurzame-energie/bestellen/overzicht

[4] Central Bureau for Statistics (CBS). (2019) Share of renewable energy up to 7.4 percent. [Online]. Available: https://www.cbs.nl/en-gb/news/2019/22/share-of-renewable-energy-up-to-7-4-percent

[5] ——. (2019) Solar panel capacity up by more than half. [Online]. Available: https://www.cbs.nl/en-gb/news/2019/17/solar-panel-capacity-up-by-more-than-half

[6] R. Philipsen, G. Morales-España, M. de Weerdt, and L. de Vries, "Trading power instead of energy in day-ahead electricity markets," *Applied Energy*, vol. 233-234, pp. 802 – 815, 2019. [Online]. Available: http://www.sciencedirect.com/science/article/pii/S0306261918315241

[7] L. de Vries and R. Verzijlbergh, "How renewable energy is reshaping europe's electricity market design," *Economics of Energy & Environmental Policy*, vol. 7, no. 2, pp. 31–49, 2018.

[8] European Commission. 2030 climate & energy framework. [Online]. Available: https://ec.europa.eu/clima/policies/strategies/2030_en

[9] ——. (2019) Long term strategy: Going climate neutral by 2050. [Online]. Available: https://ec.europa.eu/clima/sites/clima/files/long_term_strategy_brochure_en.pdf

[10] K. Balamurugan, D. Srinivasan, and T. Reindl, "Impact of distributed generation on power distribution systems," *Energy Procedia*, vol. 25, pp. 93 – 100, 2012, pV Asia Pacific Conference 2011. [Online]. Available: http://www.sciencedirect.com/science/article/pii/S1876610212011757

[11] W. L. Theo, J. S. Lim, W. S. Ho, H. Hashim, and C. T. Lee, "Review of distributed generation (dg) system planning and optimisation techniques: Comparison of numerical and mathematical modelling methods," *Renewable and Sustainable Energy Reviews*, vol. 67, pp. 531 – 573, 2017. [Online]. Available: http://www.sciencedirect.com/science/article/pii/S1364032116305421

[12] F. Bastiao, P. Cruz, and R. Fiteiro, "Impact of distributed generation on distribution networks," in *2008 5th International Conference on the European Electricity Market*, May 2008, pp. 1–6.

[13] M. Karimi, H. Mokhlis, K. Naidu, S. Uddin, and A. Bakar, "Photovoltaic penetration issues and impacts in distribution network – a review," *Renewable and Sustainable Energy Reviews*, vol. 53, pp. 594 – 605, 2016. [Online]. Available: http://www.sciencedirect.com/science/article/pii/S136403211500903X

[14] Central Bureau for Statistics (CBS). (24-12-2019) Lower co2 emissions in third quarter of 2019. [Online]. Available: https://www.cbs.nl/en-gb/news/2019/52/lower-co2-emissions-in-third-quarter-of-2019

[15] NL Times. (12-10-2017) New dutch government's plans for the coming years. [Online]. Available: https://nltimes.nl/2017/10/10/new-dutch-governments-plans-coming-years

[16] Reuters. (02-05-2019) City of amsterdam to ban polluting cars from 2030. [Online]. Available: https://www.reuters.com/article/us-netherlands-pollution-amsterdam/city-of-amsterdam-to-ban-polluting-cars-from-2030-idUSKCN1S81XV

[17] Netherlands Enterprise Agency. (March 2019) Statistics electric vehicles in the netherlands. [Online]. Available: https://www.rvo.nl/sites/default/files/2019/03/2019_02_Statistics

[18] Central Bureau for Statistics (CBS). (10-05-2019) Number of all-electric cars has doubled. [Online]. Available: https://www.cbs.nl/en-gb/news/2019/19/number-of-all-electric-cars-has-doubled

[19] R. A. Verzijlbergh, L. J. De Vries, and Z. Lukszo, "Renewable energy sources and responsive demand. do we need congestion management in the distribution grid?" *IEEE Transactions on Power Systems*, vol. 29, no. 5, pp. 2119–2128, Sep. 2014.

[20] NOS. (15-09-2019) Tu delft experimenteert met stroomnet, want dat is nog niet klaar voor toekomst. [Online]. Available: https://nos.nl/artikel/2301846-tu-delft-experimenteert-met-stroomnet-want-dat-is-nog-niet-klaar-voor-toekomst.html

[21] Alliander. (2018) Annual report 2018. [Online]. Available: https://2019.jaarverslag.alliander.com//verslagen/annual-report-2018/ourresultsin8/customers6/pilsuppocustomimakchoi

[22] G. A. Putrus, P. Suwanapingkarl, D. Johnston, E. C. Bentley, and M. Narayana, "Impact of electric vehicles on power distribution networks," in *2009 IEEE Vehicle Power and Propulsion Conference*, Sep. 2009, pp. 827–831.

[23] Central Bureau for Statistics (CBS). (08-10-2018) Use of air-source heat pumps has increased. [Online]. Available: https://www.cbs.nl/en-gb/news/2018/40/use-of-air-source-heat-pumps-has-increased

[24] E. Veldman, M. Gibescu, H. Slootweg, and W. L. Kling, "Impact of electrification of residential heating on loading of distribution networks," in *2011 IEEE Trondheim PowerTech*, June 2011, pp. 1–7.

[25] Eneco. Saving energy and insight into consumption. [Online]. Available: http://eneco.nl/energieproducten/

[26] G. Doorman and L. de Vries, "Electricity market design based on consumer demand for capacity," 2017.

[27] European Parliamentary Research Service. (2017) Capacity mechanisms for electricity. [Online]. Available: https://www.europarl.europa.eu/RegData/etudes/BRIE/2017/603949/EPRS_BRI(2017)603949_EN.pdf

[28] European Commission-RES Legal. (09-01-2019) Promotion in the netherlands. [Online]. Available: https://www.tennet.eu/our-grid/our-high-voltage-grid/power-failures/

[29] A. Campoccia, L. Dusonchet, E. Telaretti, and G. Zizzo, "Feed-in tariffs for grid-connected pv systems: The situation in the european community," in *2007 IEEE Lausanne Power Tech*, July 2007, pp. 1981–1986.

[30] Netherlands Enterprise Agency. (2019) Stimulation of sustainable energy production - sde+. [Online]. Available: https://english.rvo.nl/subsidies-programmes/sde

[31] T. Couture and Y. Gagnon, "An analysis of feed-in tariff remuneration models: Implications for renewable energy investment," *Energy Policy*, vol. 38, no. 2, pp. 955 – 965, 2010. [Online]. Available: http://www.sciencedirect.com/science/article/pii/S0301421509007940

[32] M. Klein, A. Ziade, and L. de Vries, "Aligning prosumers with the electricity wholesale market – the impact of time-varying price signals and fixed network charges on solar self-consumption," *Energy Policy*, vol. 134, p. 110901, 2019. [Online]. Available: http://www.sciencedirect.com/science/article/pii/S0301421519304793

[33] Eneco. (2020) Frequently asked questions. [Online]. Available: https://www.eneco.nl/zonnepanelen/saldering/

[34] C. Triki and A. Violi, "Dynamic pricing of electricity in retail markets," pp. 21 – 36, 2009. [Online]. Available: https://doi.org/10.1007/s10288-007-0056-2

[35] S. Neuteleers, M. Mulder, and F. Hindriks, "Assessing fairness of dynamic grid tariffs," *Energy Policy*, vol. 108, pp. 111 – 120, 2017. [Online]. Available: http://www.sciencedirect.com/science/article/pii/S0301421517303129

[36] W. van Westering and H. Hellendoorn, "Low voltage power grid congestion reduction using a community battery: Design principles, control and experimental validation," *International Journal of Electrical Power & Energy Systems*, vol. 114, p. 105349, 2020. [Online]. Available: http://www.sciencedirect.com/science/article/pii/S0142061519305009

[37] I. Abdelmotteleb, T. Gómez, J. P. Chaves Ávila, and J. Reneses, "Designing efficient distribution network charges in the context of active customers," *Applied Energy*, vol. 210, pp. 815 – 826, 2018. [Online]. Available: http://www.sciencedirect.com/science/article/pii/S0306261917311236

[38] L. N. Ochoa, F. Pilo, A. Keane, P. Cuffe, and G. Pisano, "Embracing an adaptable, flexible posture: Ensuring that future european distribution networks are ready for more active roles," *IEEE Power and Energy Magazine*, vol. 14, no. 5, pp. 16–28, 2016.

[39] E. Koliou, C. Bartusch, A. Picciariello, T. Eklund, L. Söder, and R. A. Hakvoort, "Quantifying distribution-system operators' economic incentives to promote residential demand response," *Utilities Policy*, vol. 35, pp. 28 – 40, 2015. [Online]. Available: http://www.sciencedirect.com/science/article/pii/S0957178715300096

[40] D. Steen, L. A. Tuan, and O. Carlson, "Effects of network tariffs on residential distribution systems and price-responsive customers under hourly electricity pricing," *IEEE Transactions on Smart Grid*, vol. 7, no. 2, pp. 617–626, 2016.

[41] G. L. Doorman, "Capacity subscription: solving the peak demand challenge in electricity markets," *IEEE Transactions on Power Systems*, vol. 20, no. 1, pp. 239–245, Feb 2005.

[42] S. Bjarghov and G. Doorman, "Utilizing end-user flexibility for demand management under capacity subscription tariffs," in *2018 15th International Conference on the European Energy Market (EEM)*, June 2018, pp. 1–5.

[43] C. Eid, P. Codani, Y. Perez, J. Reneses, and R. Hakvoort, "Managing electric flexibility from distributed energy resources: A review of incentives for market design," *Renewable and Sustainable Energy Reviews*, vol. 64, pp. 237 – 247, 2016. [Online]. Available: http://www.sciencedirect.com/science/article/pii/S1364032116302222

[44] K. Knezović, M. Marinelli, P. Codani, and Y. Perez, "Distribution grid services and flexibility provision by electric vehicles: A review of options," in *2015 50th International Universities Power Engineering Conference (UPEC)*, Sep. 2015, pp. 1–6.

[45] TenneT TSO B.V. (2020) Security of supply. [Online]. Available: https://www.tennet.eu/our-key-tasks/security-of-supply/security-of-supply/

[46] E. C. Portante, S. F. Folga, J. A. Kavicky, and L. T. Malone, "Simulation of the september 8, 2011, san diego blackout," in *Proceedings of the Winter Simulation Conference 2014*, Dec 2014, pp. 1527–1538.

[47] M. Papic. (2013) Pacific southwest blackout on september 8, 2011 at 15:27. [Online]. Available: https://site.ieee.org/pes-cascading/files/2013/08/2a_SWPacific_Papic.pdf

[48] L. L. Lai, H. T. Zhang, S. Mishra, D. Ramasubramanian, C. S. Lai, and F. Y. Xu, "Lessons learned from july 2012 indian blackout," in *9th IET International Conference on Advances in Power System Control, Operation and Management (APSCOM 2012)*, 2012, pp. 1–6.

[49] ENTSO E-UCTE. (2004) Load-frequency control and performance. [Online]. Available: https://eepublicdownloads.entsoe.eu/clean-documents/pre2015/publications/entsoe/Operation_Handbook/Policy_1_Appendix%20_final.pdf

[50] P. Kundur, *Power System Stability and Control*, ser. EPRI power system engineering series. McGraw-Hill, 1994.

[51] TenneT TSO B.V. (2020) Fcr manual for bsps. [Online]. Available: https://www.tennet.eu/fileadmin/user_upload/SO_NL/Handboek_FCR_voor_BSPs_-_EN_version.pdf

[52] R. Yan, T. K. Saha, N. Modi, N.-A. Masood, and M. Mosadeghy, "The combined effects of high penetration of wind and pv on power system frequency response," *Applied Energy*, vol. 145, pp. 320 – 330, 2015. [Online]. Available: http://www.sciencedirect.com/science/article/pii/S0306261915002214

[53] M. Dreidy, H. Mokhlis, and S. Mekhilef, "Inertia response and frequency control techniques for renewable energy sources: A review," *Renewable and Sustainable Energy Reviews*, vol. 69, pp. 144 – 155, 2017. [Online]. Available: http://www.sciencedirect.com/science/article/pii/S1364032116309212

[54] H. Bevrani, A. Ghosh, and G. Ledwich, "Renewable energy sources and frequency regulation: Survey and new perspectives," *Renewable Power Generation, IET*, vol. 4, pp. 438 – 457, 10 2010.

[55] M. Yilmaz and P. T. Krein, "Review of benefits and challenges of vehicle-to-grid technology," in *2012 IEEE Energy Conversion Congress and Exposition (ECCE)*, 2012, pp. 3082–3089.

[56] ——, "Review of the impact of vehicle-to-grid technologies on distribution systems and utility interfaces," *IEEE Transactions on Power Electronics*, vol. 28, no. 12, pp. 5673–5689, Dec 2013.

[57] S. Weckx and J. Driesen, "Load balancing with ev chargers and pv inverters in unbalanced distribution grids," *IEEE Transactions on Sustainable Energy*, vol. 6, no. 2, pp. 635–643, April 2015.

[58] M. Datta and T. Senjyu, "Fuzzy control of distributed pv inverters/energy storage systems/electric vehicles for frequency regulation in a large power system," *IEEE Transactions on Smart Grid*, vol. 4, no. 1, pp. 479–488, March 2013.

[59] K. Knezović, M. Marinelli, P. B. Andersen, and C. Træholt, "Concurrent provision of frequency regulation and overvoltage support by electric vehicles in a real danish low voltage network," in *2014 IEEE International Electric Vehicle Conference (IEVC)*, 2014, pp. 1–7.

[60] A. O'Connell, A. Keane, and D. Flynn, "Rolling multi-period optimization to control electric vehicle charging in distribution networks," in *2014 IEEE PES General Meeting | Conference Exposition*, 2014, pp. 1–1.

[61] M. Andoni, V. Robu, D. Flynn, S. Abram, D. Geach, D. Jenkins, P. McCallum, and A. Peacock, "Blockchain technology in the energy sector: A systematic review of challenges and opportunities," *Renewable and Sustainable Energy Reviews*, vol. 100, pp. 143 – 174, 2019. [Online]. Available: http://www.sciencedirect.com/science/article/pii/S1364032118307184

[62] TenneT TSO B.V. (2018) End report fcr pilot: Fcr delivery with aggregated assets. [Online]. Available: https://www.tennet.eu/fileadmin/user_upload/SO_NL/FCR_Final_report_FCR_pilot__alleen_in_Engels_.pdf

[63] Equigy. (2020) The platform-equigy. [Online]. Available: https://equigy.com/the-platform/

[64] X. Cao, X. Dai, and J. Liu, "Building energy-consumption status worldwide and the state-of-the-art technologies for zero-energy buildings during the past decade," *Energy and Buildings*, vol. 128, pp. 198 – 213, 2016. [Online]. Available: http://www.sciencedirect.com/science/article/pii/S0378778816305783

[65] P. H. Shaikh, N. B. M. Nor, P. Nallagownden, I. Elamvazuthi, and T. Ibrahim, "A review on optimized control systems for building energy and comfort management of smart sustainable buildings," *Renewable and Sustainable Energy Reviews*, vol. 34, pp. 409 – 429, 2014. [Online]. Available: http://www.sciencedirect.com/science/article/pii/S1364032114001889

[66] S. Teleke, M. E. Baran, S. Bhattacharya, and A. Q. Huang, "Rule-based control of battery energy storage for dispatching intermittent renewable sources," *IEEE Transactions on Sustainable Energy*, vol. 1, no. 3, pp. 117–124, 2010.

[67] F. Brahman, M. Honarmand, and S. Jadid, "Optimal electrical and thermal energy management of a residential energy hub, integrating demand response and energy storage system," *Energy and Buildings*, vol. 90, pp. 65 – 75, 2015. [Online]. Available: http://www.sciencedirect.com/science/article/pii/S0378778814011128

[68] W. Tushar, C. Yuen, S. Huang, D. B. Smith, and H. V. Poor, "Cost minimization of charging stations with photovoltaics: An approach with ev classification," *IEEE Transactions on Intelligent Transportation Systems*, vol. 17, no. 1, pp. 156–169, 2016.

[69] Wiljan Vermeer, Gautham Ram Chandra Mouli, Pavol Bauer, "Real-time building smart charging system based on pv forecast and li-ion battery degradation," *Energies*, vol. 13, pp. 1–25, 02-07-2020. [Online]. Available: https://www.mdpi.com/1996-1073/13/13/3415#cite

[70] NREL. (2015) Battery ownership model. [Online]. Available: https://www.nrel.gov/docs/fy16osti/66140.pdf

[71] Tesla Inc. (2020) Tesla powerwall. [Online]. Available: https://www.tesla.com/en_gb/powerwall/design

[72] B. NEF, "New energy outlook 2019," Bloomberg NEF, -, 2019.

[73] M. Bortolini, M. Gamberi, A. Graziani, C. Mora, and A. Regattieri, "Multi-parameter analysis for the technical and economic assessment of photovoltaic systems in the main european union countries," *Energy Conversion and Management*, vol. 74, pp. 117 – 128, 2013. [Online]. Available: http://www.sciencedirect.com/science/article/pii/S019689041300232X

[74] J. Wang, J. Purewal, P. Liu, J. Hicks-Garner, S. Soukazian, E. Sherman, A. Sorenson, L. Vu, H. Tataria, and M. W. Verbrugge, "Degradation of lithium ion batteries employing graphite negatives and nickel–cobalt–manganese oxide + spinel manganese oxide positives: Part 1, aging mechanisms and life estimation," *Journal of Power Sources*, vol. 269, pp. 937 – 948, 2014. [Online]. Available: http://www.sciencedirect.com/science/article/pii/S037877531401074X

[75] W. Vermeer, G. R. C. Mouli, and P. Bauer, "Working paper: Optimal system sizing in future buildings based on optimal power flows and battery degradation," *TBA*, vol. TBA, p. TBA, 2020. [Online]. Available: TBA

[76] ELaad. (2020) Analyses. [Online]. Available: https://platform.elaad.io/analyses.html

[77] Electric Vehicle Database. (2020) Tesla model 3 standard range. [Online]. Available: https://ev-database.org/car/1060/Tesla-Model-3-Standard-Range

[78] G. Ram Chandra Mouli, "Charging electric vehicles from solar energy: Power converter, charging algorithm and system design," Ph.D. dissertation, Delft University of Technology, 2018.

[79] Centraal Bureau voor de Statistiek. (2019) Solar panel capacity up by more than half. [Online]. Available: https://www.cbs.nl/en-gb/news/2019/17/solar-panel-capacity-up-by-more-than-half

[80] NVE. (2020) The norwegian water resources and energy directorate. [Online]. Available: https://www.nve.no/english/

[81] PV Magazine. (2020) Netherlands to support residential pv through net metering for the entire decade. [Online]. Available: https://www.pv-magazine.com/2020/04/01/netherlands-to-support-residential-pv-through-net-metering-for-the-entire-decade/

[82] Zonefabriek. (2020) Net metering in the netherlands. [Online]. Available: https://www.zonnefabriek.nl/en/solar-panels/net-metering-in-the-netherlands/

[83] C. Zhang, J. Wu, C. Long, and M. Cheng, "Review of existing peer-to-peer energy trading projects," *Energy Procedia*, vol. 105, pp. 2563–2568, 2017. [Online]. Available: http://www.sciencedirect.com/science/article/pii/S1876610217308007

[84] Sweco and PwC, "Study on the effective integration of distributed energy resources for providing flexibility to the electricity system," European Council, Tech. Rep., 2015.

[85] Vandebron. (2020) Energy from renewable sources. [Online]. Available: https://vandebron.nl/energie

[86] Lichtblick. (2020) Das neue normal. [Online]. Available: https://www.lichtblick.de/

[87] A. Picciariello, J. Reneses, P. Frias, and L. Söder, "Distributed generation and distribution pricing: Why do we need new tariff design methodologies?" *Electric Power Systems Research*, vol. 119, pp. 370 – 376, 2015. [Online]. Available: http://www.sciencedirect.com/science/article/pii/S0378779614003927